LITHIUM-7 NMR INVESTIGATIONS OF THE BIOLOGICAL BEHAVIOUR OF THE LITHIUM ION

Janice Bramham

A Thesis Submitted for the Degree of PhD
at the
University of St Andrews

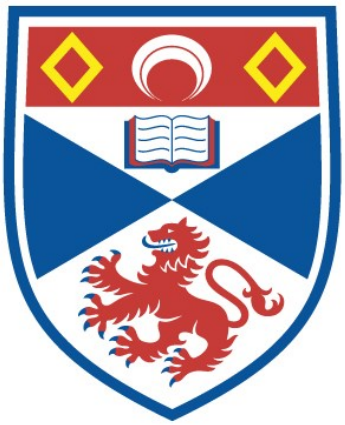

1993

Lithium-7 NMR Investigations of the Biological Behaviour of the Lithium Ion

Janice Bramham

A thesis submitted for the degree of Doctor of Philosophy

Faculty of Science, University of St. Andrews

January 1993

ProQuest LLC.
789 East Eisenhower Parkway
P.O. Box 1346
Ann Arbor, MI 48106 – 1346

Declarations

I, Janice Bramham, hereby certify that this thesis is of my own composition and that it is based upon the results of my own work. Work other than my own is clearly indicated in the text by reference to the relevant researchers or to their publications. This thesis has not in whole, or in any part, been previously presented for any other degree or professional qualification.

I was admitted to the Faculty of Science of the University of St. Andrews under the Ordinance General N^0. 12 in October 1989 and as a candidate for the degree of Doctor of Philosophy in October 1990.

Janice Bramham

I hereby certify that Janice Bramham has fulfilled the conditions of the Resolution and Regulations appropriate to the degree of Doctor of Philosophy.

Dr. F.G. Riddell

Reader in Chemistry

Copyright

Acknowledgements

First, I must thank Dr. F.G. Riddell for introducing me to this unusual and interesting application of NMR spectroscopy, and for enthusiastically volunteering to be a human guinea-pig for this research. I express my utmost gratitude to the consultant psychiatrist from the Royal Liff Hospital in Dundee, Dr. G. Naylor, for his expert advice and encouragement, and for coordinating the necessary interactions between myself and the psychiatrists. I am also deeply indebted to Sister Murray and Dr. Robertson, of the Occupational Health Unit at the University of St. Andrews, for their expert assistance throughout. This work would not have been possible without the numerous volunteers and patients who donated their blood, usually without complaint, and I extend my thanks to everyone.

Thanks are also due to Dr. A. Leech and Professor D. Gani of the Chemistry Department, University of St,. Andrews, for the provision of the enzyme used in this work; to Nigel Carter, Professor C.P.Downes and Dr. I. Batty of the Department of Biochemistry, University of Dundee, for the provision of the cultured cells, and for the materials and advice for the electrophoresis work; and to Kim Thompson and Dr. J. Henderson of the N.E.R.C. Unit, University of Stirling, for their help and loan of equipment for the TLC and densitometry experiments.

I acknowledge my debt to the S.E.R.C. for providing financial support to enable me to carry out this work.

Finally, I thank Nigel and my mum for their invaluable support over the last three years.

Abstract

This thesis reports an investigation of the uptake of Li^+ into human erythrocytes using quantitative ^{7}Li-nmr spectroscopy. It was found that the erythrocytes of psychiatric patients, who were on long term lithium therapy for the treatment of bipolar affective disorder, accumulated more Li^+, and attained an apparent steady-state concentration more rapidly than did the erythrocytes of healthy controls, not taking lithium. This phenomena was shown to be due, at least in part, to a Li^+-induced effect resulting from the treatment of these patients with Li^+. Indeed, prior to treatment the uptake of Li^+ into the erythrocytes from all the patients was similar to that in the erythrocytes of the healthy controls. This Li^+-induced effect is consistent with the inhibition of the Na^+-Li^+ countertransport mechanism, the predominant Li^+ efflux pathway in erythrocytes, which has previously been shown to be inhibited by Li^+.

The uptake of Li^+ into cultured cells was also monitored by ^{7}Li-nmr spectroscopy, by growing the cells upon the surfaces of microcarrier beads. Excellent spectra were obtained from which the uptake of Li^+ was found to be approximately ten-fold faster than that into erythrocytes, with the steady-state being achieved more rapidly.

In an attempt to rationalise the altered transport behaviour of erythrocytes exposed to Li^+ *in vivo*, the effect of this cation upon the major components of the erythrocyte membrane were investigated by TLC and gel electrophoresis. However, no significant differences were observed in either the relative amounts of the lipids, or in the major protein content of the erythrocyte membranes from Li^+-treated patients and from healthy controls not taking lithium.

^{7}Li-nmr spectroscopy was also employed to investigate the interaction between Li^{+} and the enzyme, inositol monophosphatase, however under the conditions of the experiment no interaction was observed.

Finally, a brief study of the transport behaviour of the Cs^{+} ion across the human erythrocyte membrane using ^{133}Cs-nmr spectroscopy is reported. The uptake of Cs^{+} into the erythrocytes of patients suffering from alcohol-dependence syndrome, the erythrocytes of whom are reported to contain abnormally high levels of Cs^{+}, was found to be virtually identical to that of abstinent controls.

Contents

Chapter 1

Introduction

1.1 Introduction

In recent years, considerable success has been achieved using nuclear magnetic resonance spectroscopy to study the lithium ion in biological systems, with the intention of probing the possible mechanisms of action of this cation in psychiatric therapy. This thesis is primarily concerned with the use of high-resolution, nuclear magnetic resonance spectroscopy to study the lithium ion in cell systems, in particular to investigate the effect of lithium therapy on the transport of the lithium ion in human erythrocytes. The effect of the lithium ion on membrane composition, using chromatographic techniques, and the interaction of the lithium ion with the enzyme inositol monophosphatase, using nuclear magnetic spectroscopy, are also investigated. Finally, a preliminary study on the transport behaviour of the caesium ion in human erythrocytes is discussed.

In this chapter, following an introduction to the medical applications of lithium, the membrane transport behaviour of the lithium ion is described and then the application of the high-resolution nuclear magnetic resonance spectroscopy of the alkali metal ions to biological research is discussed.

1.2 Lithium in Medicine

Throughout history many theories concerning the therapeutic qualities of the lithium ion have been proposed covering a wide range of illnesses, including gout, gallstones, rheumatism and eczema. For one reason or another, most of these claims have now been discredited. However, the therapeutic effect of lithium salts in the treatment of bipolar affective disorder has been confirmed and they are now the treatment of choice for the control of acute mania and in the relapse-prevention of bipolar affective disorder. Currently, approximately 1 person in 1000 in the UK is receiving lithium therapy. A significant amount of research is also underway into the

efficacy of lithium salts for the treatment of other disorders, such as schizophrenia, alcoholism, aggression, premenstrual tension and epilepsy. In addition, topical applications of lithium salts have been shown to be clinically effective in the treatment of a number of inflammatory skin disorders, including seborrhoeic dermatitis and herpes.

1.2.1 Psychoses

The most common forms of psychoses in man are schizophrenia and manic depression, and both of these illnesses flare up episodically. Patients suffering from manic depression often experience periods of relative normality between the episodes of affective illness. Schizophrenia takes a more deteriorating course and people suffering from this illness lose contact with reality, suffering delusions and hallucinations.

1.2.2 Affective Disorders

The affective disorders are illnesses which affect the mood of a person and are divided into two categories: bipolar affective disorder and unipolar affective disorder. People suffering from bipolar affective disorder, also known as manic-depressive illness or bipolar II, experience recurrent episodes of both mania and depression whereas people suffering from unipolar disorder, also referred to bipolar I, experience the depression but not the mania. The term 'schizoaffective disorder' has also been employed where there is an apparent co-existence of manic and schizophrenic symptoms in a patient.

In bipolar affective disorder, the periods of mania and depression occur in either regular or irregular sequences. Some patients experience swings in mood on a daily basis but more often the episodes of mania and depression are less frequent and less

regular, with intervening periods of normal mental function. During a manic phase the patient is in a state of overexcitement and is characteristically elated, hyperactive, excessively self-confident, talkative, aggressive, over-indulgent and impulsive. Conversely, the depressive phase of the illness is characterized by sadness, inactivity, indecision, low self-esteem and suicidal thoughts. In some cases a person suffering from bipolar affective disorder may experience only a few episodes of illness during their lifetime.

1.2.3 Lithium in Psychiatry

In 1949, it was discovered that the salts of lithium had therapeutic properties in some types of psychiatric illness *(1)*. The discovery of the therapeutic effects of the lithium ion, Li^+, was totally unexpected since it was actually the toxicity of urea and uric acid which was under investigation at that time. It had been proposed that people experiencing acute mania excreted higher levels of uric acid in their urine than did normal controls and, on this basis, a series of animal experiments were performed involving the administration of injections of mixtures of urea and lithium urate to guinea pigs, the lithium ion being chosen because of its ability to dissolve uric acid. The predicted toxicity with the urate salts was not observed, however the researchers were surprised to discover that the animals had lost their usual timidity; they did not become distressed when handled and were generally very lethargic. Further investigation showed that this effect was caused by Li^+ alone. After administration of lithium carbonate and lithium citrate to healthy humans, the salts were then given to a number of patients suffering from mania, schizophrenia and chronic depression *(1)*. The manic patients all showed a significant and rapid improvement. These results led to a number of other studies showing similar positive results for manic patients. However, at about the same time, the severe side effects which occurred in a totally separate use of lithium salts, including several fatalities, when LiCl was substituted for NaCl in the diet of

patients suffering from cardiovascular illnesses or hypertension, gave lithium salts a bad reputation which naturally resulted in a severe restriction of their use in the clinic and of the necessary research *(2)*. Thus the initial acceptance of lithium therapy was slow and controversial.

Li^+ has been shown to exert its therapeutic effect against mania and, to a lesser extent, against depression in bipolar affective disorder. However, the main use of Li^+ is in relapse-prevention of both the manic and the depressive episodes with the same efficacy, in bipolar and unipolar affective disorders *(3)*. Treatment with Li^+ usually produces an attenuation of the manic and the depressive recurrences. In healthy individuals and in bipolar patients commencing Li^+ therapy during the interval between psychotic episodes, there is surprisingly very little effect on normal mood and cognitive functions. Li^+ is not effective in all cases; 1-2% of bipolar patients and approximately 20% of manic patients fail to respond to treatment with Li^+. In addition, the effectiveness of Li^+ in the treatment of a number of other disorders has been reported, including acute depression (both bipolar and unipolar), schizoaffective disorder, schizophrenia, alcoholism and aggression. Further medical applications of lithium salts under investigation include: herpes simplex virus, aplastic anaemia, headaches, premenstrual tension, hyperthyroidism, granulocytopenia, Menieres syndrome and AIDS.

1.2.4 Li^+ Medication

Li^+ salts are predominantly administered in tablet form. The carbonate is the most convenient, and hence the most common salt of Li^+ employed and its extensive use has shown no problems specific to this salt. In contrast, the citrate contains a lower proportion of Li^+ and hence more drug has to be administered for the same clinical response, however the taste of lithium citrate is more acceptable and it is commercially

available in syrup form. Other salts, such as the sulphate and the acetate, are also commercially available although the chloride is far too deliquescent for convenient use.

Sustained-release formulations of lithium carbonate have been designed to modify the rate of release of Li^+ and thus lower the rate of absorption of Li^+, in order to reduce the frequency and the intensity of the side effects. However, in a comparison of the pharmacokinetics of a sustained-release and a standard-release formulation, no significant differences were found in either the maximum Li^+ concentrations in the serum or in the time that this peak occurred *(4)*.

The nature of the clinical response and the intensity of the side effects upon patients as a consequence of lithium therapy is related to the concentration of Li^+ in the blood plasma. A significant increase in toxic side effects with no corresponding increase in efficacy is observed above a plasma level of approximately 1.4mM, however below 0.4mM the drug is ineffective. Thus, Li^+ has a very narrow therapeutic window, with a tenuous balance between its therapeutic efficacy and the unwanted side effects. Therefore, monitoring of plasma Li^+ levels, particularly during the initial stages of treatment is necessary to ensure a safe and effective dose is administered to the patient. It is now standard practice to monitor the levels of Li^+ in the blood plasma of patients 8-12 h after the last dose. The recommended range varies between health authorities and countries, but in the UK a range of 0.3 - 1.0mM is now generally accepted *(5)*. This is achieved by the daily administration of 600-1000mg Li_2CO_3 (approximately 15-30mmoles Li^+). However, higher levels are sometimes required for the relief of acute episodes of mania.

1.2.5 Side Effects and Toxicity of Li^+

Lithium therapy is associated with numerous, relatively common side effects, most of which can be alleviated by adjusting the dose administered or sometimes by

switching from standard release to slow release drugs. These side effects occasionally occur at acceptable serum Li^+ levels indicating an unusual sensitivity to Li^+. The milder side effects include thirst, polyuria, gastric irritation, weight gain and fine hand tremor, whereas more intense effects include nausea, vomiting, diarrhoea, increased hand tremor and muscle weakness, trembling, headaches, impaired concentration, vertigo, blurred vision and tinnitus, with patients feeling fatigued and lethargic. Cases of severe intoxication are characterised by increased cognitive impairment and restlessness, slurred speech, and confusion, which can precede brain damage, delirium, coma, seizures, and finally death.

Li^+ treatment can result in adverse effects upon the thyroid gland *(6)* - the primary effect is the inhibition of hormone release, which reduces the amount of thyroxine reaching circulation and consequently some Li^+-treated patients develop goitre. It has been suggested that the inhibitory effects of Li^+ are compensated for by a raised secretion of TSH and thus an increase in the stimulation of the thyroid. The elevation of thyroid stimulating hormone, TSH, sometimes observed during the early stages of Li^+ treatment usually disappears but can occasionally lead to hypothyroidism. TSH measurement is the most sensitive commonly available test of thyroid function.

Li^+ treatment can lead to precipitation of some skin disorders, such as acne and psoriasis. Also, some adverse drug interactions have been observed, for instance with diuretics and nonsteroidal antiinflammatory drugs, primarily due to a decrease in the efficiency of the renal clearance of Li^+ resulting in higher serum levels. ACE inhibitors (angiotensin-converting enzyme) may also increase serum [Li^+], possibly due to inhibition of the formation of angiotensin II, a potent stimulator of thirst, and thus leading to dehydration.

Although teratogenesis in animals, as a consequence of Li^+ administration, has occasionally been reported, the incidence of foetal abnormality in humans does not appear to be higher than normal. However, Li^+ does cross the human placenta and the

foetus is exposed to the same concentrations of Li^+ as the mother *(7)*, therefore the risk of continuing Li^+ treatment during pregnancy should be weighed against the risk involved by stopping the therapy and the likely return of the previous psychiatric disorder.

1.3 Mechanism of Action of Li^+

Despite the widespread clinical use of Li^+, its mode of action in psychiatric therapy remains unknown. It is possible that the answer may not be found until the genes responsible for the affective disorders are characterised. Research has uncovered numerous biological systems which are influenced by Li^+. However, which of these effects, if any, are important and how they are involved in the treatment of affective disorders is unknown. It may be that a cocktail of several Li^+-induced effects is responsible for its therapeutic action. The mode of action needs to account for both the acute and the prophylactic efficacy in mania and depression, and for the slow onset of its effectiveness.

Li^+ effects have been demonstrated on membrane transport systems, cyclic AMP-dependent systems, phosphoinositide metabolism, viral replication and prostaglandin synthesis. In some of these effects Li^+ appears to compete with Mg^{2+}, a cofactor for many enzymes.

Li^+ clearly affects the second messenger systems, inhibiting stimulated adenylate cyclase leaving basal activity unaltered, and inhibiting stimulated phosphoinositol turnover leaving basal activity unaltered. Many hormones and neurotransmitters exert their effect by stimulating the synthesis of cyclic AMP. Adenylate cyclase activity, stimulated by such an agonist, is mediated by a Mg^{2+}-dependent, guanine nucleotide-binding protein. It has been shown that Li^+ interferes with the binding of the G-protein resulting in an inhibition of accumulation of

cyclic AMP *(8)*. The effect of Li^+ on the phosphoinositide-dependent signalling system is discussed in Chapter 6.

Li^+ interferes with the biosynthesis of prostaglandins by inhibiting the cyclooxidation of the fatty acids - Mg^{2+} is a cofactor in the cyclooxygenase system *(9)*. Manic patients have abnormally high levels of PGE1, thus this inhibitory behaviour may offer an explanation for the antimanic action of Li^+.

Li^+ influences a number of cell types in the immune system, stimulating protective host responses, and the haemotopoietic system, increasing the production of granulocytes and platelets *(10)*. Li^+ inhibits DNA synthesis and therefore effectively interferes with the replication of DNA viruses. The stimulation of immune responses and inhibition of viral replication are responsible for the efficacy of Li^+ in the treatment of herpes. It appears that Li^+ inhibits Type I and Type II herpes simplex viruses. This antiviral effect of Li^+ has stimulated research of its effects in the treatment of HIV and AIDS. In AIDS, it has been shown that Li^+ increases the number of T_4 helper lymphocytes and may also permit patients to receive higher doses of AZT.

A number of enzymes, apart from those involved in the above systems, have also been shown to be influenced by Li^+, and many of these are Mg^{2+}-dependent. For instance, Li^+ stimulates Na^+/K^+-ATPase in a dose dependent manner and inhibits pyruvate kinase *(11)*.

1.4 Membrane Transport

An essential characteristic of biological membranes is their selectivity in permeability with respect to the movement of molecules and ions, thus providing environments favourable for the processes required to sustain life. Membrane transport mechanisms are responsible for the maintenance of intra-, and extracellular ionic and molecular composition and pH, and for the regulation of cell volume. The production

of ion gradients across membranes is essential in cellular systems as the resulting electrical potentials are a source of the potential energy required for several functions, including the transport of other species. In neurons, for instance, the electrical potential derived from trans-membrane ion gradients is involved in the propagation of signals as ion currents.

The movement of a substrate across a membrane is a consequence of either a passive or an active transport mechanism, and can occur by either a mediated or a non-mediated process. Non-mediated transport occurs by dissolution of the transporting species into the membrane lipids and subsequent diffusion to the other side, the primary barrier to diffusion being the hydrophobic lipid core of the membrane. In mediated, or facilitated transport, specific proteins within the membrane containing both hydrophobic and hydrophilic regions, increase the permeability of the membrane towards particular molecules and ions. Specific complexes are formed between the transporting protein and the substrate, and conformational changes of the protein are often involved during the transport process. At least three steps are involved in the mediated transport processes; the formation of a complex between the transporter and the substrate; the diffusion across the membrane; and the dissociation of the substrate from the transporter at the other side of the membrane. Channel proteins are so called because they form hydrophilic channels which span the bilayer of the membrane forming an aqueous environment for the diffusion of substrates down the concentration gradient. These proteins do not interact strongly with the translocating substrates and hence their selectivity arises from the size and charge of the substrates.

The transport of one substrate is often coupled to that of another and, in this cases, is described as being either a co-, or a countertransport process. When only one substrate is transported the process is termed uncoupled transport, and transport is initiated by the formation of the substrate:protein complex.

The research into membrane transport processes has been facilitated by the use of artificial vesicles whose size and composition, with respect to both phospholipids and transport proteins, can be strictly controlled to study particular mechanisms. For instance, the involvement of ATPase in the Na^+/K^+ pump was confirmed by observing the activity of the pump when the purified protein was inserted into vesicles *(12)*.

Mammalian transport systems involve both facilitative diffusion systems and active transport to similar extents; many of these processes appear to be coupled to the hydrolysis of ATP or are Na^+ symports.

1.4.1 Free Energy of Transport

The free energy change (ΔG) involved in the diffusion of a substrate, of charge Z, across a membrane, from side 1 where the concentration is C_1 to side 2 where the concentration is C_2, is given by:

$$\Delta G = RT \ln \frac{C_2}{C_1} + ZF\Delta V \qquad (1.1)$$

where R is the gas constant ($8.31 JK^{-1}mol^{-1}$); T is the temperature (K); F is the Faraday ($96.48 kJV^{-1}mol^{-1}$); and ΔV is the trans-membrane potential difference (V). Obviously for uncharged substrates, Z is zero and hence the free energy change for the transport is simply $RT \ln \frac{C_2}{C_1}$.

1.4.2 Passive Transport

In passive transport, the change in free energy is negative. The driving force for these processes is generally the electrochemical gradient across the membrane; the translocating substrate moves from an environment of higher to one of lower

concentration. The rate of transport is dependent on the permeability of the membrane with respect to the substrate.

1.4.3 Active Transport

In active transport, the change in free energy is positive. An active transport mechanism can transport a substrate across a membrane against its electrochemical gradient; the energy required for the process is provided by a chemical reaction. The most ubiquitous transport process in animal cells is the Na^+/K^+ pump, an active system in which the energy is produced by the hydrolysis of ATP by the enzyme Na^+/K^+-ATPase.

1.4.4 Cotransport and Countertransport

Co-, and countertransport occur when the transport of one substrate is coupled to the movement of one or more other substrates, the driving force usually being the electrochemical gradient of one of the substrates. All the substrates must be available for transport to occur, however the molecular mechanisms for the transport of each of the substrates are not necessarily the same. The transport of the substrates can be either simultaneous or sequential, and the stoichiometry of the process is not necessarily one to one. A cotransport, or symport, is a system in which the substrates are carried in the same direction, and a countertransport, or antiport, is one in which the substrates move in opposing directions across the membrane. The membrane protein responsible for the transport is called either a symporter or an antiporter, respectively. In animal cells these systems are mostly driven by the trans-membrane Na^+ gradients which are maintained by the Na^+/K^+ pump. For example, glucose is actively cotransported into cells by the simultaneous entry of Na^+ down its concentration gradient.

1.5 Li^+ in Biological Systems

Li^+ does not normally occur in biological materials and no biological system in humans has been shown to be dependent upon this cation. Since there is no radioisotope of lithium with a convenient half-life, the main methods for the clinical analysis of Li^+ are atomic absorption spectrophotometry (AAS) and flame emission spectrophotometry (FES). More recently, nuclear magnetic resonance spectroscopy (NMR), ion-selective electrodes (ISE) and neutron activation methods have been employed to study Li^+ in biological materials *(13)*. Both AAS and FES are susceptible to interference from other elements present in the sample and, in the case of biological material, the relatively high concentrations of Na^+ and K^+ interfere with the analysis of the lower levels of Li^+, and must be allowed for by the use of appropriate standards.

1.5.1 Distribution of Li^+ *in vivo*

The hydrated Li^+ ion has the largest effective diameter, lowest diffusion coefficient and least lipid solubility of all the alkali metals *(14)*. It might therefore be expected that the movement of this cation may be more limited than that of either Na^+ and K^+ and therefore that the distribution of this cation *in vivo* may be difficult to predict. The atomic and ionic radii of lithium are more similar to those of magnesium, and the hydrated radius and electronegativity are more similar to those of calcium than to those of sodium. Consequently, it may be that the physiological behaviour of Li^+ is more like Mg^{2+} and Ca^{2+} than either Na^+ or K^+ *(15)*.

The concentration of lithium ions, $[Li^+]$, in the blood plasma of patients taking Li^+ is carefully monitored and maintained in the range 0.3 - 1.0mM by adjustment of the dose, the blood samples having been taken 12h after the previous dose. During lithium therapy, Li^+ is widely, and unevenly distributed throughout the body fluids and tissues. In the brain the average $[Li^+]$ was originally reported to be approximately the

same as that in the plasma, whereas in the saliva it is about twice as high and in the cerebrospinal fluid it is much lower *(16)*. However, recent preliminary studies using *in vivo* magnetic resonance techniques on living patients, suggest that the [Li^+] in the brain and muscle are lower than that in the serum *(17)*. Compared to the [Li^+] in serum, studies on animals have shown higher levels in the kidneys, bone *(18)*, and endocrine glands, especially the thyroid *(6)*, and lower levels have been found in the liver *(19, 20)*. The distribution of Li^+ may be due in part to the relative rates of entry and efflux in the different tissues. For instance, the uptake of Li^+ from the blood is rapid into the kidney, is slower into the liver, bone and muscle, and is very slow into brain, and it was concluded that the relatively slow uptake into the brain is due to the low permeability of the blood-brain barrier *(21)*. Lower Li^+ uptake rates into the brain and muscle compared to serum have also been observed using *in vivo* magnetic resonance studies *(22)*. Table 1.1 shows the *post mortem* Li^+ distribution of a male patient who had been on a maintenance dose of 1200mg/day Li_2CO_3 for the treatment of manic depression, for three months prior to his death *(20)*.

The distribution of Li^+ in different regions of the brain is uneven but no particular region appears to accumulate Li^+ to any significant extent *(20,23)*. Table 1.2 shows the result of a *post mortem* examination of the Li^+ distribution in the brains of two patients, both of whom had received 900mg/day Li_2CO_3 for the treatment of mania for only a few days prior to death. The [Li^+] was higher in the pons than in the cerebral white or grey tissue or in cerebellar tissue *(23)*. The distribution of $^6Li^+$ in a section of mouse brain has been imaged by a neutron irradiation technique *(24)*. This clearly shows a variation in Li^+ accumulation, with, for example, higher Li^+ levels in both the hippocampus and hypothalmus, and a lower level in the thalamus.

Table 1.1 The distribution of Li^+ in man *post mortem* (mmol. kg^{-1}) *(20)*

TISSUE	$[Li^+]$
Whole blood*	0.86
Bile*	7.8
Bone	2.54
Cardiac muscle	1.4
Lymphoid tissue	1.3
Thyroid	1.1
Pituitary	0.9
Kidney	0.9
Lung	0.8
Fat	0.7
Spleen	0.7
Alveolar connective tissue	0.6
Liver	0.4
Testis	0.3
Femoral Nerve	0.2

Table 1.2 The distribution of Li^+ in human brain (mmol.kg^{-1})*(23)*

TISSUE	PATIENT 1	PATIENT 2
Serum*	0.25	0.35
Grey Matter	0.15	0.24
White Matter	0.18	0.34
Cerebellum	0.17	0.35
Pons	0.35	0.65

*Values for whole blood, bile and serum are expressed in mM Li^+

1.5.2 Li^+ Transport in Erythrocytes

Studies of Li^+ transport across membranes have predominantly employed erythrocytes since these are readily and ethically available, with individual cells freely flowing in suspension. If the movement of Li^+ across the erythrocyte membrane is purely passive, the ratio of the $[Li^+]$ in erythrocytes to that in plasma (Li^+_{in} /Li^+_{out}) should reach approximately 1.5 at steady-state *in vivo* (from equation 1.1, where ΔV is 10mV for erythrocytes). However, during lithium treatment, the actual $[Li^+]$ in erythrocytes is lower than that in plasma *(25)*, indicating the presence of active transport mechanisms which can extrude Li^+ from erythrocytes. It has been suggested that the concentration of Li^+ in erythrocytes or the erythrocyte:serum concentration ratio may be correlated with the clinical state or the response to Li^+ treatment *(26)*. Additionally, the concentration of Li^+ in the brain correlates with that in erythrocytes better than that in the plasma *(27)*, and some transport processes in erythrocytes are qualitatively similar to those in neurons, for example the Na^+/K^+ pump. Thus, the transport mechanisms for Li^+ operating in erythrocytes have been extensively investigated. However, it should be noted that erythrocytes have an atypical morphology and no nucleus, compared to most cells.

Five processes which can operate as pathways for the movement of Li^+ across the human erythrocyte membrane have been elucidated and characterised, and are depicted in Figure 1.1: a Na^+-Li^+ countertransport, the Na^+/K^+ pump, a 'leak', an anion exchange and a Na^+-K^+ cotransport. These pathways have been characterised *in vitro* by manipulation of the composition of, and by the use of known transport inhibitors in the incubating media of suspensions of erythrocytes. The relative contribution of each of these processes to the overall fluxes of Li^+, both the influx and the efflux, is greatly influenced by the composition and pH of the incubating medium, in particular with respect to the $[Na^+]$ and $[K^+]$. Under artificial conditions of ion concentration, temperature and pH, Li^+ can be transported into, or out of eythrocytes by any of these mechanisms. However, under pseudo-physiological conditions and at

extracellular [Li^+] typically found in the plasma during lithium therapy (0.3 - 1.0mM), the transport of Li^+ by many of these processes is inhibited. For example, the uptake of Li^+ into cells by the Na^+/K^+ pump is inhibited by physiological concentrations of extracellular K^+ *(28)*. It is generally agreed that under physiological conditions and, by inference, *in vivo* during lithium therapy, the uptake of Li^+ into erythrocytes is predominantly by the two passive diffusion processes, the 'leak' and the anion exchange pathway, and that Li^+ is actively transported out of the erythrocyte by the Na^+-Li^+ countertransport route. The five Li^+ transport pathways are discussed in detail below.

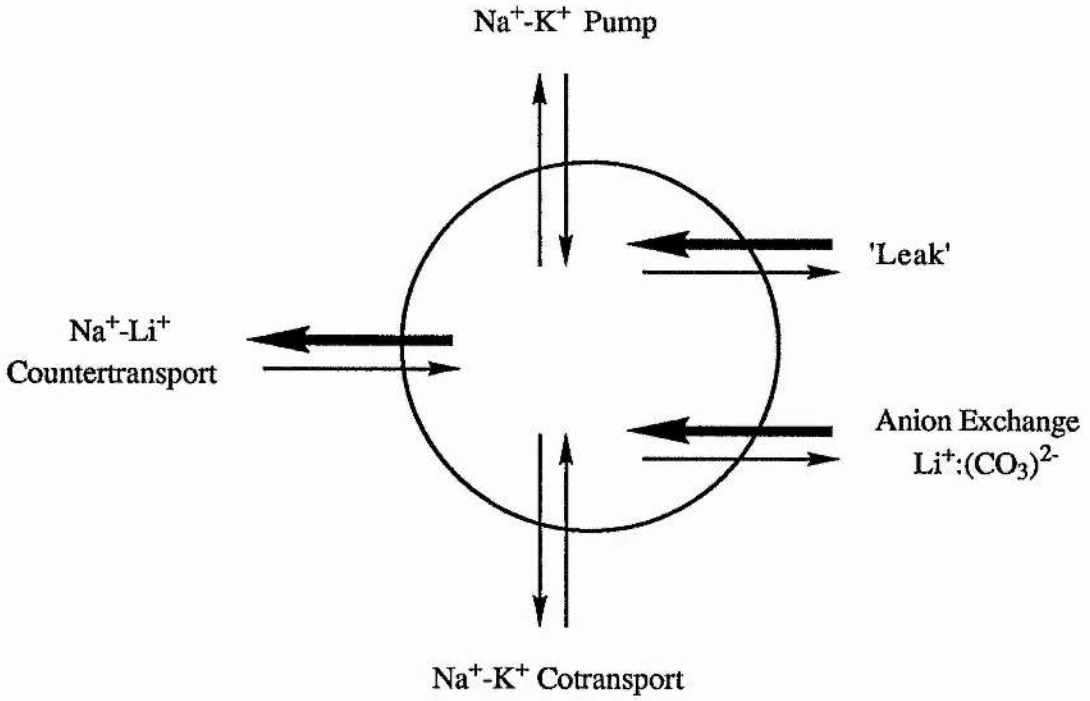

Figure 1.1 Transport pathways for Li^+ in human erythrocytes

(Li^+ can be transported by any of the pathways shown; the bold arrows indicate mechanisms operating under physiological conditions)

The 'leak' is a passive diffusion pathway which transports Li^+ into erythrocytes down its concentration gradient. The rate of uptake increases linearly with increasing extracellular [Li^+] and for a 1mM difference in [Li^+] the magnitude of the leak is 0.016 mmol. Li^+(ml cells)$^{-1}h^{-1}$ *(29)*. This mechanism is inhibited partly by phloretin and is also inhibited by dipyridamole which, interestingly, inhibits the uptake of Na^+ and K^+ by leak pathways in rat erythrocytes to a similar extent, suggesting the pathways may have the same mechanism *(30)*.

The passive transport of Li^+ is enhanced in the presence of the bicarbonate anion, HCO_3^- *(31)*, and this effect is approximately four times greater than that of the similar transport of Na^+ *(32)*. In this process, Li^+ forms an ion pair with the carbonate ion CO_3^{2-}, which is in equilibrium with HCO_3^- in solution and the resulting single-negatively charged species, $(Li{:}CO_3)^-$, provides a substrate which can then cross the erythrocyte membrane by the anion exchange mechanism; the transporter for this pathway is part of the band 3 protein which spans the erythrocyte membrane *(33)*. This countertransporter mediates the movement of monovalent anions such as halides, HCO_3^-, NO_3^-, phosphate and sulphate, in a one for one exchange. The mechanism for Li^+ transport was characterized by its inhibition by compounds known to inhibit the anion exchange system in erythrocytes for example: dipyridamole, SITS, phloretin, phlorizin, phenylbutazone, ethacrynic acid and furosemide *(29,30)*. The rate of transport is linearly dependent on both the extracellular [Li^+] and the [HCO_3^-] and is very similar to that of the leak, being 0.019 mmol. Li^+(ml cells)$^{-1}h^{-1}$ for a 1mM difference in [Li^+] and an extracellular [HCO_3^-] of 24mM *(29)*.

The Li^+-Na^+ countertransport is an active pathway which can transport Li^+ in either direction depending on the distribution of Li^+ and Na^+ on the two sides of the membrane *(34,35)*. The stoichiometry of the process is one to one and can involve homo-, or heteronuclear exchange; for every Li^+ and/or Na^+ transported in one direction, one Na^+ and/or Li^+ is transported in the opposite direction across the membrane. The movement of Li^+ is dependent upon the presence of either Na^+ or Li^+

on the *trans* side, and is inhibited by Na^+ on the *cis* side of the membrane such that Li^+ can be transported into the erythrocyte only in the presence of intracellular Na^+ or Li^+, and *vice versa.* The mechanism for this transport is believed to be the same as the Na^+-Na^+ exchange system found in erythrocytes, as the two share many characteristics: both involve one for one exchange of the cation *(36)*, both are insensitive to ouabain *(34,35)* and are inhibited by phloretin, phlorobenzophenone and N-ethylmaleimide *(36)*; both observe Michaelis-Menten kinetics *(36,37)*; and the transport rates of the two processes are similar. The system has a much higher affinity for Li^+ than Na^+ and, apparently, no affinity for any other cations *(35)*. The respective values of K_m for Li^+ and Na^+ are 0.5mM and 9.0mM at the internal, and 1.5mM and 25.0mM at the external side of the erythrocyte membrane *(37)*, where K_m is the concentration of cation required to give half-maximum activation of the transport system. Thus the affinities of this transport system for both cations is approximately three times greater at the internal than the external side of the erythrocyte membrane.

Under physiological conditions this process transports Li^+ out of erythrocytes against its concentration gradient and is thus responsible for maintaining the intracellular [Li^+] lower than that in the plasma *in vivo*. The driving force is the Na^+ gradient across the erythrocyte membrane ([Na^+] extracellular is approximately 150mM and intracellular is approximately 5-10mM); this process is not directly dependent on ATP *(35)*.

The Na^+/K^+ pump is the most ubiquitous ion transport system in animal cells, creating and maintaining the Na^+ and K^+ gradients across membranes and also maintaining the osmotic equilibrium. The driving force for the pump is the energy produced during the hydrolysis of ATP by the enzyme Na^+/K^+-ATPase, a protein which spans the membranes of cells. For each molecule of ATP hydrolysed to ADP and P_i, $2K^+$ are transported into, and $3Na^+$ are transported out of the cell. Ouabain, a cardiac glycoside, is a potent inhibitor of Na^+/K^+-ATPase, competing with K^+ at the external pump sites: the pump is also inhibited by oligomycin and ethacrynic acid *(28)*.

Li^+ can be transported by this route either into, or out of, erythrocytes only in the absence of extracellular K^+, or intracellular Na^+ respectively. Extracellular K^+ and, to a lesser extent Na^+, inhibit Li^+ uptake in a competitive manner, and intracellular Na^+ and/or K^+ completely inhibit the transport of Li^+ by this route *(28,38)*. The external site of the Na^+/K^+ pump has a lower affinity for Li^+ than K^+ and the internal site has a much lower affinity for Li^+ than Na^+. Under physiological conditions of $[K^+]$ and $[Na^+]$ and at the low $[Li^+]$ found in blood plasma *in vivo* during therapy, the movement of Li^+ through the erythrocyte membrane mediated by the Na^+/K^+ pump is negligible

In the Na^+-K^+ cotransport system, $1Na^+$, $1K^+$ and $2Cl^-$ are transported together in the same direction across the cell membrane, and the direction of movement can be in either direction *(39)*. This process is blocked by 'loop' diuretics such as furosemide, bumetanide and piretanide, and is insensitive to ouabain. The movement of Li^+ can also be mediated by this cotransport by replacing the Na^+ *(37,40)*.

1.5.4 Variability in Li^+ Transport

The ratio, Li^+_{in}/Li^+_{out}, in human erythrocytes ranges from 0.2-0.9, illustrating a large interindividual variability *(41)*. However, this ratio is relatively constant over long periods of time for individuals and there is evidence that this phenomena is under genetic control *(42)*. During the first days of Li^+-treatment, the ratio increases gradually until a steady-state value is attained *(25)*. Higher ratios have been reported in patients with affective illnesses compared to healthy subjects *(43,44)* and in females compared to males *(45)*. There have been attempts to correlate the higher Li^+ ratio to a better clinical response of patients to Li^+ therapy *(46,47)*.

Since the steady-state Li^+ ratio depends upon the balance between the efflux and influx processes, the countertransport system, and the leak and the anion exchange

routes respectively, a number of groups have investigated these variations in Li^+ ratio by looking for differences in the Li^+ transport processes. These studies were performed with erythrocytes from both normal controls and psychiatric patients. Neither of the passive transport routes, the leak and the bicarbonate pathway appear to vary amongst healthy controls *(36)*. However, significant variability amongst individuals was found in *in vitro* studies of the transport of Li^+ by the Na^+-Li^+ countertransport mechanism *(36,37)*. Hence the variation in the steady state Li^+ ratios is believed to be due primarily to differences in the Na^+-Li^+ countertransport mechanism; a higher Li^+ ratio arising almost exclusively from a lower activity of this mechanism *(36,48)*. Significant individual variation in the maximal transport activity, V_{max}, has been reported by a number of groups *(36,38)*. Sarkadi *(37)* reported a range of 0.1- 0.37 mmol.Li^+(l cells)$^{-1}h^{-1}$. Interestingly, this transport process appears to show little variability over time within an individual *(36,49)*, indicating that the magnitude of this transport process is a characteristic property of the erythrocyte membranes of an individual and thus suggesting the involvement of a genetic component *(42)*.

Differences in the Na^+-Li^+ countertransport process have also been observed in the erythrocytes of psychiatric patients *(50,51,52)*. Pandey reported that this process was generally slower in bipolar patients than in normal controls, leading to higher Li^+ ratios *(51)*. There was a great deal of variability amongst the patients and many had Li^+ ratios in the 'normal' range.

A decrease in the efficiency of the Na^+-Li^+ countertransport also appears to be a direct result of Li^+ administration *(44,49)*; a 50% inhibition in efflux of Li^+ from the erythrocytes of people on Li^+ therapy has been reported *(44)*. This reduction in the transport rate is not an immediate effect of commencing Li^+ treatment; the decrease in activity has been observed 2-4 days after commencing therapy and the maximum reduction appears within 7 days. The rate of transport returns to normal soon after the Li^+ therapy is ceased *(53)*.

This Li^+-induced reduction in the transport rate appears to be distinct from the interindividual variation, as the two show different kinetics *(49)*: In the Li^+-induced change, K_m increases threefold but V_{max} does not change, whereas in the interindividual case, it is V_{max} which varies *(53)*. Ehrlich suggests that the protein responsible for this transport mechanism may be modified in a way which involves no change in the number of these proteins available for transport per cell, thus explaining the lack of effect on the V_{max} *(53)*.

One interesting study reported that the *in vitro* exposure of erythrocytes to Li^+ caused an inhibition of the Na^+-Li^+ countertransport mechanism similar to that seen *in vivo (54)*. It was proposed that Li^+ might alter the lipid composition of the erythrocyte membrane, for example by altering the rate of choline production from phospholipid, or that Li^+ might alter the transport process of some other solute, the resulting altered concentration of which might affect the countertransport mechanism.

Variations in the Na^+-Li^+ transport mechanism in other mammalian species namely: sheep, beef, horses and rabbits have also been observed *(55)*. Here, as in the cases of the interindividual differences, the maximal transport activity, V_{max}, is altered, being lowest in humans and significantly higher in the others. Interestingly, there was no corresponding Na^+-Li^+ countertransport process found in rat erythrocytes *(55)*; Li^+ transport *via* the 'leak' route is approximately 3-fold greater in rat erythrocytes than in humans *(30)*.

1.5.5 Li^+ Transport in Other Cells

Erythrocytes share transport mechanisms with many other cells although surprisingly the Li^+ transport pathways in other cell types has received little attention and the available data is not very informative. Most work shows that, as in the case of erythrocytes, the intracellular [Li^+] is lower than the extracellular and is below that

expected for passive diffusion of the cation across the cell membrane, although there some reports which contradict this. The transport mechanisms are not well understood in any of these systems and have not been fully characterised. As with erythrocytes, the composition of the incubating medium, particularly with respect to [Na^+] and [K^+], can significantly affect the transport behaviour of Li^+. The Na^+/K^+ pump can transport Li^+ in most cell systems but it is considerably inhibited in physiological media just as in erythrocytes. Many tissues, including brain and muscle exhibit a similar Na^+-Na^+ exchange system to that observed in human erythrocytes *(29)*, however the majority of cells lack the anion transporter present in erythrocytes. The intestinal absorption of Li^+ following oral administration occurs primarily in the small intestine *(56)*. Transport into the bloodstream is a passive process via a paracellular route, with very little Li^+ accumulating in the intestinal cells *(56,57,58)*. One significant feature of excitable cells, such as nerves, is the presence of the voltage-dependent Na^+ channel which is not found in erythrocytes and in non-excitable cells in general. The permeability of this transporter to Li^+ is almost the same as that to Na^+ (Table 1.3) and, as with Na^+, the cell membrane may become dramatically more permeable to Li^+ in the excited state. Veratridine, an alkaloid which activates these Na^+-channels, significantly increases the initial rate and the extent of Li^+ uptake in mouse neuroblastoma cells *(59)* and in mouse neuroblastoma x glioma hybrid cells *(60)*.

Table 1.3 Relative permeabilities of the Na^+-channel and the K^+-channel in axon membranes *(61)*

Cation	Na^+-channel	K^+-channel
Li^+	0.93	<0.01
Na^+	1.00	<0.01
K^+	0.09	1.00
Rb^+	<0.01	0.91
Cs^+	<0.01	<0.08

The reported studies on cultured cells emphasise the variability in the intracellular Li^+ concentrations which might be expected if these result from the integration of several transport pathways in each cell type. Expressed as a ratio of Li^+_{in}/ Li^+_{out}, values of 5.6, 1.5, 0.3 and 0.7 have been reported for rat glioma cells *(62)*, mouse neuroblastoma cells *(59)*, mouse neuroblastoma x glioma cells *(60,63)* and primary chick embryo brain containing mixed populations of neuronal and glial cells *(64,65)*, respectively. In general, these cells have faster transport rates than those observed for erythrocytes since the intracellular Li^+ achieves steady-state within 20-60 minutes, compared to several hours for erythrocytes. The involvement of voltage-dependent Na^+-channels and a Na^+/Li^+ countertransport mechanism, similar to that operating in erythrocytes, has been reported for neuroblastoma x glioma cells, and the Na^+/K^+ pump appears to have a role in Li^+ transport in a human neuroblastoma cell line *(66)*.

1.6 Nmr of Alkali Metals in Biological Systems

The chemical shift of all of the alkali metal ions in aqueous systems, except Cs^+, is virtually independent of the environment of the cation. Therefore, in biological systems where the cations can be distributed among several environments, for example intra-, and extracellular, in perfusate or in tissue, the nmr spectrum of a particular cation generally only contains a single peak corresponding to the overlapping signals from each environment. The resonance from a cation in a specific environment can be distinguished from those of the cation in other regions by the addition of a 'contrast' reagent to that environment.

1.6.1 Contrast Reagents

There are two types of contrast reagent: shift reagents, which produce a chemical shift of the resonance from the cation in the same environment; and relaxation reagents which result in a significant increase in the line-width of the resonance from the cation in the same environment until the signal is no longer visible. The use of contrast reagents in the nmr spectroscopy of the alkali metal ions in biological systems results in the resolution of signals from cations in distinct environments, thus allowing the behaviour of the cations in these pools to be investigated independently and the transport of the cations to be studied by this non-invasive methodology. In order to be effective in these studies, the contrast reagent must be stable and soluble in physiological conditions, it must be non-toxic to the cells or organisms, it must not penetrate or interact with the cell membrane, and it must not bind strongly with the cation to the extent that the transport behaviour and trans-membrane gradient of the cation are disturbed.

In this study, a paramagnetic shift reagent has been employed to distinguish the intra-, and extracellular Li^+ resonances in the nmr spectra.

1.6.2 Shift Reagents

A number of anionic complexes of the paramagnetic lanthanides, Dy^{3+} and Tb^{3+}, have been investigated as potential chemical shift reagents for the alkali metal cations, as these lanthanides have been shown to produce relatively large shifts *(67)*. In general, larger shifts are obtained using complexes with highly negative charges; the structures of those discussed here are shown in Figure 1.2.

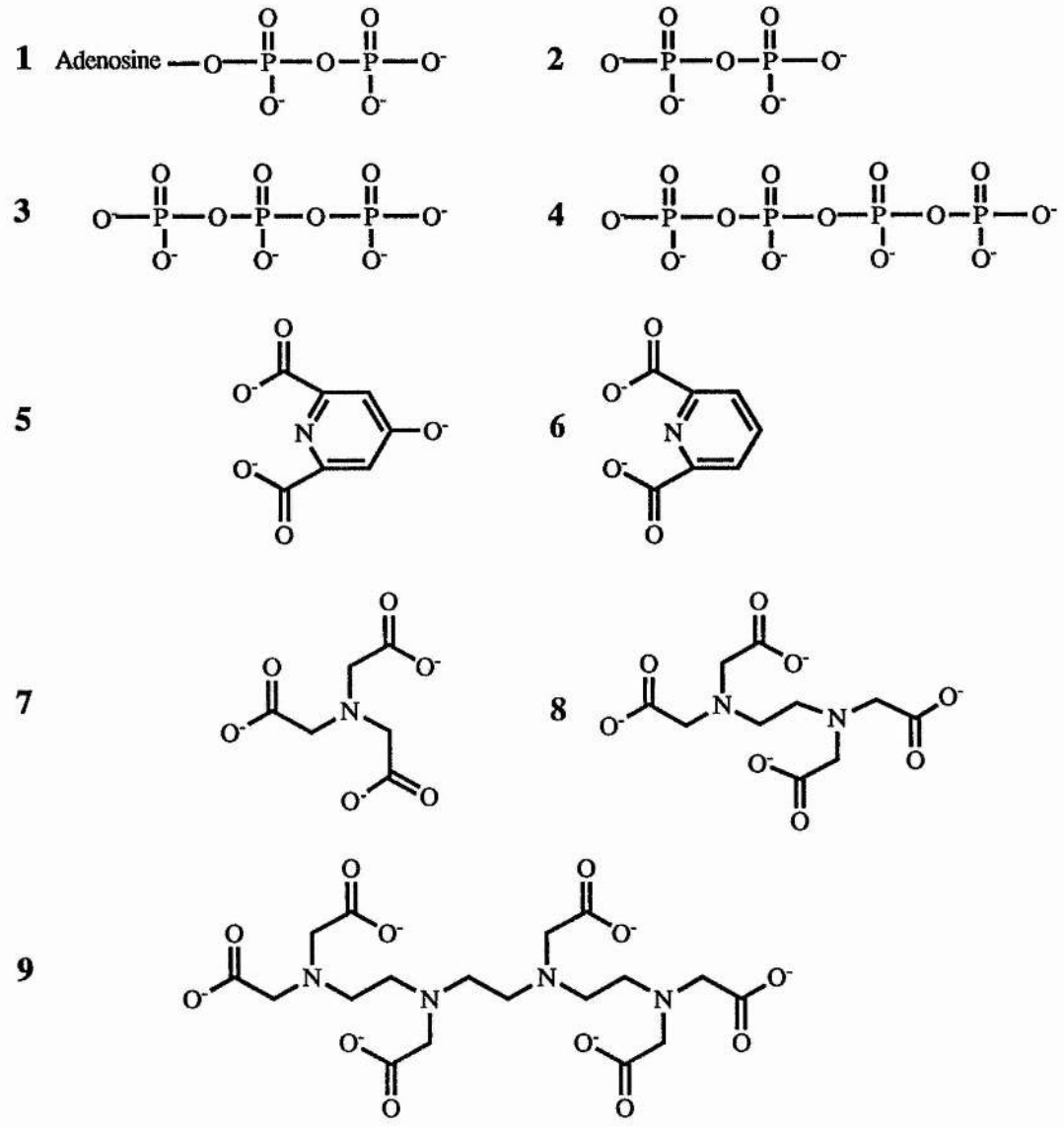

Figure 1.2 Structure of ligands of the lanthanide shift reagents

1 ADP^{3-}, adenosine diphosphate; **2** $P_2O_7^{4-}$, pyrophosphate;
3 $P_3O_{10}^{5-}$, tripolyphosphate; **4** $P_4O_{13}^{6-}$, tetrapolyphosphate;
5 CA^{3-}, chelidamate, 4-oxypyridine-2,6-dicarboxylate; **6** DPA^{2-}, dipicolinate, pyridine-2,6-dicarboxylate;
7 NTA^{3-}, nitrilotriacetate; **8** $EDTA^{4-}$, ethylenediaminetetraacetate;
9 $TTHA^{6-}$, triethylenetetraminehexaacetate)

Both of the higher negatively-charged complexes, $Dy(NTA)_2^{3-}$ and $Dy(DPA)_3^{3-}$, produce larger upfield shifts of the ^{23}Na resonances than the single-negatively charged complex, $Dy(EDTA)^-$ *(68)*. $Dy(CA)_3^{6-}$ produces significant upfield shifts of the ^{23}Na, ^{39}K, ^{87}Rb and ^{25}Mg resonances, whereas $Tm(CA)_3^{6-}$ produces a downfield shift of the ^{23}Na resonance *(69)*. In an investigation of various polyphosphate ligands with Dy^{3+}, the highly negatively-charged 1:2 complex between Dy^{3+} and tripolyphosphate, $Dy(P_3O_{10})_2^{7-}$, was found to be an extremely effective shift reagent for ^{23}Na, producing larger shifts than the Dy^{3+} complexes of either ADP, pyrophosphate or tetrapolyphosphate *(70)*. Although the shifts produced by $Dy(P_3O_{10})_2^{7-}$ and $Tm(P_3O_{10})_2^{7-}$ are the largest, they are strongly pH-dependent and are significantly decreased by the presence of either Ca^{2+} or Mg^{2+}, which compete both with the monovalent cation for the shift reagent, and with the lanthanide ion for the ligand *(71,72)*. In comparison, the complexes $Dy(TTHA)^{3-}$ and $Tm(TTHA)^{3-}$ are also effective as shift reagents albeit to a lesser extent than the complexes of $P_3O_{10}^{5-}$; the shifts produced are downfield but are much less sensitive to pH and to the presence of divalent cations *(71,72)*.

1.6.3 Shift Reagents for the Alkali Metals in Biological Systems

In the first reported biological application of the use of these reagents, the ^{23}Na- nmr spectra of samples of gently packed erythrocytes showed two well-resolved resonances when maintained in a medium containing 140mM Na^+, 10mM K^+ and concentrations of $Dy(P_3O_{10})_2^{7-}$ of 2mM and 5mM *(70)*. The magnitude of the upfield shift of the resonance from the extracellular Na^+, (Na^+_{out}), increased with increasing concentration of the shift reagent, and only a small amount of line-broadening was induced by the shift reagent. The resonance from the intracellular Na^+, (Na^+_{in}), was unshifted from the resonance of Na^+ in the spectrum of the cell-free medium containing no shift reagent, indicating that the $Dy(P_3O_{10})_2^{7-}$ had not penetrated the cell

membrane. The application of this shift reagent in the study of Na^+ in different environments in frog skeletal muscle was also demonstrated *(70)*. Similarly, $Dy(P_3O_{10})_2^{7-}$ was employed to shift the resonance from $^{39}K^+_{out}$ in samples of human erythrocytes *(73)*, however $Tb(P_3O_{10})_2^{7-}$ was shown to be a more effective shift reagent for K^+ producing a slightly larger chemical shift with a correspondingly smaller induced line-broadening *(74)*.

^{23}Na-nmr studies were carried out on samples of human erythrocytes using $Dy(P_3O_{10})_2^{7-}$ and $Tm(TTHA)^{3-}$ which shifted the resonance from the Na^+_{out} upfield, and also $Dy(TTHA)^{3-}$ and $Tm(P_3O_{10})_2^{7-}$ which shifted this resonance downfield *(75)*. The Tm^{3+} complexes producing substantially lower shifts than the corresponding Dy^{3+} complexes. Quantification of both the intra-, and the extracellular $[Na^+]$ was achieved by the construction of a calibration curve from the integrals of the Na^+ resonances in the spectra of NaCl standards. The results were within ± 5% of the values determined by flame emission spectrophotometry indicating the absence of nmr invisibility for Na^+ in this system.

Similarly, $Dy(P_3O_{10})_2^{7-}$ and $Dy(TTHA)^{3-}$ were investigated as potential shift reagents for Li^+ in erythrocyte suspensions and, as expected from the results on Na^+, $Dy(P_3O_{10})_2^{7-}$ produced the larger separation of the two resonances, but the shifts produced by $Dy(TTHA)^{3-}$ were virtually independent of pH and were less dependent upon $[Ca^{2+}]$ and $[Mg^{2+}]$ *(76)*. The use of these shift reagents in ^{7}Li-nmr spectroscopy is described in more detail in Chapter 3 of this thesis.

No adverse effect on either the energy metabolism or the morphology of erythrocytes was observed due to either of the shift reagents $Dy(P_3O_{10})_2^{7-}$ and $Dy(TTHA)^{3-}$, following investigation by ^{31}P-nmr and by scanning electron microscopy (SEM) *(76,77)*. The shape and size of the erythrocytes remained virtually unchanged in the presence of the relatively low concentrations of $Dy(P_3O_{10})_2^{7-}$, $Dy(TTHA)^{3-}$, $Tm(P_3O_{10})_2^{7-}$ and $Dy(PO_2(CH_2PO_3)_2)^{5-}$ typically used in the nmr

experiments. However, as the concentrations increased above about 10mM an increasing amount of shrinkage occurred in the cells *(77)*. Additionally with the exception of $Dy(TTHA)^{3-}$, these shift reagents produced significant changes in the membrane potential of the erythrocytes, and therefore it was suggested that these agents should be employed with caution *(77)*.

1.6.4 Structure of $Dy(P_3O_{10})_2^{7-}$

In this thesis, $Dy(P_3O_{10})_2^{7-}$ has been employed to distinguish between the intra-, and extracellular Li^+ resonances in suspensions of erythrocytes and cultured cells. The proposed structure of the 1:2 complex between Dy^{3+} and $P_3O_{10}^{5-}$ is shown in Figure 1.3 with a coordination number of 9 for the metal centre *(78)*. $P_3O_{10}^{5-}$ acts as a tetradentate ligand in which one of the PO_3 groups is bidentately coordinated, the other PO_3 group and the PO_2 group are monodentately coordinated, and one molecule of H_2O is coordinated in the first coordination sphere *(79)*. The interconversion of the coordination of the two PO_3 groups is rapid. This model predicts that there are no specific binding sites for the alkali metal cations, but that up to seven cations can bind in the second coordination sphere to neutralise the negative charge. At pH 7.5 several protonated forms of the complex exist: $Dy(P_3O_{10})_2^{7-}$, $Dy(P_3O_{10})(P_3O_9OH)^{6-}$ and $Dy(P_3O_9OH)_2^{5-}$ *(80)*. As the pH is lowered an increasing amount of protonation occurs and as the negative charge on the complex decreases, the interaction with the cation is weaker and the resulting chemical shift of the cation in the nmr spectrum is reduced *(72)*. The shifts produced by $Dy(P_3O_{10})_2^{7-}$ in the nmr spectra are also reduced by the presence of other cations which compete for the shift reagent and the relative order of competition is: $Ca^{2+} \geq Mg^{2+} > Li^+ > Na^+ \geq K^+$. All these cations compete for the binding sites in the second coordination sphere in a reaction of the type:

$$xNa^{+}:Dy(P_3O_{10})_2^{7-} + M^{n+} \rightleftharpoons yNa^{+}M^{n+}:Dy(P_3O_{10})_2^{7-} + nNa^{+}$$

where, $M^{n+} = Li^{+}, Na^{+}, K^{+}, Mg^{2+}, Ca^{2+}$; $1 \leq x \leq 7$; $n=1, 2$

whereas the divalent cations also compete with the Dy^{3+} for the ligand in a reaction of the type:

$$Dy(P_3O_{10})_2^{7-} + M^{2+} \rightleftharpoons M(P_3O_{10})^{3-} + Dy(P_3O_{10})^{2-}$$

where, $M^{2+} = Ca^{2+}$ or Mg^{2+}

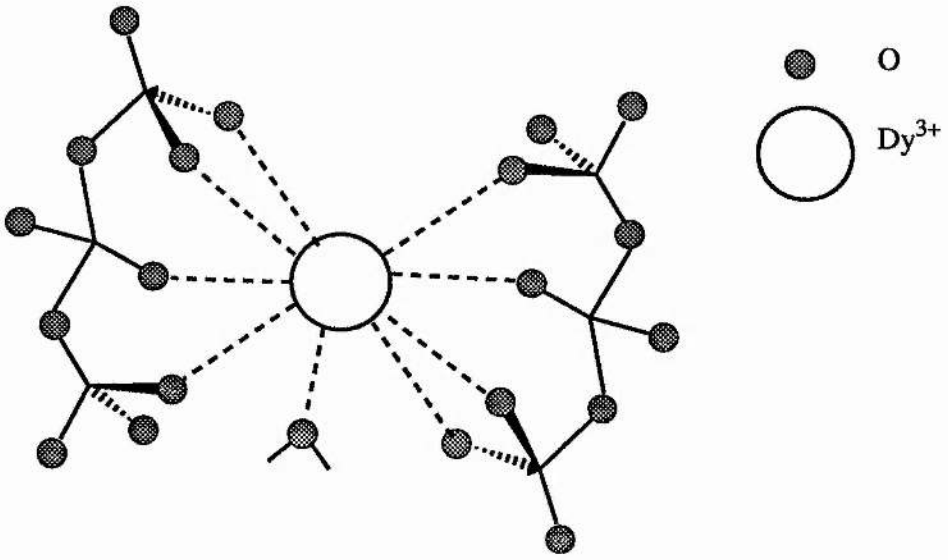

FIGURE 1.3 Structure of $Dy(P3O10)2^{7-}$

1.7 References

1 Cade, J.F.J. (1949), *Med. J. Aus.*, **36**, 349-352.

2 Hanlon, L.W., Romaine, M., Gilroy, F.J. and Dietrick,.J.E. (1949), *J. Am. Med. Assoc.*, **139**, 688-692.

3 Schou, M. (1988), in *Lithium: Pharmacology and Psychiatric Use*, Birch, N.J. (ed.), IRL Press, Oxford, chapter 1.

4 Phillips, J.D. (1991), in *Lithium and the Cell*, Birch N.J. (ed.), Acad. Press, London, chapter 17.

5 Schou, M. (1991), in *Lithium and the Cell*, Birch N.J. (ed.), Acad. Press, London, chapter 1

6 Berens, S.C. and Wolff, J. (1975), in *Lithium Research and Therapy*, Johnson, F.N. (ed.), Academic Press, London, chapter 27.

7 Weinstein, M.R. and Goldfield, M.D. (1975), in *Lithium Research and Therapy*, Johnson, F.N. (ed.), Academic Press, London.

8 Geisler, A. and Mork, A. (1990) in *Lithium and Cell Physiology*, Bach, R.O. and Gallicchio, V.S. (eds), Springer-Verlag, N.Y., chapter 10.

9 Horrobin, D.F. (1990) in *Lithium and Cell Physiology*, Bach, R.O. and Gallicchio, V.S. (eds), Springer-Verlag, N.Y., chapter 11.

10 Gallicchio, V.S (1990) in *Lithium and Cell Physiology*, Bach, R.O. and Gallicchio, V.S. (eds), Springer-Verlag, N.Y., chapter 6.

11 Birch, N.J., Hughes, M.S., Thomas, G.M.H. and Partridge, S. (1986), *Mag. Bull.*, **8**, 145-147.

12 Stahl,W.L. (1986), *Neurochem. Int.* ,**8**, 449-476.

13 Thellier, M. and Wissocq, J.C. (1991) in *Lithium and the Cell*, Birch N.J. (ed.), Acad. Press, London, chapter 4.

14 Cotton, F.A. and Wilkinson, G. (eds), (1980), in *Advanced Inorganic Chemistry*, John Wiley and Sons, N.Y., chapter 7.

15 Birch, N.J. (1973), *Biol. Psychiat.*, **7**, 269-272.

16 Schou, M.(1976), *Ann. Rev. Pharmacol. Toxicol.*, **16**, 231-253.

17 Gyulai, L., Wicklund, S., Greenstein, R., Bauer, M.S., Ciccione, P., Whybrow, P.C., Zimmerman, J., Kovachich, G. and Alves, W. (1991), *Biol. Psychiat.*, **29**, 1161-1170.

18 Birch, N.J. (1974), *Clin. Sci. Mol. Med.*, **46**, 409-413.

19 Birch, N.J. and Hullin, R.P (1972), *Life Sci.*, **11**, 1095-1099.

20 Spirtes, M.A. (1976), *Pharmacol. Biochem. Behaviour.*, **5**, 143-147.

21 Schou, M. (1958), *Acta Pharmacol. Toxicol.*, **15**, 115-124.

22 Renshaw, P.F. and Wicklund, S. (1988), *Biol. Psychiat.*, **23**, 465-475.

23 Francis, R.I. and Trail, M.A. (1970), *Lancet*, 523-524.

24 Thellier, M., Wissocq, J.C. and Heurteaux, C. (1980), *Nature*, **283**, 299-302.

25 Maggs, R. (1963), *Br. J. Psychiat.*, **109**, 56-65.

26 Elizur, A. et al (1972), *Clin. Pharmacol. Ther.*, **13**, 947-952.

27 Frazer, A., Mendels, J., Sekunda, S.K. and Bianchi, C.P. (1973), *J. Psychiat. Res.*, **10**, 1-8.

28 Duhm, J. and Becker, B.F. (1977), *Pflugers Arch.*, **367**, 211-219.

29 Duhm, J. and Becker, B.F. (1978), in *The Red Cell*, Brewer, G. (ed.), Alan R. Liss Inc., N.Y., 551-570.

30 Duhm, J. (1982), in *Basic Mechanisms in the Action of Lithium*, Emrich H.M., Aldenhoff, J.B. and Lux, H.D. (eds), Excerpta Medica, Amsterdam, chapter 1.

31 Wieth, J.O. (1970), *Acta. Physiol. Scand.*, **79**, 76-87.

32 Wieth, J.O. and Funder, J. (1965), *Scand. J. Clin. Invest.*, **17**, 399-400.

33 Steck, T.L. (1974), *J. Cell Biol.*, **62**, 1-19.

34 Haas, M., Schooler, J. and Tosteson, D.C. (1975), *Nature*, **258**, 425-427.

35 Duhm, J., Eisenreid, F., Becker, B.F. and Greil, W. (1976), *Pflugers Arch.*, **364**, 147-155.

36 Duhm, J. and Becker, B.F. (1977), *Pflugers Arch.*, **370**, 211-219.

37 Sarkadi, B., Allimoff, J.K., Gunn, R.B. and Tosteson, D.C. (1978), *J. Gen. Physiol.*, **72**, 249-2

38 Pandey, G.N., Sarkadi, B. Haas, M. Gunn, R.B., Davis, J.M. and Tosteson, D.C. (1978), *J. Gen. Physiol.*, **72**, 233-247.

39 Wiley, J.S. and Cooper, R.A. (1974), *J. Clin. Invest.*, **53**, 745-755.

40 Canessa, M. Bise, I., Adragna, N. and Tosteson, D. (1982), *J. Gen. Physiol.*, **80**, 149-168.

41 Rybakowski, J.K. (1990), *Lithium*, **1**, 75-85.

42 Dorus, E., Pandey, G.N. and Davis, J.M. (1975), *Arch. Gen. Psychiat.*, **32**, 1097-1102.

43 Lyttkens, L., Soderberg, U. and Wetterberg, L. (1973), *Lancet*, **i**, 40.

44 Rybakowski, J.K., Frazer, A., Mendels, J. and Ramsey, T.A. (1978), *Commun. Psychopharmacol.*, **2**, 99-104.

45 Rybakowski, J.K. and Strzyzewski, W. (1976), *Lancet*, **i**, 1408-1409.

46 Mendels, J. and Frazer, A. (1973), *J. Psychiat. Res.*, **10**, 9-16.

47 Mendels, J., Frazer, A., Baron, J. (1976), *Lancet*, **i**, 966.

48 Greil, W., Eisenried, F., Becker, B.F. and Duhm, J. (1977), *Psychopharmacol.*, **53**, 19-26.

49 Ehrlich, B.E., Diamond, J.M., Kaye, W., Ornitz, E.M. and Gosenfeld, L. (1979), *Am. J. Psychiat.*, **136**, 1477-1478.

50 Ostrow, D.G., Pandey, G.N., Davis, J.M., Hurt, S.W. and Tosteson, D.C. (1978), *Am. J. Psychiat.*, **135**, 1070-1078.

51 Pandey, G.N., Dorus, E., Casper, R.C., Janicek, P. and Davis, J.M. (1984), *Prog. Neuropsychopharmacol. Biol. Psychiat.*, **8**, 547-555.

52 Rybakowski, J.K. and Lehmann, W. (1991), *Biol. Psychiat.*, **29**, 340-346.

53 Ehrlich, B.E. and Diamond, J.M. (1981), *Biochem. Pharmacol.*, **30**, 2539-2543.

54 Ehrlich, B.E., Diamond, J.M., Fry, V. and Meier, K. (1983), *J. Memb. Biol.*, **75**, 233-240.

55 Duhm, J. and Becker, B.F. (1979), *J. Memb. Biol.*, **51**, 263-286.

56 Diamond, J.M., Ehrlich, B.E., Morawski, S.G., Santa Ana, C.A. and Fordtran, J.S. (1983), *J. Memb. Biol.*, **72**, 153-159.

57 Phillips, J.D., Davie, R.J., Kmiot, W.A., Poxon, V.A., Keighley, M.R.B. and Birch, N.J. (1988), *Br. J. Pharmacol.* **96**, 253P.

58 Phillips, J.D., Davie, R.J., and Birch, N.J. (1988), *Br. J. Pharmacol.* **95**, 836P.

59 Gorkin, R.A. and Richelson, E. (1981), *Neuropharmacol.*, **20**, 791-801.

60 Reiser, G., Scholz, F. and Hamprecht, B. (1982), *J. Neurochem.*, **39**, 228-234.

61 Stryer, L. (ed.) (1988), in *Biochemistry*, Freeman, N.Y., p1012.

62 Gorkin, R.A. and Richelson, E. (1979), *Brain Res.*, **171**, 365-368.

63 Reiser, G. and Duhm, J. (1982), *Brain Res.*, **252**, 247-258.

64 Szentistvanyi, I., Janka, Z., Rimanoczy, A., Latzkovits, L. and Juhasz, A. (1980), *Cell. Mol. Biol.*, **25**, 315-321.

65 Janka, Z., Szentistvanyi, I., Rimanoczy, A. and Juhasz, A. (1980), *Psychopharmacol.*, **71**, 159-163.

66 Saneto, R.P. and Perez-Polo, J.R. (1982), *J. Neurosci. Res.* , **7**, 413-41.

67 Bryden, C.C. and Reilly, C.N. (1981), *Anal. Chem.*, **81**, 1418-1425.

68 Pike, M.M. and Springer, C.S. (1982), *J. Mag. Res.*, **46**, 348-353.

69 Pike, M.M., Yarmush, D.M., Balschi, J.S., Lenkinsk, R.E. and Springer, C.S. (1983), *Inorg. Chem.*, **22**, 2388-2392.

70 Gupta, R.K. and Gupta, P. (1982), *J. Mag. Res.*, **47**, 344-350.

71 Chu, S.C., Pike, M.M., Fossel, E.T., Smith, T.W., Balschi, J.A. and Springer, C.S. (1984), *J. Mag. Res.*, **56**. 33-47.

72 Ramasamy, R., Espanol, M.C., Long, K.M., Mota de Freitas, D. and Geraldes, C.F.G.C. (1989), *Inorg. Chim. Acta*, **163**, 41-52.

73 Brophy, P.J., Hayer, M.K. and Riddell, F.G. (1983), *Biochem. J.*, **210**, 961-963.

74 Hayer, M.K. and Riddell, F.G. (1984), *Inorg. Chim. Acta*, **92**, L37-L39.

75 Pike, M.M., Fossel, E.T., Smith, T.W. and Springer, C.S. (1984), *Am. J. Physiol.*, **246**, C528-C536.

76 Mota de Freitas, D., Espanol, M.C. and Ramasamy, R. (1987), *Biophys. J.*, **51**, 73a.

77 Ramasamy, R., Mota de Freitas, D., Jones, W., Wezeman, F., Labotka, R. and Geraldes, C.F.G.C. (1990), *Inorg. Chem.*, **29**, 3979-3985.

78 Ramasamy, R., Mota de Freitas, D. Geraldes, C.F.G.C. and Peters, J.A. (1991), *Inorg. Chem.*, **30**, 3188-3191.

79 Nieuwenhuizen, M.S., Peters, J.A., Sinnema, A., Kieboom, A.P.G. and van Bekkum, H. (1985), *J. Am. Chem. Soc.*, **107**, 12-16.

80 Khan, M.M.T., Reddy, P.R. (1974), *J. Inorg. Nucl. Chem.*, **36**, 607-610.

Chapter 2

Experimental

2.1.1 Human Erythrocytes for Li^+ Uptake Studies

Venous blood (usually 20ml) was drawn from healthy volunteers from within the Chemistry Department, University of St. Andrews, by qualified staff at either the Occupational Health Department or at the Health Centre in St. Andrews. Blood from patients was obtained from either the psychiatric clinic at the Ninewells Hospital, Dundee or from the Royal Liff Hospital, Dundee. The blood was immediately transferred into tubes containing either sodium heparin or citrate-based anticoagulant (7mM citric acid, 93mM trisodium citrate, 139mM dextrose). In the latter, the ratio of blood:anticoagulant was 1:9. The blood was centrifuged for approximately 5min. and the plasma was removed by aspiration. The erythrocytes were then washed with the intended incubation medium, centrifuged and the supernatant aspirated. This procedure was repeated at least three times before the isolated erythrocytes were resuspended in the incubating medium.

2.1.2 Rat and Rabbit Erythrocytes for Li^+ Uptake Studies

All animal handling was performed by A.N. Carter of the University of Dundee. Immediately after killing the rats using CO_2, whole blood was obtained by cardiac puncture from 3 female rats and pooled together (approximately 16ml), and by venepuncture of the inferior vena cava of 1 rat (approximately 15ml), and transferred into tubes containing citrate anticoagulant (3ml). Whole blood (20ml) was obtained by venepuncture of the peripheral ear vein of the live rabbit and transferred immediately into a tube containing sodium heparin. The erythrocytes were then isolated as above.

2.1.3 Li^+ Uptake Into Erythrocytes

The fresh erythrocytes were incubated overnight as a dilute suspension (approximately 4% haematocrit) at room temperature in an isotonic medium (Buffer A: 40.0mM NaCl, 16.8mM KCl, 2.0mM $CaCl_2$, 1.2mM $MgCl_2$, 4.75mM Na_3PO_4, 10mM dextrose, 15mM $Na_5P_3O_{10}$, 0.5mM $DyCl_3$, pH 7.4). This removed most, but not all, of the intracellular Li^+ found in the erythrocytes of the people taking lithium salts. At the start of an experiment the incubating medium was changed to Buffer B (Buffer A + 2mM LiCl) by centrifuging and washing the erythrocytes three times in Buffer B before resuspending the erythrocytes at approximately 8% haematocrit. The suspension was incubated at 37°C in a thermostatted water bath and was intermittently agitated gently to prevent the erythrocytes settling. Zero time for the experiment was taken as the time when the erythrocytes were first exposed to Buffer B. For each nmr measurement an aliquot of gently packed erythrocytes (2ml) was obtained by centrifuging a pre-determined volume of the suspension for 2min.; the supernatant was aspirated and discarded, and the erythrocytes were transferred to a 10mm nmr tube which was then fitted with a 4mm outside-diameter (o.d), coaxial insert containing ^2H_2O. The haematocrit of the sample was typically 85%. The time point recorded for each spectrum was the midpoint of the data acquisition period. After recording the spectrum the erythrocytes were returned to the stock suspension and simultaneously fresh buffer was added (the same volume as that previously discarded) to maintain both the Li^+ concentration and the haematocrit of the suspension.

2.1.4 Nmr Spectroscopy of Erythrocytes

All the nmr spectra were recorded using the high-resolution probes on either a Bruker AM300 or a Bruker MSL500 Fourier-transform spectrometer at the frequencies shown in Table 2.1. Spectra recorded on the MSL500 spectrometer had at least twice the signal-to-noise ratio than those from the AM300 spectrometer. Each spectrum was

field/frequency locked on the ^2H resonance of ^2H_2O contained in a 4mm-o.d. insert tube placed coaxially in the 10mm sample tube. Free induction decays (FID's) were acquired in a data block just sufficiently large to contain all the visible decay. After applying an appropriate line-broadening factor to improve the signal-to-noise ratio the FID's were subsequently transformed in a larger data block to improve the digital resolution in a process known as 'zero-filling' *(1)*.

Table 2.1 The respective nuclear frequencies on the Bruker AM300 and Bruker MSL500 nmr spectrometers (MHz)

Nucleus	AM300	MSL500
^7Li	116.638	194.366
^{23}Na	79.388	132.294
^{39}K	14.006	23.336
^{133}Cs	39.367	65.597
^{31}P	121.513	202.458

For all quantitative work, spectra were recorded and transformed under identical conditions. 90° pulse widths were determined, by first obtaining the 180° pulse width by adjustment of the pulse length until no signal is produced, and then dividing the pulse length by 2 *(2)*. That the resulting pulse length generated the maximum signal intensity was double checked. T_1 values were determined by the standard inversion-recovery method *(3)*. 90° pulses were applied with a repetition rate of greater than 5 times the relaxation time of the slowest relaxing nuclei, thus allowing sufficient time for all the nuclei to be completely relaxed before applying the next pulse. The Li^+ resonances of both suspensions of erythrocytes and aqueous solutions, containing

known concentrations of LiCl over the concentration range 0.05-1.00mM, were compared directly. For a given [Li^+], there was no significant difference between the integral of the Li^+ resonance in the erythrocyte sample and the aqueous solution, confirming the validity of the quantitative method employed in this work.

2.1.5 ^{7}Li Nmr Spectroscopy of Erythrocytes

Typically 100 FID's were collected into 1K data points with a sweep width of 1000Hz (1.95Hz/pt). The repetition rate between pulses was generally 30s and therefore the total acquisition time for a spectrum was 50min. The FID's were zero-filled to 8K data points (0.24Hz/pt) and transformed with a line-broadening factor of typically 4Hz. A typical spectrum is shown in Figure 2.1(A). Assignment of the resonance from the extracellular Li^+ was achieved by comparison of the spectra of the erythrocyte samples with a spectrum of a reference sample of the incubating medium Figure 2.1(B), the two resonances having the same chemical shift. Therefore, the second resonance in the spectra of the erythrocyte samples was from the intracellular Li^+, being unaffected by the extracellular shift reagent. This second resonance occurs at the same chemical shift as that arising from Li^+ in aqueous solutions of LiCl in the absence of shift reagents. In all spectra the chemical shift of the extracellular Li^+ resonances was referenced to the intracellular Li^+ resonance which was consistently set at 0ppm. The line widths at half height, $\omega_{1/2}$, are 10Hz and 16Hz for the intracellular and extracellular signals respectively and the separation between the peaks is 0.64ppm.

Quantification of the intracellular Li^+ levels in each sample of packed erythrocytes was achieved by comparing the ^{7}Li spectrum of the sample (2ml) with a reference spectrum of the incubating medium (2ml) containing 2mM Li^+, which was recorded and transformed under identical conditions. The spectrum of the incubating medium, Figure 2.1(B), was integrated and the area under the peak set at 100 for convenience (i.e. 100% of the sample was occupied by the incubating medium at 2mM

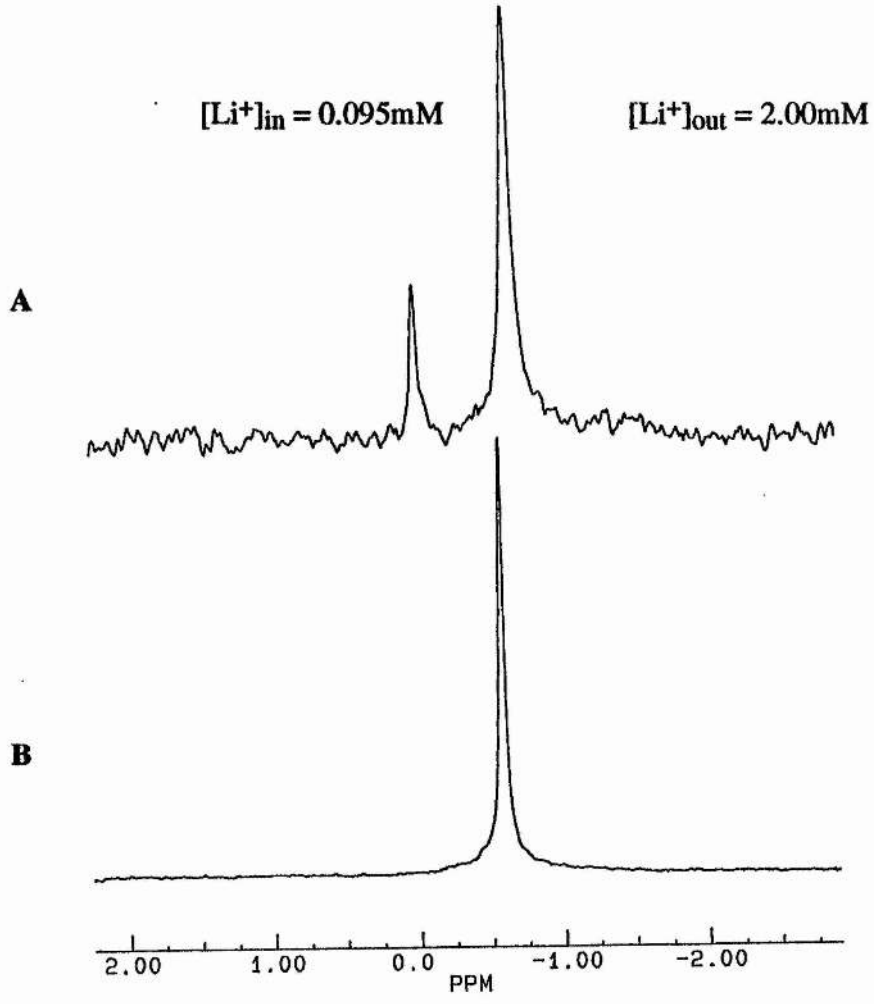

Figure 2.1 ^{7}Li nmr spectra of **(A)** a sample of erythrocytes after 428min. incubation in Buffer B (2mMLi^{+}) at 37°C, and **(B)** Buffer B (Each spectrum is the sum of 100 acquisitions recorded at 194MHz on the MSL500 nmr spectrometer)

Li^+). Each sample spectrum was then transformed with the same absolute intensity. The percentage volume occupied by the extracellular medium was given by the integral of the signal from the extracellular Li^+, I_{out}, since the concentration was the same as that of the reference sample (2mM). Therefore the remaining volume in the sample was that occupied by the erythrocytes (i.e. the haematocrit) and was thus given by:

$$\text{Haematocrit (\%)} = 100 - I_{out}$$

The intracellular Li^+ resonance corresponding to this haematocrit was integrated, I_{in}, and the intracellular $[Li^+]$ was thus given by:

$$[Li^+]_{in} = I_{in} \times \frac{[Li^+]_{ref}}{I_{ref}} \times \frac{100}{100-I_{out}}$$

Substituting for $[Li^+]_{ref} = 2mM$, and $I_{ref} = 100$, then the intracellular Li^+ concentration in all the samples of packed erythrocytes could be calculated from the integrals of the two resonances by:

$$[Li^+]_{in} = \frac{2I_{in}}{100-I_{out}}$$

2.1.6 ^{31}P Nmr Spectroscopy of Erythrocytes

A sample of fresh blood in the citrate-based anticoagulant was centrifuged approximately 2h after it had been drawn. The buffy coat and white cells were removed by aspiration and an aliquot of the gently packed erythrocytes (2ml) was transferred to a 10mm nmr tube, which was then fitted with a 4mm-o.d. coaxial insert containing ^2H_2O. The ^{31}P nmr spectrum of the sample was then recorded. The remaining erythrocytes were collected, isolated and incubated as in the Li^+ uptake experiments. ^{31}P spectra of samples of gently packed erythrocytes were recorded at time intervals throughout the incubation period. Typically 240 FID's were acquired with a repetition rate of 2s, in a 2K data block with a sweep width of 10^4Hz

(9.77Hz/pt), and transformed in an 8K data block (2.44Hz/pt) with 15Hz line-broadening. All spectra were referenced to the ^{31}P resonance of a solution of H_3PO_4 (10% w/v) set at 0ppm.

2.1.7 Erythrocyte Viability

The viability of the erythrocytes throughout the lifetime of the experiments was demonstrated in a number of ways: by the absence of haemolysis, which was indicated by the non-appearance of the red colour of haemoglobin in the supernatant; by periodic monitoring of the morphology of the erythrocytes by microscopic examination, to ensure that the normal biconcave shape was maintained; and by the use of ^{31}P nmr spectroscopy. Haemolysis was usually accompanied by a significant increase in the apparent intracellular [Li^+].

^{31}P nmr spectroscopy is a potent method to investigate the intracellular environment, particularly intracellular pH. Figure 2.2A shows the ^{31}P nmr spectrum of a sample of packed erythrocytes which was recorded just 2h after the blood had been drawn and prior to the incubation procedure. This was compared to the ^{31}P nmr spectra of erythrocyte samples after 0.5 and 24h incubation in Buffer B at 37°C, Figure 2.2B and Figure 2.2C respectively. The signals at 3.10 and 2.14ppm are assigned to the 3- and 2-phosphate groups of 2,3-diphosphoglycerate (2,3-DPG), and the signals at -5.54, -10.55, and -19.27ppm are assigned to the γ, α and β phosphate groups of ATP *(4)*. The two additional peaks in Figure 2.2B and 2.2C, at -7.09 and -20.87ppm, are assigned to the α and β resonances from $P_3O_{10}^{5-}$ in the extracellular medium.

The consistencies of the intensities and the chemical shifts of the resonances from both ATP and 2,3-DPG confirm that the levels of phosphorous metabolites in the erythrocytes are unchanged, even after 24h incubation, and also that the intracellular pH is constant. The chemical shift difference between the γ, and α resonances of ATP

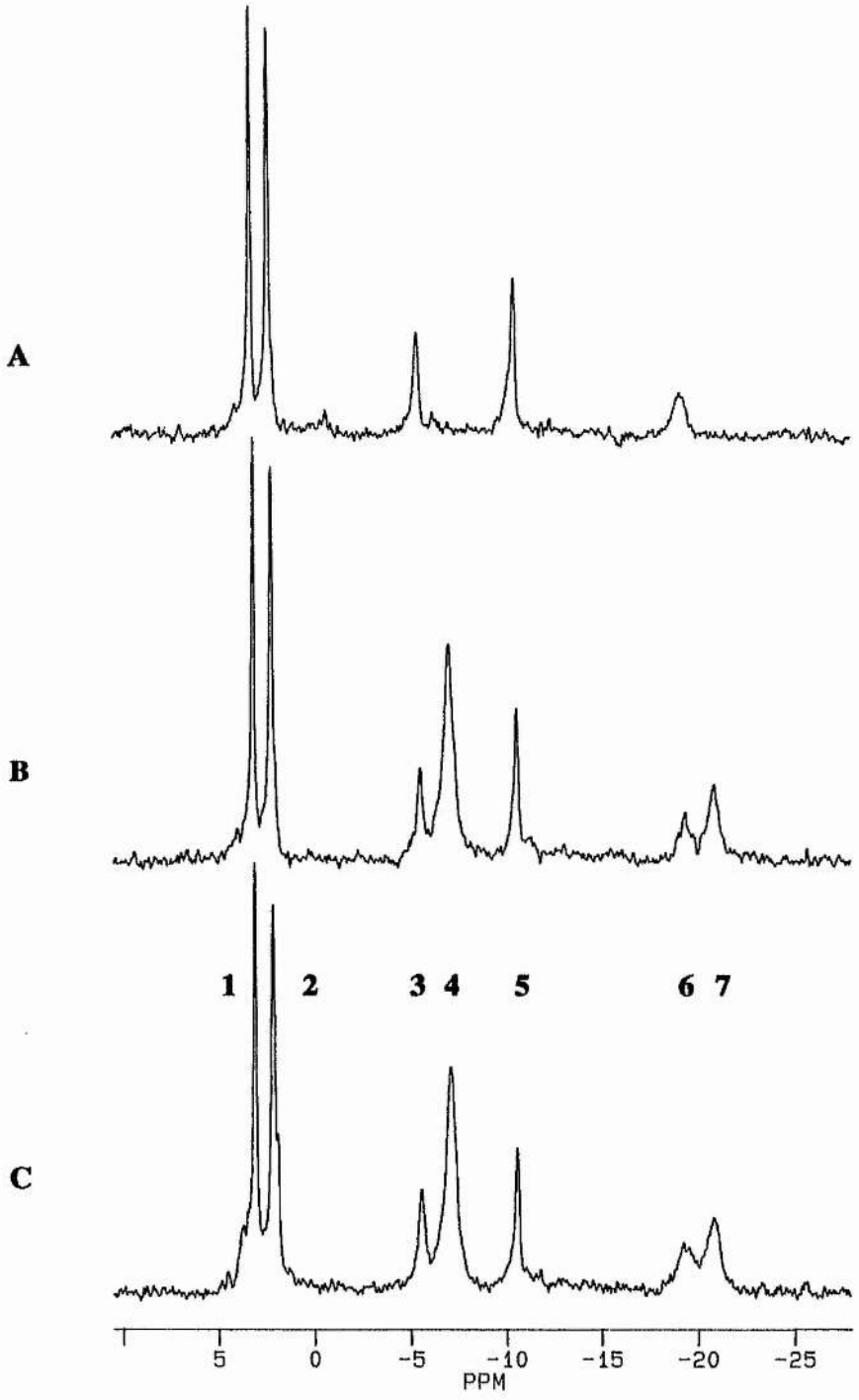

Figure 2.2 ^{31}P nmr spectra of human erythrocytes in **(A)** blood plasma, 2h after collection, **(B)** Buffer B, after 0.5h incubation at 37°C, and **(C)** Buffer B, after 24h incubation at 37°C

(**1,2** 2,3-DPG, **3** γ-ATP, **4** α-$P_3O_{10}^{5-}$, **5** α-ATP, **6** β-ATP, **7** β-$P_3O_{10}^{5-}$)

($\delta_{\alpha\gamma}$) is a good indicator of intracellular pH *(4)*. Thus, the viability of the erythrocytes throughout the lifetime of the experiments was confirmed.

A particular problem with erythrocyte viability was experienced at one stage during this work. A slight haemolysis during the initial washing procedure, followed by a gradually increasing amount of lysis during the incubation period of the uptake experiment was observed for a number of such experiments. This was accompanied by much higher intracellular [Li^+] being attained than in previous experiments. Microscopic examination showed the erythrocytes with a considerably altered shape with an abundance of irregularities on the normally smooth exterior surface (crenation). The problem was investigated and was eventually identified as an adverse osmotic effect due to a new batch of $Na_5P_3O_{10}$, which was used in the incubating medium. This had been acquired from Aldrich as opposed to that previously used from BDH. The BDH material contained a higher amount (approximately 18%) of $P_2O_7^{4-}$ than the Aldrich material (approximately 6%) and also contained a small amount of $P_3O_9^{3-}$ (approximately 0.1%), as determined by ^{31}P nmr spectroscopy of the aqueous solutions. The ionic composition of the incubating medium was originally designed using $Na_5P_3O_{10}$ from BDH. The consequence of using the Aldrich salt when preparing the buffer was a significant difference in the ionic strength , i.e.the buffer was no longer isotonic and resulted in lysis of the erythrocytes. All experiments using this material were therefore repeated using the BDH salt.

2.1.8 Effect of Overnight Incubation Upon the Uptake of Li^+

The effect of the overnight incubation procedure required for the erythrocytes already containing Li^+, on the uptake of Li^+ into erythrocytes was investigated. The isolated erythrocytes from a blood sample from one healthy individual were divided equally; a Li^+ uptake experiment was carried out immediately using one half of the erythrocytes and the remaining erythrocytes were incubated in Li^+-free buffer for 23h

before the uptake experiment was performed. The results are illustrated in Figure 2.3 and, although there was no significant effect caused by the incubation procedure, as illustrated by the similarity in the two profiles, it was decided to follow identical procedures for all the Li^+ uptake experiments so that valid comparisons could be made. Therefore, the erythrocytes from both patients and controls were incubated overnight, in a Li^+-free medium, prior to the experiment.

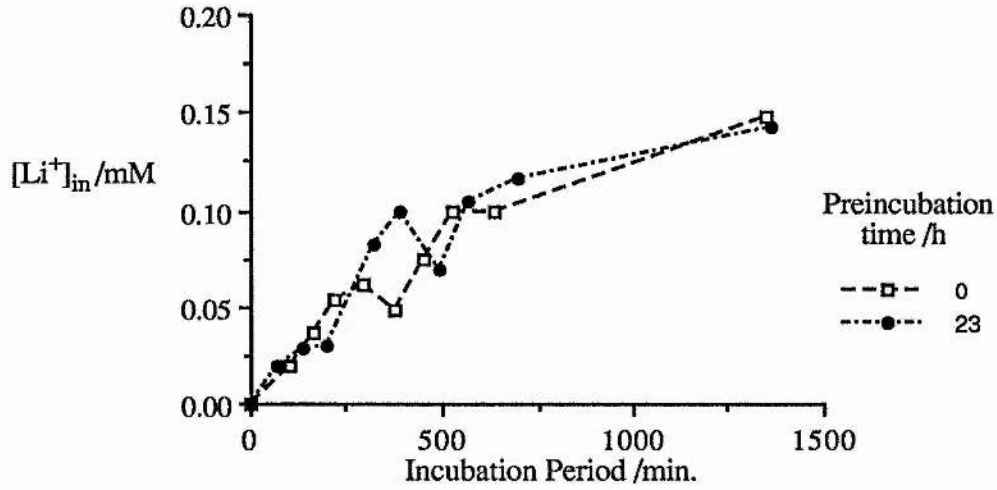

Figure 2.3 A comparison of the uptake of Li^+ into fresh erythrocytes and into erythrocytes incubated for 23h in a Li^+-free medium

2.2 Human 1321 N1 Astrocytomas

This is a cell line originally derived from a human brain tumour in the early 1970's. The cells were cultured on the surface of microcarrier beads (Nunc Biosilon, diameter 250μm), by A.N.Carter of the University of Dundee. These beads allow very high density cultures to be obtained, having a surface area in the range 250-300cm^2 per gram of beads, thus allowing a maximum density of approximately 10^8 cells g^{-1} beads to be obtained.

The cells were cultured in Dulbecco's-modified Eagles medium containing foetal calf serum (10% v/v), Gentamicin - a broad spectrum antibiotic (5μg ml^{-1}) and Amphotericin B - an anti-fungal agent (2.5μg ml^{-1}). The cells (2 x 10^7) were seeded onto the microcarrier beads (5g) in a 75cm^2 culture flask containing culture medium (25ml). The flask was then transferred to a humidified incubator in an atmosphere of 5% CO_2, 95% air and left for 2 days with periodic gentle mixing. After this time the beads were allowed to settle and the medium aspirated. The beads were transferred to a 175cm^2 flask, fresh medium added (100ml), and they were then replaced in the incubator for 2 days with periodic mixing. The medium was replaced in this way every 2 days for a further 10 days, after which time the beads, now carrying the cells, were used for an experiment. For one particular experiment, LiCl (16.7mM) was included in the culture medium in the 24h preceding the nmr experiment in order to obtain a significant intracellular [Li^+].

2.2.1 Nmr Studies of Astrocytomas

Prior to an nmr experiment, Hepes (20mM, pH 7.2) was included in the culture medium and the suspensions were maintained at 37°C in a thermostatted water bath. For each nmr experiment, an aliquot of the suspension was transferred to a 10mm nmr tube, the beads were allowed to settle under gravity and the supernatant was aspirated. This process was repeated until a sufficient volume of beads was obtained. By repeated washings and aspirations, the extracellular medium was changed to Buffer C (10mM Hepes, 10mM LiCl, 80mM NaCl, 10mM $Na_5P_3O_{10}$, 3mM $DyCl_3$, 2.7mM KCl, 0.5mM $MgCl_2$, 1.4mM $CaCl_2$, 0.04mM NaH_2PO_4, 30mM dextrose, adjusted to pH 7.2 with Tris base). This buffer was adapted from that employed in the ^{23}Na-nmr study of rat mucosal mast cells *(5)*. For the experiment at the higher [Li^+] of 50mM, LiCl was substituted for NaCl in the buffer.

All spectra were recorded on the MSL 500 spectrometer. The spectrometer was field/frequency locked, and the magnet was shimmed using a sample tube containing a fixed volume of the microcarrier beads in a fixed volume of aqueous solution containing D_2O (20%v/v), LiCl and NaCl. Thereafter, no further shimming was performed and the spectra were recorded unlocked with all samples containing the same volumes of beads and solution as the above sample.

For the ^{23}Na spectra, typically 1200 FID's were collected into 1K data points with a sweep width of 10^4Hz (19.53Hz/pt) and a repetition rate of 0.2s, thus giving an acquisition time of 4min. The FIDs were zero-filled to 8K data points (2.44Hz/pt) and transformed with a line-broadening factor of typically 20Hz. ^7Li spectra were collected into 2K data points with a sweep width of 8000Hz (7.88Hz/pt) and a repetition rate of 30s. The FID's were zero-filled to 8K data points (1.97Hz/pt) and transformed with a line-broadening factor of typically 20Hz. Reference spectra for both Na^+ and Li^+ were obtained on samples of the buffers alone and on samples of the buffers containing beads without cells. ^{31}P spectra were collected into 2K data points with a sweep width of 15000Hz (14.80Hz/pt) and a repetition rate of 2s. The FID's were zero-filled to 8K data points (3.70Hz/pt) and transformed with a line-broadening factor of typically 20Hz. The chemical shifts were referenced to the ^{31}P resonance in an aqueous solution of H_3PO_4 (10% w/v).

2.2.2 Cell Viability

^{31}P nmr spectra were recorded on the suspensions in both the culture medium and in Buffer C to ensure the viability of the cells. Not having the necessary equipment for perfusing the cell suspensions in the spectrometer it was found that, by ensuring sufficient buffer was present to almost completely fill the nmr tube, the suspension could be periodically mixed by gentle inversion of the tube, thus ensuring that the cells were not depleted of oxygen or other necessary nutrients. If left without this mixing

procedure for long periods of time, the shape of extracellular resonance, in both the ^{23}Na and ^{7}Li-nmr spectra, altered significantly. A broad shoulder appeared on the upfield side of the extracellular signal which is probably due to the action of a pyrophosphatase, associated with the cells. This enzyme will catalyse the decomposition of the $P_3O_{10}^{5-}$ to orthophosphate, thus reducing the concentration of shift reagent in the immediate extracellular environment of the cation. The activity of such an enzyme with this shift reagent has been observed in a number of other mammalian tissues *(6)*. Interestingly, by mixing the cell suspension by inversion of the nmr tube, the subsequent spectra no longer showed this abnormality in the extracellular peak, presumably due to the replacement of the decomposed $P_3O_{10}^{5-}$. The ^{31}P spectra recorded prior to, and subsequent to the nmr experiment of the cells in the growth medium are shown in Figure 2.4A and 2.4B, respectively. The spectra are very similar indicating no significant changes in either the phosphorous metabolites or the intracellular pH, thus confirming the viability of the cells and, therefore, the experiment.

The viability of the cells was also confirmed by assay of the inositol uptake behaviour using [^{3}H]-inositol by Dr I. Batty of the University of Dundee *(8)*. This assay also gave an approximate value of 80mg protein (4×10^7 cells) per ml beads packed under gravity.

2.2.3 Determination of Intracellular [Li^+] in Astrocytomas

A very approximate value for the intracellular [Li^+] was determined from the nmr data on the astrocytoma samples, by establishing an approximate value for the intracellular volume as a percentage of the sample volume. This method assumes no loss of nmr-visibility for any of the ^{23}Na-, or the ^{7}Li-nmr resonances and assumes an intracellular [Na^+] of 20mM *(9)*.

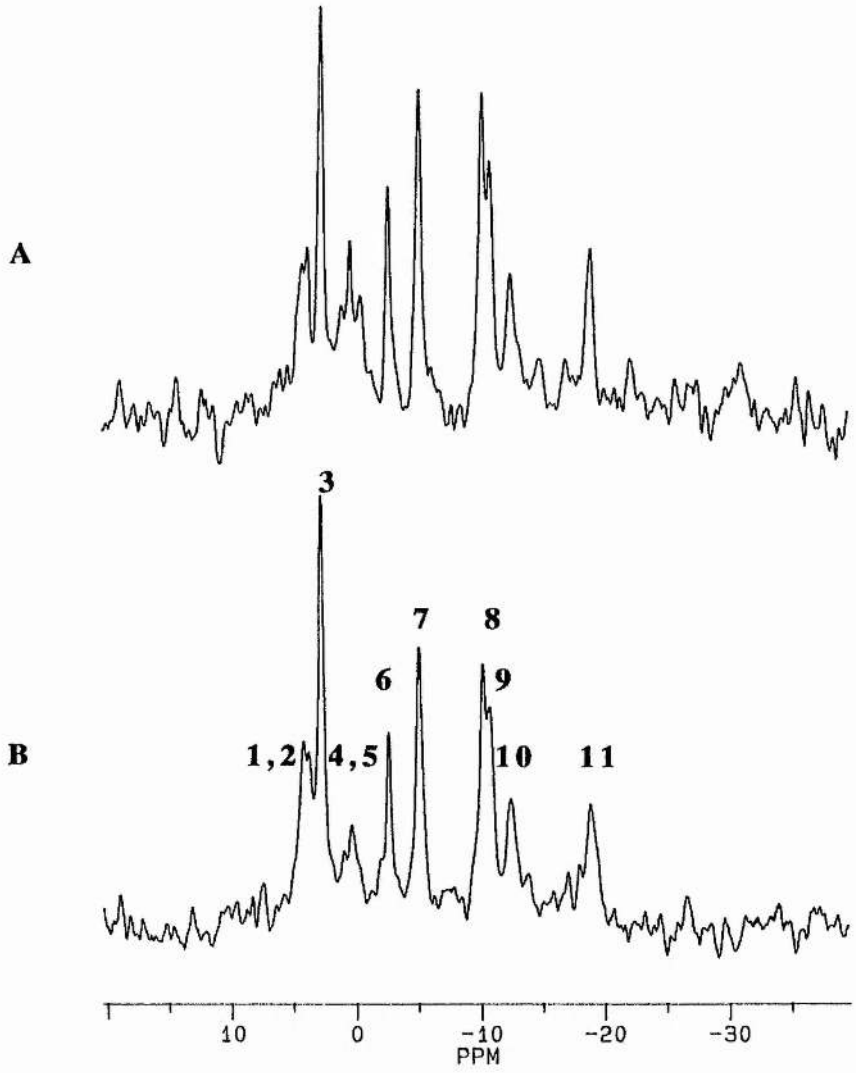

Figure 2.4 ^{31}P nmr spectra of human 1321 N1 astrocytomas on microcarrier beads recorded prior to **(A)**, and subsequent to **(B)** a Li^+-nmr experiment

(1 PE; **2** PC; **3** P_i; **4** GPE; **5** GPC; **6** PCr; **7** γ-NTP; **8** α-NTP; **9, 10** UDPG; **11** β-NTP *(7)*)

The integral of the Na^+ resonance from the reference spectrum of the buffer is set at 100. Therefore, the percentage volume occupied by the buffer ($V_{Na\text{-}out}$) in the suspensions of beads/cells is given by the integral of the extracellular Na^+ resonance ($I_{Na\text{-}out}$). The intracellular Na^+ at 20mM occupies a percentage volume $V_{Na\text{-}in}$, and gives a signal of integral $I_{Na\text{-}in}$, where:

$$I_{Na\text{-}in} = I_{Na\text{-}out} \times \frac{[Na^+]_{in}}{[Na^+]_{out}} \times \frac{V_{Na\text{-}in}}{V_{Na\text{-}out}}$$

and since $V_{Na\text{-}out} = I_{Na\text{-}out}$, the intracellular volume is given by:

$$V_{Na\text{-}in} = I_{Na\text{-}in} \times \frac{[Na^+]_{out}}{[Na^+]_{in}}$$

Using this value, the $[Li^+]_{in}$ was determined from the $[Li^+]_{out}$ and the integrals of the intra-, and extracellular resonances in the corresponding ^{7}Li-nmr spectrum by:

$$[Li^+]_{in} = \frac{I_{Li\text{-}in}}{I_{Li\text{-}out}} \times \frac{V_{Li\text{-}out}}{V_{Li\text{-}in}} \times [Li^+]_{out}$$

The volume occupied by the beads is given by: $100 - (V_{in} + V_{out})$.

2.3.1 Rats for *in vivo* ^{7}Li-Nmr Spectroscopy

Sprague-Dawley rats weighing approximately 250g were provided by SmithKline Beecham Research Ltd and were handled by Dr D. Reid. The rats were administered doses of LiCl, varying from 1-5mmol.kg^{-1}, by intraperitoneal (i.p.) injection prior to the nmr experiment. Repeat dosages were administered to some animals at intervals over 1 or 2 days, to allow accumulation of Li^+ in tissues and organs. The rats were anaesthetised with a barbiturate (Sagital) administered i.p. before being secured in a purpose built holder to maintain the animal in a fixed vertical position within the magnet. The contrast reagents were introduced into the bloodstream by intravenous (i.v.) injection into the tail vein. The rats were sacrificed after the experiment.

2.3.2 *In vivo* Nmr Spectroscopy of Rat Brain

In vivo ^{7}Li-, and ^{31}P-nmr spectra were recorded using a Bruker AM360 spectrometer at 139.960 and 145.785 MHz, respectively. A surface coil, which could be retuned without moving the rat, was positioned on the surface of the scalp. The homogeneity of the magnetic field was adjusted using the ^{1}H signal from the rat brain. For ^{7}Li-nmr spectra, 100-1000 FID's were collected into 1K data points with a sweep width of 5000Hz (9.76 Hz/pt), and were transformed in 8K (1.22Hz/pt) with a line-broadening of 25Hz. In order to keep the acquisition time as a short as possible, a repetition rate of typically 2s was employed. Although the relaxation times were not determined, this delay is probably insufficient for full relaxation of all the Li^{+} species present; a T_1 in rat brain of 4.1s has previously been reported *(10)*. This was demonstrated in a study using interpulse delays of 0, 2 and 5s which gave relative integrals of 4.6, 8.4 and 1.0. Therefore no quantitative data could be obtained from this data. For ^{31}P-nmr spectra, 512 FID's were collected into 2K data points with a sweep width of 8000Hz (7.81Hz/pt) and a repetition rate of 4s, giving an acquisition time of 34min. The FID's were transformed in 8K (1.95Hz/pt) with a line-broadening of 15Hz. ^{31}P-nmr spectroscopy was employed to monitor the metabolic state of the rats. A typical spectrum from a healthy anaesthetised rat is shown in Figure 2.5.

2.4 Extraction and Separation of Erythrocyte Membrane Lipids

The extraction of the lipids from erythrocyte membranes and their subsequent separation by high-performance, thin-layer chromatography (HP-TLC) was based on a method used at the NERC unit, University of Stirling *(11)*. The lipid extraction is adapted from a procedure described by Folsch *(12)* and the HP-TLC of the lipids is as according to Vitiello *(13)*.

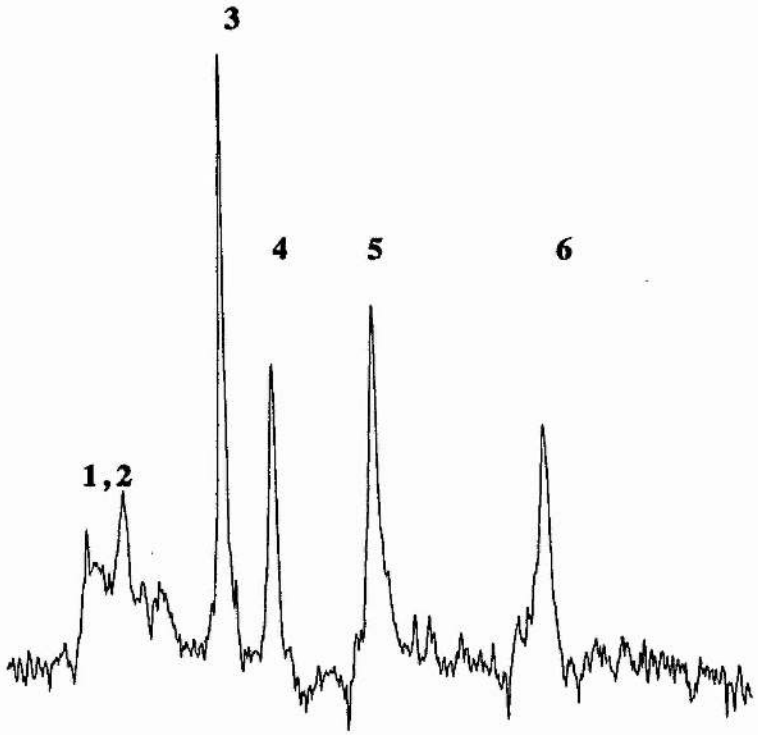

Figure 2.5 *In vivo* ^{31}P nmr spectrum of the head of an anaesthetised rat

(1 PME; 2 P_i; 3 PCr; 4 γ-NTP; 5 α-NTP; 6 β-NTP *(10)*)

2.4.1 Extraction of Lipids from Erythrocyte Membranes

The following extractions were performed in duplicate. Erythrocytes were isolated from the venous blood of healthy volunteers and of Li^+-treated psychiatric patients, as described previously in Section 2.1.2, and an aliquot of gently packed erythrocytes in aqueous medium (0.5ml) was transferred to a glass-stoppered centrifuge tube (15ml) for lipid extraction. The erythrocyte membranes were disrupted by repeated freeze-thawing (3 times). H_2O (0.5ml) and $CHCl_3$-MeOH (2:1), with an antioxidant, butylated hydroxy-toluene (BHT, 0.01%w/v), (8ml) were added to the tube. The mixture was shaken vigorously and then left on ice for 1h, with intermittent shaking. KCl (0.88%w/v, 1ml) was then added and the mixture was shaken before being centrifuged to separate the 2 phases. The aqueous phase (upper) was removed gently by pipette and the organic phase (lower) was then filtered though a prewashed filter (Whatmans N° 1). The residue was rinsed with $CHCl_3$-MeOH (2 x 1ml) and the combined filtrates were brought to dryness under a stream of N_2. The lipids were immediately resuspended in $CHCl_3$-MeOH (1ml), transferred to a weighed sample bottle, dried under N_2 and desiccated in the dark for 30min. The weight of lipid was determined before being resuspended in $CHCl_3$-MeOH (1%w/v) and stored at -5°C under N_2 until required. A further aliquot of packed erythrocytes from the same sample (0.1ml) was transferred to a volumetric flask (50ml) which was filled to the mark with isotonic buffer. The cells were then counted using a haemocytometer (B.D.H.).

2.4.2 Thin-Layer Chromatography of Erythrocyte Membrane Lipids

HP-TLC plates (Merck, pre-coated silica gel-60, 10 x 10cm) were prerun with $CHCl_3$-MeOH (2:1) and then desiccated. The plates were activated at 110°C for 30min. prior to use. Lipid extracts (approximately 10µg) were applied, as a small horizontal line (-), 1cm from the bottom of the plate and ascending chromatography

was then performed at room temperature with the first solvent system: chloroform - *i*-propanol - methyl acetate - methanol - 0.25% w/v KCl (25 : 25 : 25 : 10 : 9) until the solvent front had travelled for approximately 5cm. The plate was then transferred to a desiccator for 30min. Chromatography was then performed in the same direction to within 0.5cm of the top of the plate, using the second solvent system: hexane - diethyl ether - acetic acid (80 : 10 : 2). The plate was dried in air and the lipids were revealed by spraying with a solution of cupric acetate (3% w/v) and phosphoric acid (8% w/v) and charring at 160°C for 15min. This produced simultaneous detection of all the lipids as black spots. The plates were stored in foil and analysed by a flying-spot, scanning densitometer (Shimadzu CS-9000) as soon as possible (within 1 day) as the spots faded very quickly.

2.5 Solubilisation and Separation of Erythrocyte Membrane Proteins

The solubilisation of the proteins from human erythrocyte membranes using sodium dodecyl sulphate (SDS) and the subsequent fractionation by polyacrylamide gel electrophoresis (SDS-PAGE) was based on the method of Laemmli *(14)*.

2.5.1 Preparation of Protein Samples

Erythrocytes were isolated from the venous blood of healthy controls and of Li^+-treated psychiatric patients, as described in Section 2.1.2. Gently packed erythrocytes in aqueous medium (2ml) were lysed by adding ice-cold Tris/HCl (20ml, 20mM, pH 7.4) containing EDTA (1mM), and leaving on ice for 10min. The cells were then centrifuged at 16000rpm for 20min. (Beckman J2-21 centrifuge with JA 20 rotor) after which the supernatant was aspirated. The residual pellet was washed 8 times in the lysis buffer followed by centrifugation and aspiration of the supernatant, to

produce white erythrocyte ghosts containing no cytosolic material. The ghosts were stored at -20°C until required. The following solubilisation and fractionation was performed in duplicate. Aliquots of the ghosts (100µl) were diluted with SDS-PAGE sample buffer (400µl) and heated in a boiling water bath for 5min. The SDS-PAGE sample buffer contained: H_2O (4ml), Tris/HCl (1ml, 0.5M, pH 6.8), glycerol (0.8ml), SDS (1.6ml, 10%), 2-mercaptoethanol (0.4ml) and bromophenol blue (0.2ml, 0.05% in H_2O).

2.5.2 SDS-PAGE of Erythrocyte Membrane Proteins

The separating gel (7.5% monomer) was prepared from acrylamide/bis (25ml, from acrylamide (146g) and N'N'-bis-methylene-acrylamide (4g) in H_2O (500ml)), Tris/HCl (25ml, 1.5M, pH 8.8), SDS (1ml, 10% in H_2O), H_2O (48.5ml) and N,N,N',N'-tetramethylethylenediamine (TEMED, 50µl). Polymerisation was initiated by the addition of fresh ammonium persulphate (AMPS, 500µl, 10% in H_2O) and the solution was poured into the prepared glass plate sandwich. Butan-1-ol (0.5ml) was carefully layered onto the gel surface to exclude atmospheric O_2 which inhibits the polymerisation. After 45min. the butanol was removed and the surface of the gel was rinsed with H_2O.

The stacking gel (4% monomer) was prepared from acrylamide/bis (1.3ml), Tris/HCl (2.5ml, 0.5M, pH6.8), SDS (100µl, 10%), H_2O (6.1ml) and TEMED (10µl). Polymerisation was initiated by the addition of AMPS (50µl, 10%) and the solution was applied to the top of the polymerised separating gel. A 15-place teflon comb was inserted into this solution to produce 15 sample wells on polymerisation. The final gel was 16cm long and 0.75mm thick.

The samples were applied to the gel such that there was an equal protein loading in each lane. The gels were then run under constant current, using 30mA for the

stacking gel and 50mA for the separating gel, in the running buffer: Tris base (25mM), glycine (192mM) and SDS (0.1%). Once the bromophenol blue tracker dye had reached 5mm from the bottom of the gel (~3h), the current was switched off and the gel was immersed in the staining solution, Coomassie brilliant blue R250 (prepared from Coomassie blue (1g) dissolved in methanol (500ml), followed by the addition of glacial acetic acid (100ml) and H_2O (400ml)). The gel was stained for 30min. and then washed in destaining solution (prepared from methanol (500ml), glacial acetic acid (100ml), and H_2O (400ml)). The gel was then dried onto filter paper or photographed.

2.6 ^{7}Li-Nmr Spectroscopy of Interaction of Li^+ with Inositol Monophosphatase

Bovine brain inositol monophosphatase was supplied by Dr A. Leech, University of St. Andrews. ^{7}Li-nmr spectroscopy of inositol monophosphatase was performed using a Bruker MSL500 spectrometer fitted with a solenoid probe. This gave higher sensitivity (approximately 2.5 times) than the high resolution probe at the expense of the resolution. Sample tubes, specially adapted from standard 5mm nmr tubes, were made in order to contain a small sample volume (200-250µl), and which could be secured in a horizontal position within the detection coils of the probe. The homogeneity of the magnetic field was adjusted using the ^{31}P signal from H_3PO_4, after which the homogeneity was not altered for the remainder of the experiment. For the ^{7}Li-spectra, typically 200 FID's were collected with a sweep width of 10^4Hz. Aqueous solutions of homogeneous bovine brain inositol monophosphatase (0.2-0.3mM) containing K^+ (250mM), Mg^{2+} (3mM) and Tris (50mM) at pH 7.5, with varying concentrations of LiCl, inositol 1-phosphate, HPO_4^{2-}, and $Dy(P_3O_{10})_2^{7-}$ (from $DyCl_3$ and $K_5P_3O_{10}$) were investigated by ^{7}Li-nmr spectroscopy. T_1 values were determined using the standard inversion-recovery method *(3)*.

2.7.1 Chemical Shift of the ^{133}Cs-Nmr Resonance

^{133}Cs-nmr spectroscopy was performed at either 39.4MHz or 65.6MHz using the Bruker AM300 or MSL500 spectrometer, respectively. The chemical shift of the ^{133}Cs resonance in various aqueous solutions was investigated to find a suitable solution for the incubation of the erythrocytes for Cs^+ uptake experiments and the results are shown in Table 2.2. The dramatic effect of phosphate anions on the chemical shift of ^{133}Cs has been observed previously *(15)*, however the largest shift observed here was in the solution containing no phosphates, Solution 1; the only anion in this solution was Cl^-. In suspensions of erythrocytes, the chemical shift difference between the intra-, and the extracellular Cs^+ resonances produced by Solutions 1, 2 and 4 in Table 2.2 were 0.94ppm, 1.05ppm and 0ppm, respectively. Therefore, in order to allow the incubation medium to be buffered, solution 2 was employed in the following Cs^+ uptake experiments.

Table 2.2 The chemical shift of ^{133}Cs resonance in various aqueous solutions*, relative to that of Cs^+ (10mM) in H_2O

Solution	PO_4^{3-}/mM	$P_3O_{10}^{5-}$/mM	$Mg^{2+}(Ca^{2+})$/mM	δ/ppm
1	0	0	0	-5.87
2	4.75	0	0	-5.69
3	0	15	0	-3.76
4	4.75	15	1(2)	-4.66

*solutions all contain 130mM Na^+, 7mM K^+, 10mM Cs^+ and 10mM dextrose

2.7.2 Cs^+ Uptake into Human Erythrocytes

Venous blood (20ml) was drawn from healthy volunteers and from patients from the alcoholism clinic at the Ninewells Hospital, Dundee, and the erythrocytes

isolated as in Section 2.1.1. The erythrocytes were incubated in an isotonic medium (115mM NaCl, 20mM KCl, 4.75mM Na_3PO_4 and 10mM dextrose, pH 7.4) until required for an experiment. At the start of an experiment the incubating medium was changed to a Cs^+-containing buffer (115mM NaCl, 10mM KCl, 10mM CsCl, 4.75mM Na_3PO_4, and 10mM dextrose, pH 7.4).

^{133}Cs nmr spectra were recorded and the intracellular [Cs^+] concentrations were determined using the same methods employed in the study of Li^+ in erythrocytes in Section 2.1.5. Typically, 8 FID's were collected into 2K data points with a sweep width of 2000Hz (1.95Hz/pt) and a repetition rate of 60s. The FID's were transformed in 8K (0.49Hz/pt) with a line-broadening of 5Hz.

2.7.3 ^{23}Na-, and ^{39}K-Nmr Spectroscopy of Erythrocytes

Quantitative ^{23}Na-, and ^{39}K-nmr spectroscopy was employed to monitor the change in the intracellular concentrations of these cations, in erythrocytes incubated in isotonic medium containing increasing concentrations of Cs^+. A sample of erythrocytes, isolated as in Section 2.1.1, was divided equally into 5 and each aliquot was incubated overnight at ambient temperature in one of the Buffers A-E in Table 2.3.

Intracellular Na^+ concentrations were determined by the same methods employed in the ^7Li-nmr spectroscopy of erythrocytes in Section 2.1. However under these conditions, the intra-, and the extracellular K^+ resonances were not resolved and the intracellular K^+ concentrations had to be determined by difference spectroscopy. The spectra from the erythrocyte samples were subtracted from that of the corresponding buffers such that the extracellular K^+ signal disappeared leaving just the intracellular signal, of integral I_{in}. This produced a subtraction factor which was used to determine the haematocrit of the sample. I_{in} was subtracted from the integral of the total original signal to give the integral of the extracellular signal, I_{out}. The intracellular

concentrations were then determined using the same calculations as for Li^+, in Section 2.1.5.

The values obtained for Na^+ and K^+ are not absolute since the reported nmr invisibility of these cations was not considered. However, in this study only the change in the intracellular concentrations was investigated.

Table 2.3 The composition of the aqueous buffers*

Buffer	[NaCl] /mM	[CsCl] /mM
A	70	0
B	60	10
C	45	25
D	20	20
E	0	70

*buffers all contain 15mM KCl, 4.75mM Na_3PO_4, 10mM dextrose, 10mM $Na_5P_3O_{10}$, and 2.5mM $DyCl_3$

2.8 References

1 Derome, A.E. (ed.) (1990), in *Modern NMR Techniques for Chemistry Research,* Pergamon Press, Oxford, p22.

2 Fukushima, E. and Roeder, S.B.W (eds) (1981), in *Experimental Pulse NMR,* Addison-Wesley Publishing Co., Inc., London, p434.

3 Derome, A.E. (ed.) (1990), in *Modern NMR Techniques for Chemistry Research,* Pergamon Press, Oxford, p166.

4 Mitsumori, F. (1985), *J. Biochem.*, **97**, 1551-1560.

5 Pilatus, U., Degani, H. and Pecht, I. (1990), *Febs Letts*, **269**, 292-296.

6 Matwiyoff, N.A., Gasporovic, C., Wenk, R., Wicks, J.D. and Rath, A. (1986), *Mag. Res. Med.*, **3**, 164-168.

7 Neeman, M., Rushkin, E., Kadoun, A. and Degani, H. (1988), *Mag. Res. Med.*, **7**, 236-242.

8 Batty, I., *personal communication.*

9 Downes, C.P., *personal communication.*

10 Ramaprasad, S., Newton, J.E.O., Cardwell, D., Fowler, A.H. and Komoroski, R.A. (1992), *Mag. Res. Med.*, **25**, 308-318.

11 Thompson, K. and Henderson, J., *personal communication.*

12 Folch, J., Lees, M. and Sloane Stanley, G.H. (1957), *J. Biol. Chem.*, **226**, 497-509.

13 Vitiello, F. and Zanetta, J.P. (1978), *J. Chromatogr.*, **166**, 637-640.

14 Laemmli, U.K. (1970), *Nature*, **227**, 680-685.

15 Wittenkeller, L., Mota de Freitas, D., Geraldes, C.F.G.C. and Tome, A.J.R. (1991), *Inorg. Chem.*, **31**, 1135-1144.

Chapter 3

Lithium NMR Spectroscopy of Erythrocytes

3.1 Li Nmr Spectroscopy

Both of the naturally occurring isotopes of lithium, ^{6}Li and ^{7}Li, are nmr visible. Table 3.1 shows the nuclear properties relevant to nmr spectroscopy of both isotopes of lithium compared to the other alkali metals. The relatively high sensitivity of ^{7}Li, its small quadrupole moment (Q), and its high natural abundance are all conducive to the relatively facile study of ^{7}Li by nmr. The very small values of Q for both isotopes (^{6}Li has the smallest known Q) means that quadrupolar relaxation mechanism is relatively inefficient in these nuclei and therefore the relaxation tends to be dominated by the dipolar mechanism.

Table 3.1 Nuclear properties of the alkali metals *(1)*

Nucleus	^{6}Li	^{7}Li	^{23}Na	^{39}K	^{133}Cs
Natural Abundance (%)	7.4	92.6	100	93.1	100
Spin Quantum Number	1	3/2	3/2	3/2	7/2
Quadrupole Moment ($10^{-28}m^2$)	-0.0008	-0.045	0.12	0.055	-0.003
Frequency (MHz)*	14.72	38.87	26.48	4.67	13.21
Receptivity†	3.58	1540	525	2.69	269

(* relative to ^{1}H = 100 MHz, † relative to ^{13}C = 1)

3.1.1 Shift Reagents for Studying Membrane Transport of Li^+

Several techniques using shift reagents can be employed to study the transport of cations across membranes and the choice of method depends on the time-scale of the process under study: dynamic line-broadening is used for very rapid processes (where the rate is > $5s^{-1}$), however no Li^+ transport process has yet been observed that is fast enough for study by this method; magnetisation transfer is used for slower process which are on similar time-scale to the nmr relaxation times (rate < $5s^{-1}$ for ^7Li): and, for very slow processes, the signal intensities can be measured as a function of time. The latter method has been employed to study the relatively slow transport of Li^+ across the erythrocyte membrane.

3.1.2 Li-Nmr Spectroscopy for Transport Studies in Erythrocytes

The identification of $Dy(P_3O_{10})_2^{7-}$ as a shift reagent for the alkali metals led to the development of ^7Li-nmr studies of isolated erythrocytes incubated in lithium containing media. For typical [Li^+] found in the blood plasma during lithium therapy (i.e. 0.5 - 1.2 mM), a concentration of 5mM $Dy(P_3O_{10})_2^{7-}$ was found to be sufficient to resolve the signals from the intra-, and the extracellular Li^+ producing a chemical shift difference of approximately 4ppm *(2)*. At this concentration of Li^+ and shift reagent the signals were still resolved by approximately 3ppm in the presence of physiological concentrations of other cations which compete with Li^+ for the shift reagent (Na^+, K^+, Mg^{2+} and Ca^{2+}) *(3)*.

Using $Dy(P_3O_{10})_2^{7-}$, a few studies on the transport of Li^+ across the erythrocyte membrane have been carried out, initially using high concentrations of Li^+ in order to obtain adequate signal-to-noise. Quantification was usually achieved by comparing the integrals of the signals from the erythrocyte samples relative to that from a reference sample. The integrals of the signals were monitored as a function of time.

For efflux measurements, the erythrocytes were usually preloaded with Li^+ by incubating overnight in a medium containing a high, non-physiological [Li^+]. In general, it was found that the uptake of Li^+ is a slow process in erythrocytes and very little Li^+ is taken up relative to the concentration in the extracellular medium, as observed in the previous studies using AAS.

Li^+ uptake into erythrocytes from a medium containing 50mM Li^+ (25°C, 5mM $Dy(P_3O_{10})_2^{7-}$) followed single-exponential kinetics with a time constant of 14.7±1.2h, and the efflux of Li^+ from erythrocytes into a Li^+-free buffer at 25°C (preloading with Li^+ by incubating in 50mM LiCl for 24h, 37°C) was found to be extremely slow (approximately 1% per h) *(4)*. Similar uptake kinetics, with a time constant of 16.5h, were observed at 50mM Li^+ (85% haematocrit, 25°C, 5mM $Dy(P_3O_{10})_2^{7-}$) whereas a time constant of 11.6h was observed under more physiological conditions (1.8mM Li^+, 45% haematocrit, 37°C, 5mM $Dy(P_3O_{10})_2^{7-}$) *(5)*.

In another study, the uptake of Li^+ into erythrocytes incubated in a buffer containing 34mM Li^+ was slow with very little Li^+ entering the cells compared to the extracellular concentration *(6)*. The uptake was linear over the time period studied (1h) with no evidence for saturation of the intracellular [Li^+]. A similar experiment using 40mM Li^+ showed that the [Li^+] entering the erythrocytes was only approximately 10% of the $[Li+]_{out}$ *(7)*. The uptake of Li^+ into erythrocytes at a more therapeutically relevant $[Li^+]_{out}$ (2mM) was followed for 33h *(8)* and appeared to follow first order kinetics with a rate constant of 3.33×10^{-4} min^{-1}. After 24h the $[Li^+]_{in}$ was only 0.34mM giving a value for the $[Li^+]_{in} / [Li^+]_{out}$ ratio of 0.17, confirming the reluctance of erythrocytes to take up Li^+ to any extent. After 24h, half the erythrocytes were resuspended in a buffer containing 2mM $^6Li^+$ instead of 2mM $^7Li^+$, and the $[^7Li^+]_{in}$ was seen to decrease very rapidly. This was ascribed to a $^7Li^+$ - $^6Li^+$ exchange rate which was approximately 16 times faster than the rate of $^7Li^+$ uptake. In this experiment the Li-nmr spectra were recorded with a 44s delay between 90° pulses, thus obtaining the maximal signal intensity with full relaxation between pulses. Using

extracellular concentrations of 100mM for both isotopes, the uptake of $^{6}Li^{+}$ into erythrocytes was significantly faster than that of $^{7}Li^{+}$, with rates of 1.56 ± 0.12 and 1.32 ± 0.14 mmol.Li^{+} (l cells)$^{-1}h^{-1}$ and rate constants of $(6.92 \pm 0.57) \times 10^{-3}$ h^{-1} and $(5.93 \pm 0.64) \times 10^{-3}$ h^{-1} respectively *(9)*.

3.1.3 Relaxation Behaviour of Li^{+} in Erythrocytes

The T_1 and T_2 values for $^{7}Li^{+}$ blood plasma are of the same order of magnitude, that is 4.89±0.49s and 2.93±0.09s respectively. However, the T_1 and T_2 values for intracellular $^{7}Li^{+}$ in suspensions of erythrocytes are 5.10±0.56s and 0.145±0.02s, respectively, all values being determined at 25°C *(4)*. The significantly shorter T_2 inside the erythrocytes indicates the presence of some interaction with a long correlation time. Binding of Li^{+} to haemoglobin does not appear to be a contributory factor as the interaction is very weak or nonexistent; the 2 relaxation times for Li^{+} in solutions containing both LiCl and isolated haemoglobin are of the same order of magnitude *(4)*. The short T_2 inside the erythrocytes was, therefore, proposed to be due either to the relative immobilization of Li^{+} by the intracellular membrane-associated cytoskeleton, or to the slow diffusion of Li^{+} through the heterogeneous electrostatic field gradients produced by the cytoskeleton *(4)*.

3.1.4 Li^{+} Transport in Erythrocytes by the Inversion-Recovery Method

A further method for studying Li^{+} transport in erythrocytes by Li-nmr spectroscopy uses the natural differences in the T_1 relaxation times between intra-, and extracellular Li^{+} using an inversion-recovery pulse sequence. The pulse sequence is designed such that no signal is observed from the Li^{+}_{out} where T_1 is long

(approximately 20s in the absence of shift reagent), and that all the signal is observed from the Li^+_{in} where T_1 is much shorter (5s). The pulse sequence employed is:

$$D - 180° - D_1 - 90°$$

where D is a long delay to ensure the complete relaxation of the magnetizations of both the Li^+_{in} and Li^+_{out}; the 180° pulse inverts the magnetisation of both onto the -z axis; D_1 is a delay which is chosen to allow partial relaxation of Li^+_{out} signal such that, when the 90° pulse is applied, the component of magnetisation of the Li^+_{out} along the y'-axis is negligible and no signal is detected, and the relaxation of the Li^+_{in} is such that the maximum signal can be detected by the 90° pulse. Extreme care has to be taken with this method to ensure that accurate values for T_1 are obtained and, since T_1 is temperature dependent, the temperature of the samples during spectral acquisition has to be controlled. This ensures that the signal from Li^+_{out} in samples of erythrocytes will be nullified by the pulse sequence and will not contribute to the signal measured for the Li^+_{in}. The advantage of this method is that it does not involve the use of shift reagents which, by their very nature, have the potential to interfere with the transport of the cations under investigation.

A modified inversion-recovery method (MIR) was first employed to study intracellular $^{39}K^+$ *(10)*, and this was recently applied to the study of Li^+ transport in erythrocytes *(11,12)*. This modified pulse sequence employed a 60° instead of a 90° pulse, giving a faster repetition rate, and the delays used for $^7Li^+$ were 60.0 and 11.5s, for D and D_1 respectively. This value of D_1 provided only partial relaxation of the Li^+_{in} resonance and resulted in only 81% of the maximum possible signal for Li^+_{in}. After preloading a sample of erythrocytes with Li^+, the efflux of Li^+ into a choline-containing medium, due to passive transport, and into a Na^+-containing medium, due to both passive transport and to Na^+-Li^+ exchange, was investigated by this method. The difference between the two rates was taken as being due to the Na^+-Li^+ countertransport alone and the rates determined by this method were compared with

those obtained using shift reagents in Li-nmr spectroscopy and by AAS (Table 3.2) *(11)*. The rates determined by MIR were virtually identical to those obtained by using either the shift reagent $Dy(TTHA)^{3-}$ or by AAS, however those obtained using the shift reagent $Dy(P_3O_{10})_2^{7-}$ were significantly higher. Similarly, the steady-state ratio $[Li^+]_{in}$ / $[Li^+]_{out}$ was found to be similar using the MIR method, $Dy(TTHA)^{3-}$ and AAS (0.35±0.02, 0.36±0.02 and 0.36±0.02 respectively) whereas with $Dy(P_3O_{10})_2^{7-}$, the ratio was higher (0.48±0.03) *(12)*. This discrepancy was attributed to a significant amount of extracellular Li^+ complexing with the highly negatively charged $Dy(P_3O_{10})_2^{7-}$, resulting in the altered transport rate; this problem was not experienced with the lower charged, $Dy(TTHA)^{3-}$.

The MIR method also demonstrated the use of non-invasive nmr techniques to compare the Li^+ transport rates in erythrocytes from patients suffering from either bipolar disorder or hypertension and from healthy control subjects *(11,13)*. The Na^+-Li^+ countertransport rate in erythrocytes was significantly higher in the hypertensive patients, and lower in the bipolar patients than in the controls (Table 3.2), with rate constants of $0.61 \pm 0.01h^{-1}$ for the hypertensives and $0.18 \pm 0.01h^{-1}$ in the controls *(14)*. In a similar study the Na^+-Li^+ countertransport rates in erythrocytes from a group of psychiatric patients on lithium therapy were compared to those of healthy controls *(15)*. The patients studied were suffering from either schizo-, or bipolar affective disorder and none were hypertensive. The Na^+-Li^+ countertransport rates were significantly lower in the patient group (0.13 ± 0.02mmol.Li^+(l cells)$^{-1}h^{-1}$) compared to the controls (0.23 ± 0.03mmol.Li^+(l cells)$^{-1}h^{-1}$) and also the rate constants were significantly lower for the patient group ($0.12 \pm 0.04h^{-1}$ compared to $0.24 \pm 0.01h^{-1}$). This effect on the Na^+-Li^+ countertransport rates in erythrocytes was thought to be a direct consequence of the lithium therapy of these patients.

Table 3.2 Comparison of the methods for determination of the Na^+-Li^+ countertransport rates in erythrocytes from psychiatric patients and healthy controls (mmol.Li^+(l cells)$^{-1}h^{-1}$) *(11)*

TECHNIQUE	CONTROL (n=10)	BIPOLAR (n=12)	HYPERTENSIVE (n=10)
AAS	0.20 ± 0.03	0.14 ± 0.03	0.53 ± 0.02
NMR / MIR	0.21 ± 0.02	0.13 ± 0.04	0.51 ± 0.04
NMR / $Dy(P_3O_{10})_2^{7-}$	0.34 ± 0.04		
NMR / $Dy(TTHA)^{3-}$	0.22 ± 0.02		

3.1.5 Ionophore-Mediated Li^+ Transport in Erythrocytes

Ionophores are compounds which increase the permeability of membranes to ions by forming complexes with the ions. The movement of Li^+ across membranes, mediated by ionophoric antibiotics has been demonstrated using phospholipid vesicles as model systems *(16,17,18,19)*.

After preloading a sample of erythrocytes with Li^+ by incubating overnight in a buffer containing 150mM LiCl, the ionophore-induced efflux of Li^+ into both K^+-, and Na^+-containing media (with 5mM $Dy(P_3O_{10})_2^{7-}$), was followed by Li-nmr *(3)*. With the ionophore monensin, Li^+ transport into a K^+-medium followed first-order kinetics dependent on the [monensin], whereas when the K^+ was replaced by Na^+ in the medium, no Li^+ transport was observed since monensin has a much higher affinity for Na^+ than for Li^+. Two cryptands were also tested as potential Li^+ ionophores, C221 (4,7,13,16,21-pentaoxa-1,10-diazabicyclo[8.8.5]tricosane) and C211 (4,7,13,19-tetraoxa-1,10-diazabicyclo[8.5.5]eicosane), however these induced only a very slight increase in Li^+ transport compared to the unfacilitated Li^+ efflux found in the absence of ionophores *(3,20)*. It should be noted that in these experiments the interpulse delay

was only 7.5s (only 1.5 x T_1 for the intracellular Li^+ resonance) and, although only a 45° pulse was applied, this is not thought to be sufficient for full magnetic relaxation. Therefore the absolute values for the [Li^+] must be treated with caution. Additionally, the transport is dependent upon the rates of association and dissociation of the cation:ionophore complex; C221 and C211 form relatively stable Li^+ complexes such that the dissociation rate is relatively slow, resulting in slow transport.

3.1.6 Li-Nmr Visibility

For all these quantitative studies it is essential to know whether the integrals of the Li^+ resonances observed represent the actual [Li^+] present in the sample. The presence of a pool of slowly exchanging Li^+ which is subject to either a strong quadrupolar interaction, or to a low quadrupolar interaction with a long correlation time (if the molecule is tumbling slowly) will lead to a reduction in the nmr visibility. This effect has been observed in the ^{23}Na-nmr spectra for intracellular Na^+ in erythrocytes where only 80% of the Na^+_{in} present is actually nmr-visible *(21)*. In one study all the Li^+ present in the nmr samples was reported to be nmr visible and, after lysing the erythrocytes to remove all the solubilized Li^+, no membrane-associated Li^+ was observed by Li-nmr *(4)*.

One method to assess the nmr visibility is to compare the values obtained by nmr with those obtained by other analytical techniques, such as AAS. However, for intracellular species, these techniques generally involve physical separation and washing of the cells, and great care is necessary to avoid the loss of any of the Li^+ during the procedure. By this method Hughes *(7)* found the values for the $[Li^+]_{out}$ were very similar by the two techniques, but the values for $[Li^+]_{in}$ determined by Li-nmr were 2-4 times smaller than those determined by AAS. This discrepancy was attributed to invisibility of some of the intracellular Li^+ due to binding to the cell membranes and/or to intracellular components. However the nmr spectra for both the

above experiments were recorded using only a 6s interval between the 45° pulses which is probably not sufficient for full relaxation of the intracellular Li^+ ($T_1 \approx 5s$ *(3,4)*); this would result in a lower signal intensity and correspondingly lower values for $[Li^+]_{in}$.

A method involving comparison of the integrals of the nmr resonance from Li^+ in intact cells to that after the cells have been treated with detergent has also been employed *(12)*. The detergent was used to solubilize the membrane and thus free any membrane associated Li^+ and it was found that there was no invisibility in the Li^+ signal from the intact erythrocytes. This data is in contrast to that reported by Gullapalli *et al*, who compared the integrals of the signals from Li^+ in packed erythrocytes, of known total $[Li^+]$, to the signals from Li^+ in solutions of LiCl at the same concentrations *(5)*. The results are shown in Table 3.3 and show that at levels typically observed in blood plasma during therapy the nmr visibility of $^7Li^+$ is reduced to ca. 85%. A comparison of the nmr results for both intra-, and extracellular $[Li^+]$ with those determined by ICP-AES showed the same visibility for both compartment. AAS analysis showed that very little Li^+ (1%) remained in the cell fragments produced by lysing and repeated washing of the erythrocytes indicating that the reduced visibility is probably not attributable to any strongly bound Li^+. In this work, however, no loss of signal intensity of the Li^+ resonances was experienced from the samples of packed erythrocytes when compared to those from aqueous solutions containing the same concentrations of LiCl (Section 2.1.4), in agreement with Mota de Freitas *et al (12)*.

Table 3.3 Variation in ^7Li-nmr visibility with $[Li^+]$ in erythrocyte samples *(15)*

$[Li^+]$ / mM	40	10	5	1
Visibility / %	97	92	86	84

3.2 Li^+ Uptake into Erythrocytes Using ^7Li-Nmr Spectroscopy

In this study, the uptake of Li^+ into human erythrocytes was monitored *in vitro* by isolating erythrocytes from whole blood and resuspending them at 37°C in an isotonic medium containing 2mM Li^+ - a concentration only slightly higher than that found in the blood plasma during lithium therapy. The medium was designed to maintain the viability of the erythrocytes and their transport functions. The concentration of Li^+ in the extracellular space was kept constant at 2mM and the intracellular concentration was determined by quantitative ^7Li nmr spectroscopy. 90° pulse width measurements and T_1 determinations for ^7Li were carried out to ensure that both the maximum signal intensity and full magnetic relaxation between pulses for all Li^+ species present was achieved. The T_1 values for all the Li^+ species encountered in this work are shown in Table 3.4.

The longest T_1 in the erythrocyte samples was 5.75±0.08s due to the intracellular Li^+ and is comparable to the reported values of 5.10±0.56s *(4)* and 5.7±0.06s *(5)*. Therefore, for valid quantification of the [Li^+] in the following experiments, an interpulse delay of 30s (> 5 x T_1) was employed to ensure complete relaxation of all the Li^+ species. The aqueous shift reagent, $Dy(P_3O_{10})_2^{7-}$ (from 0.5mM Dy^{3+} and 15mM $P_3O_{10}^{5-}$) was included in the incubating buffer ; at this concentration, the chemical shift difference between the nmr resonances from the intra-, and the extracellular Li^+. was typically 0.6ppm and the line widths at half-height were typically 20Hz and 10Hz, respectively.

Table 3.4 $\omega_{1/2}$ and T_1 values for the various Li^+ species encountered during the ^7Li-nmr studies of erythrocytes

Li^+-Containing Medium	$\omega_{1/2}$ / Hz	T_1^* / s
LiCl (2mM)	2	18.66 ± 0.10
Buffer B (2mM Li^+)	4	0.408 ± 0.006
Buffer B (in samples of packed erythrocytes)	12 - 18	0.319 ± 0.004
Blood plasma (0.4mM Li^+)		10.34 ± 0.38
Erythrocytes, intracellular (after 18h incubation in Li^+-free media)	8 - 10	5.679 ± 0.026
Erythrocytes, intracellular (after 24h incubation in buffer B at 37°C)	8 - 10	5.754 ± 0.083

*T_1 values are from single determinations using the inversion-recovery technique

3.2.1 $^7Li^+$ Uptake Into Erythrocytes from Healthy Controls

The blood from a healthy volunteer from within the chemistry department was obtained and the erythrocytes were isolated and resuspended in Buffer A until required. After resuspending in Buffer B and incubating at 37°C, the uptake of Li^+ into the erythrocytes was followed with time. Figure 3.1 shows a series of ^7Li nmr spectra from a typical experiment. The spectra of the erythrocytes show two signals, one at -0.64ppm assigned to the extracellular Li^+ ($\omega_{1/2}$ = 22Hz) and one at 0ppm assigned to the intracellular Li^+ ($\omega_{1/2}$ = 10Hz). The chemical shift of the resonance from the intracellular Li^+ is identical to that observed in the absence of shift reagent and does not change over the course of the experiment, confirming that the shift reagent does not

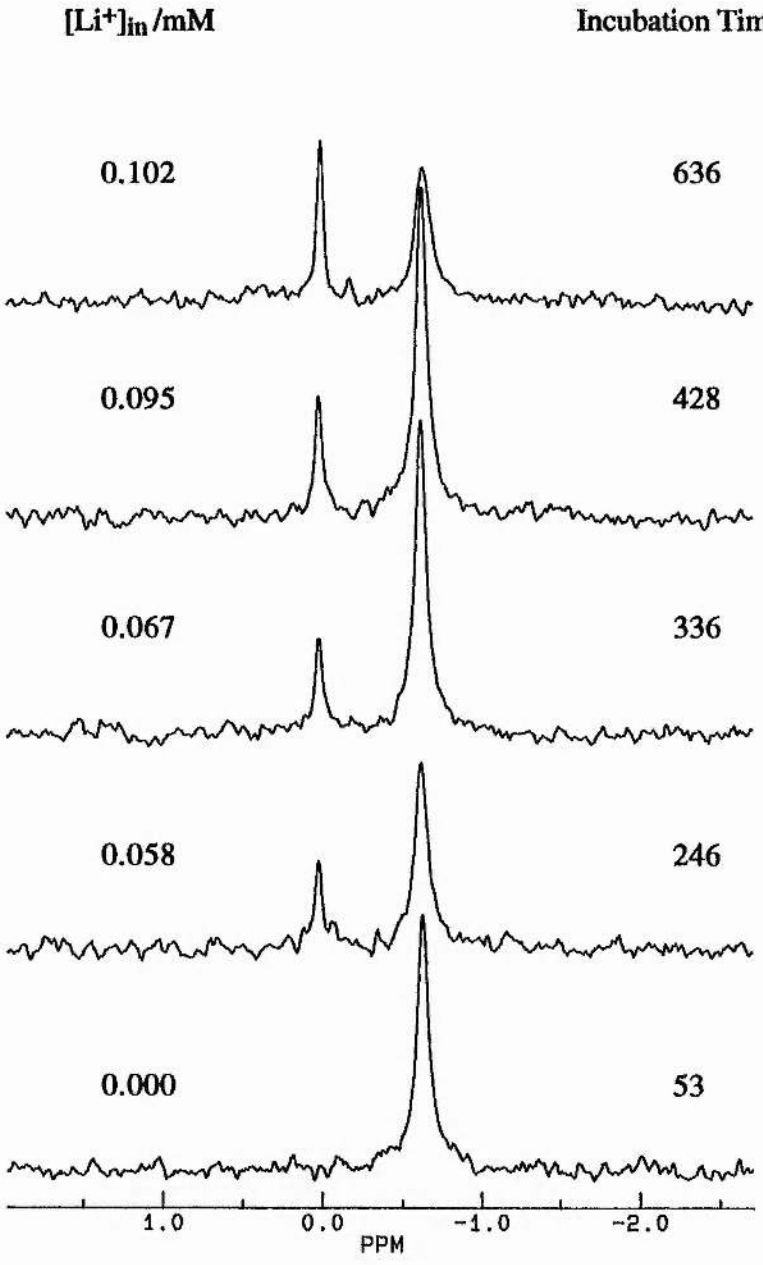

Figure 3.1 ^{7}Li-nmr spectra of human erythrocytes incubated in Buffer B (containing 2mM Li^+) showing time dependence of the intracellular [Li^+] (Each spectrum is the sum of 100 acquisitions recorded at 194MHz on the MSL500 nmr spectrometer)

penetrate the erythrocyte membrane under the conditions used. The chemical shift of the resonance from the extracellular Li^+ is also unchanged throughout the experiment confirming that the pH of the extracellular medium remains constant; the chemical shift induced by $Dy(P_3O_{10})_2^{7-}$ is very pH dependent at physiological pH *(22)*. The signal from the intracellular Li^+ increases in intensity with respect to time and, from the integrals of the peaks, the haematocrits of the samples and the corresponding intracellular Li^+ concentrations were calculated.

The experiment was repeated several times with erythrocytes from a number of healthy individuals and the results obtained were very similar. The time dependence of the $[Li^+]_{in}$ from a typical experiment is shown in Figure 3.2A. Throughout the experiment the $[Li^+]$ inside the erythrocytes is low compared with the extracellular concentration, in agreement with previous studies of this kind; after 24h the ratio $[Li^+]_{in}$ /$[Li^+]_{out}$ is only approximately 0.06. This compares with a ratio of approximately 0.1 found at 40mM Li^+_{out} *(7)*, but is lower than that observed at 2mM (0.17) *(8)*. Li^+_{out}, the latter possibly due to the difference in the composition of the incubating medium.

3.2.2 $^7Li^+$ Uptake Into Erythrocytes from Psychiatric Patients on Lithium Therapy

Similar experiments were carried out on the erythrocytes of patients suffering from bipolar affective disorder and stabilised on lithium therapy. Since Li^+ was already present in these erythrocytes as a result of the medication, the experimental protocol was designed to remove as much of this as possible before the uptake experiment was performed. The erythrocytes were incubated overnight in a Li^+-free medium prior to the uptake experiment. However, a varying amount of intracellular Li^+ persisted (0 - 0.13mM); this was quantified by Li-nmr prior to changing to the Li^+-containing medium for the uptake experiment. To investigate the reason for this prevailing $[Li^+]_{in}$,

T_1 measurements were determined for both the low $[Li^+]_{in}$ persisting after the overnight incubation in Li^+-free medium and the $[Li^+]_{in}$ accumulated after 24h incubation in Li^+-containing medium at 37°C (Table 3.4). The T_1 for any relatively immobilised Li^+, for example due to binding to the erythrocyte membrane or to the cytoplasm, should be considerably shorter than that for the free aqueous Li^+ in the intracellular water. Interestingly the two T_1 values were virtually identical, inferring that the micro-environments of the two Li^+ species were probably the same. Thus, the reason for the low level of Li^+ remaining in the erythrocytes of the patients was not elucidated.

The result from a typical Li^+ uptake experiment using the erythrocytes from a lithium-treated patient is shown in Figure 3.2B. The uptake behaviour is similar to that observed for the healthy individual in Figure 3.2A with a low $[Li^+]_{in}$ compared to the $[Li^+]_{out}$ over the time period studied. However after 24h, $[Li^+]_{in}$ / $[Li^+]_{out}$ is higher than that of the healthy individual (approximately 0.08 compared to approximately 0.06) due to the higher $[Li^+]_{in}$ accumulated in these erythrocytes.

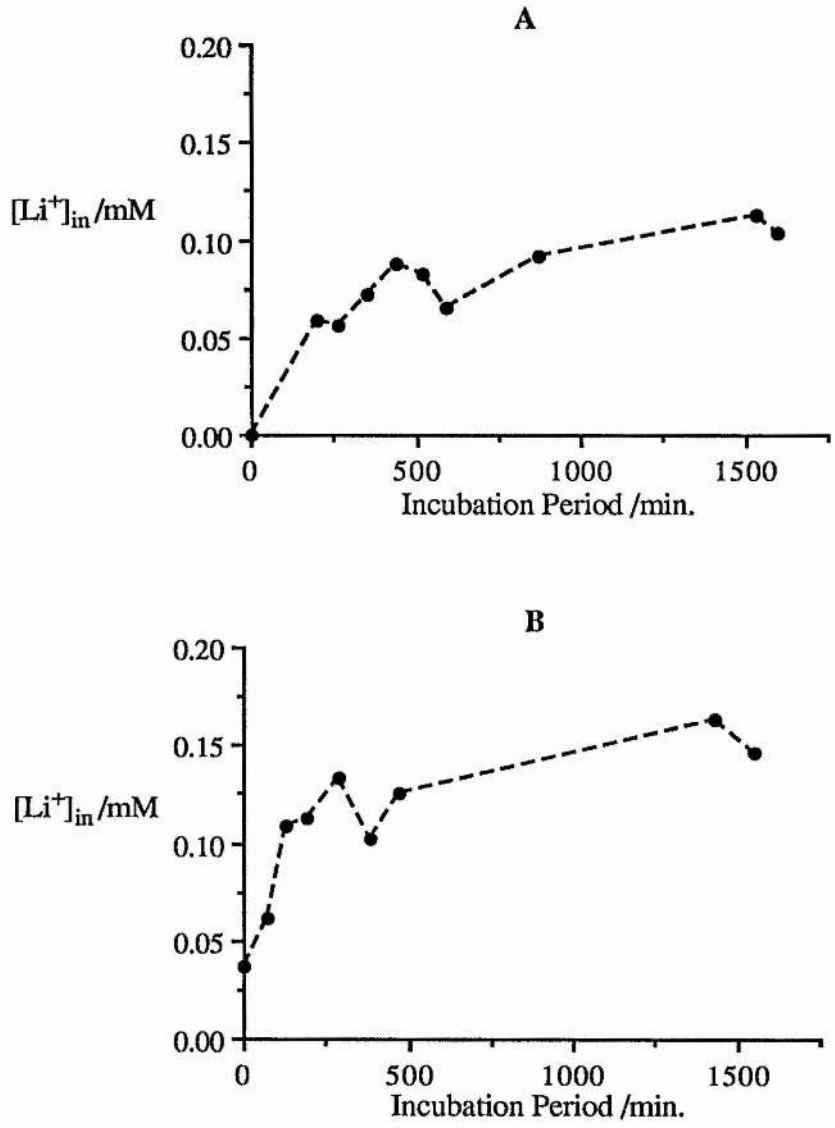

Figure 3.2 The uptake of Li^+ into the erythrocytes of a healthy individual **(A)** and a patient on lithium therapy for the treatment of bipolar disorder **(B)**

($[Li^+]_{out}$ = 2mM, 37°C)

3.2.3 Comparison of Li^+ Uptake in Erythrocytes from Psychiatric Patients on Lithium Therapy and Healthy Controls

Using identical experimental protocols Li^+ uptake experiments were then carried out on the erythrocytes from 11 healthy volunteers as controls, none of whom had any history of affective disorders or had undergone any lithium therapy, and on 9 patients on lithium therapy for the treatment of bipolar disorder. No attempt was made to match the subjects for age, sex or ethnic origin, or to control for the diet or medication of any of the subjects.

In both groups of people there was little variability in the uptake profiles between the individuals. The inter-, and intraindividual variability in the uptake of Li^+ is demonstrated in Figure 3.3 which shows the Li^+ uptake into the erythrocytes of 3 controls (A), 3 patients (B) and 1 healthy individual on 4 separate occasions spanning a 3-year period (C). The interindividual variability in the control group is similar to the variability in the repeat experiment for the single control, and is probably due to the experimental procedure rather than any variability in the transport processes. There is significantly more variation in the patient group than in the controls and obviously this may originate from the different levels of Li^+_{in} present at the start of the experiment for each patient. However this behaviour may be related to the psychiatric disorder or be a result of the different medication regimes of the patients.

Figure 3.3C also illustrates that there is no difference in the Li^+ uptake behaviour of the erythrocytes resulting from the two different anticoagulants used for collecting the blood samples in these experiments.

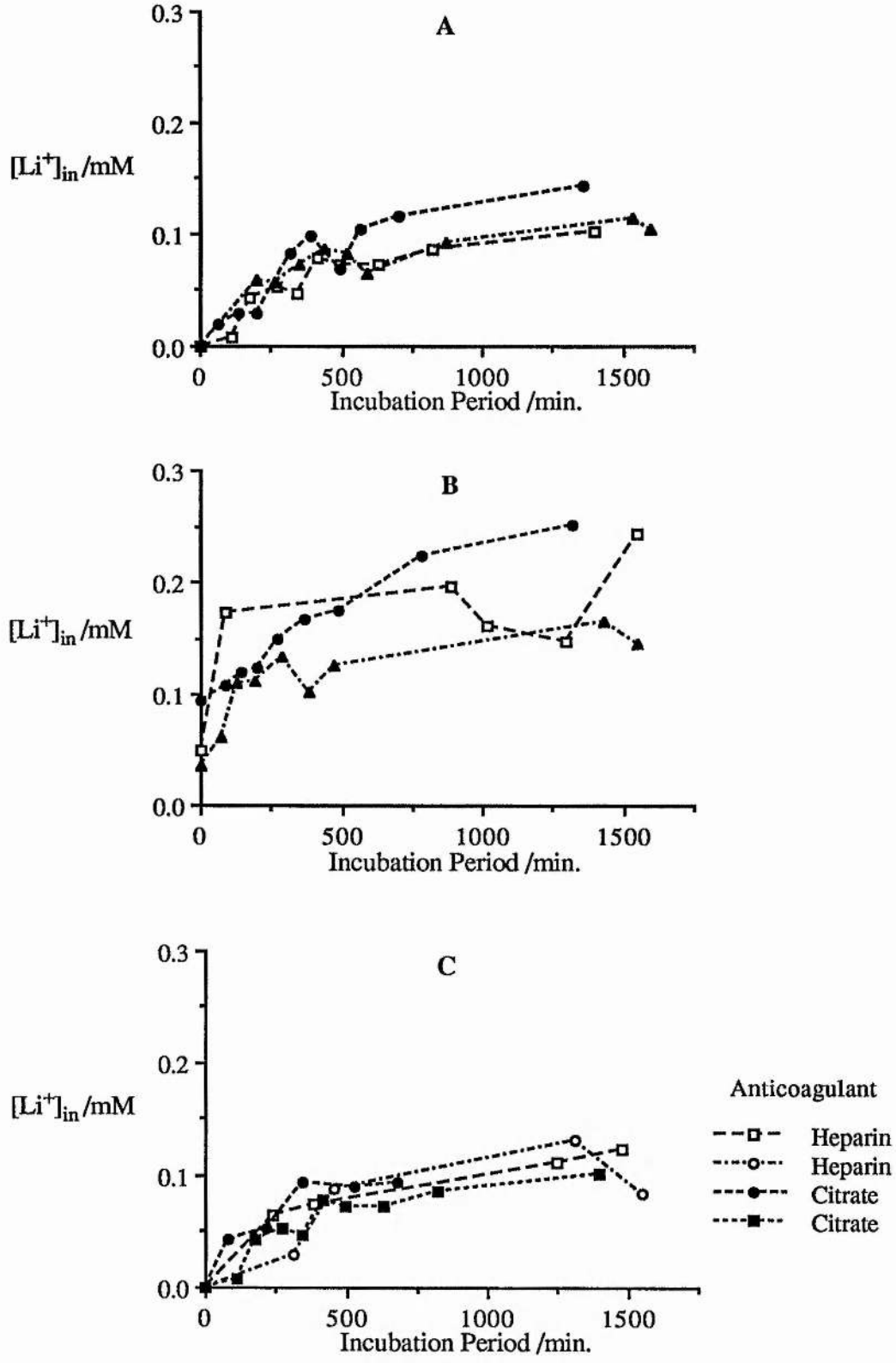

Figure 3.3 Li^+ uptake into erythrocytes from 3 healthy controls (**A**), 3 patients on lithium therapy (**B**), and 1 healthy control on 4 occasions spanning 3-years (**C**)

Figure 3.4 shows a comparison of the combined results for the 12 controls and the 9 patients. Each data point represents the mean of the $[Li^+]_{in}$ for all the controls (and patients) over 200minute periods, and the error bars comprise of both the biological variability and the experimental error. The amount of variability in the patient group is obviously greater than that for the controls. Despite the fact that the patient group contains an initial mean $[Li^+]_{in}$ of 0.080mM, a comparison of the two uptake profiles shows that the uptake of Li^+ is very similar over the first few hours however, in the patients' erythrocytes, the $[Li^+]_{in}$ attains saturation after 6-8h (at approximately 0.2mM) whereas, in the erythrocytes of the controls, the uptake is still continuing after 24h, albeit at a reduced rate. Data was not collected for longer periods of time as the appearance of the suspension altered gradually, with the cells becoming darker and signs of haemolysis developing. It is therefore possible that these erythrocytes would have eventually reached the same $[Li^+]_{in}$ as those of the patient group.

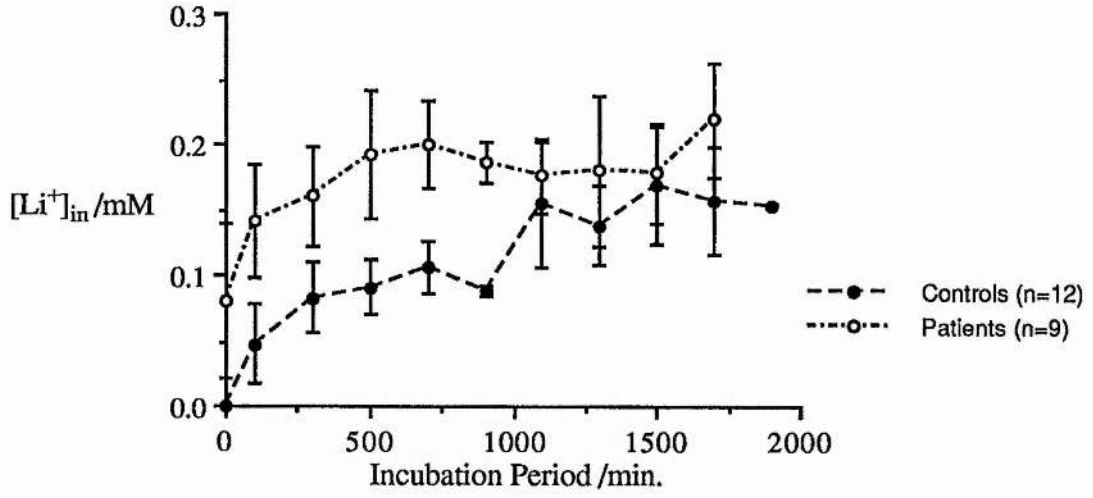

Figure 3.4 Comparison of the uptake of Li^+ into the erythrocytes of healthy controls and of psychiatric patients on lithium therapy
(The error bars indicate SEM values)

3.2.4 Effect of Lithium Therapy on Li^+ Uptake into Erythrocytes from Two Healthy Individuals

Two healthy volunteers (1 male and 1 female), with no previous experience of Li^+ treatment and no personal or familial history of psychiatric illnesses, underwent a course of Li^+ treatment (3 and 4 weeks respectively) in order to determine its the effect upon the uptake of Li^+ into erythrocytes. For each volunteer venous blood was drawn prior to starting, and at weekly intervals throughout the treatment period. For each experiment the plasma [Li^+] was determined and a Li^+ uptake study carried out as before using ^7Li nmr spectroscopy.

Lithium treatment was administered and monitored by psychiatrists from the Royal Liff Hospital, Dundee. Prior to the commencement of treatment, both volunteers underwent physical examination by the psychiatrists and their bloods were tested for electrolyte imbalance, for thyroid function and, in the case of the female, for pregnancy.

Volunteer A, a 50 year old Caucasian male, was given a daily dose of 750mg Li_2CO_3 in the form of Camcolit tablets (3 x 250mg taken at regular intervals during the day). He reported no significant ill effects for the first few days other than a slightly dry mouth, thirst and increased urination. After 1 week he reported a slight nausea and slight cognitive impairment: he described the feeling as 'like having a slight hangover'. These symptoms lasted for another week however after 3 weeks he was no longer feeling any side effects. After the first week of treatment the average plasma [Li^+] throughout the treatment period was 0.51mM (range 0.47 - 0.58mM). The results of Li^+ uptake experiments are shown in Figure 3.5A. Taking into account the initial $[Li^+]_{in}$, the uptake profiles after 7 and 14 days treatment are virtually identical to that prior to the treatment and are similar to those observed for the healthy controls in Figure 3.4. After 24h the ratio $[Li^+]_{in}$ / $[Li^+]_{out}$ is approximately 0.05. However, after 21 days the uptake profile is significantly different - the initial uptake curve is steeper and

the $[Li^+]$ taken up by the erythrocytes is higher with $[Li^+]_{in}$ / $[Li^+]_{out}$ of approximately 0.12 after 24h. This profile is similar to those observed for the patient group in Figure 3.4. One week after stopping the treatment a further uptake experiment was performed. No Li^+ was found in either the blood plasma or in the erythrocytes and the uptake profile (not shown) was very similar to that obtained prior to the treatment; the ratio $[Li^+]_{in}$ / $[Li^+]_{out}$ after 24h was 0.06.

Volunteer B, a 28 year old Caucasian female, was given a daily dose of 1000mg Li_2CO_3 in the form of Priadel tablets (5 x 200mg to be taken at night). She experienced severe discomfort during the first night and throughout the first week, with significant thirst and increased urination. Unfortunately, she was suffering from flu-like symptoms when she started the treatment and became quite ill during the first week. After seven days she suffered bad headaches, dizziness, tinnitus and vomiting, and subsequently reduced the daily dose to 800mg. Any distinct side effects caused by the Li^+ treatment were, therefore, difficult to identify. The thirst and polyuria became less significant but persisted at a reduced level over the next two weeks; occasional waves of nausea and a general feeling of lethargy were experienced throughout the treatment period. These symptoms disappeared after stopping the Li^+ medication but this may also be due to coincidental recovery from the virus. The average plasma $[Li^+]$ determined by ISE was 0.58 after 4 days, and 0.49 (range 0.48 - 0.50) after the dose had been reduced. The Li^+ uptake results are shown in Figure 3.5B and, taking into account the initial $[Li^+]_{in}$, there is no change in the uptake behaviour of the erythrocytes over the time period studied. The curves are all similar to those for the control group in Figure 3.4; the ratio $[Li^+]_{in}$ / $[Li^+]_{out}$ was approximately 0.05 after 24h.

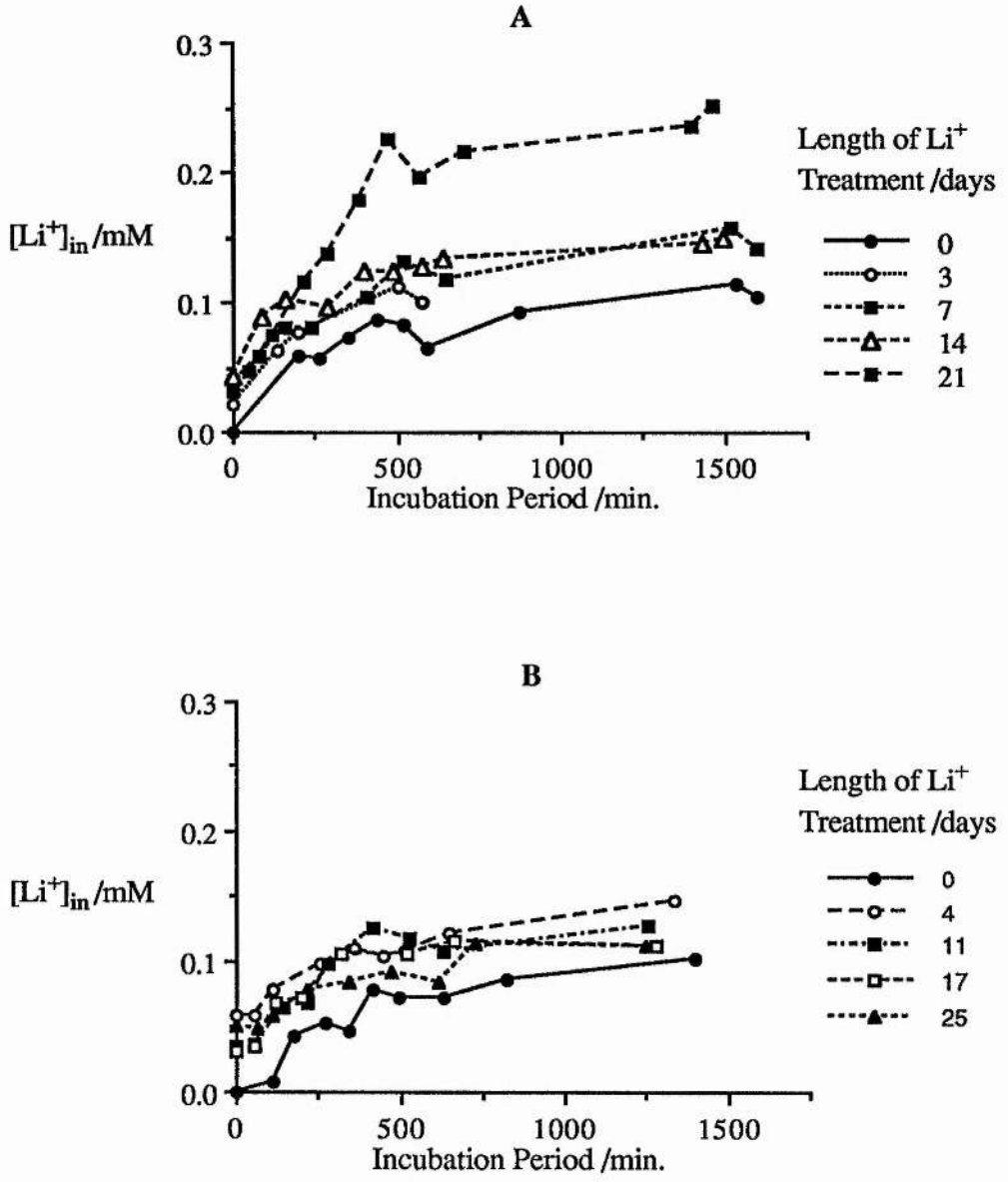

Figure 3.4 The effect of lithium treatment on the Li^+ uptake behaviour of erythrocytes from two healthy individuals (**A** male, **B** female)

3.2.5 Effect of Lithium Therapy on Li^+ Uptake into Erythrocytes from Patients Suffering from Bipolar Affective Disorder

Li^+ uptake behaviour was also studied in the erythrocytes of a number of patients diagnosed as suffering from bipolar affective disorder, when they commenced lithium treatment. These were all patients at the Royal Liff Hospital, Dundee under the supervision of the consultant psychiatrist, Dr G. Naylor.

Patient AR, a 78 year old female in-patient who had not been previously treated with Li^+, had very rapid mood swings prior to therapy. These were significantly reduced after about 10 days on lithium therapy. This patient was also taking antidepressants. The Li^+ uptake behaviour is shown in Figure 3.6A. Prior to treatment the uptake was very slow and was at the lower end of the range of that observed for the control group. There was no significant change after 4 days on Li^+ therapy however a difference was observed after 14 days. The initial uptake was faster and a higher $[Li^+]_{in}$ was attained; after 12h incubation, the ratio $[Li^+]_{in} / [Li^+]_{out}$ was approximately 0.1 compared to only 0.06 after 4 days therapy. There was no further change in the uptake behaviour during the period studied; after 21 and 28 days therapy the uptake profiles were similar to that after 14 days with, interestingly, a very similar $[Li^+]_{in}$ attained irrespective of the initial $[Li^+]_{in}$.

Patient JD, also female, had taken Li^+ previously several years ago. Unfortunately it was not possible to perform a Li^+ uptake experiment prior to the patient commencing the lithium therapy. After only 4 days treatment the uptake curve in Figure 3.6B was similar to that observed in the patient group, however after 11 and 25 days treatment, the accumulation of intracellular Li^+ was unusually excessive, even for a patient, with $[Li^+]_{in} / [Li^+]_{out}$ ratios of over 0.13. After 19 days treatment the uptake curve was almost identical to that after only 4 days. It is unlikely that these inconsistencies are due to non-compliance with the medication since this person was an in-patient at the hospital at the time of commencing lithium therapy.

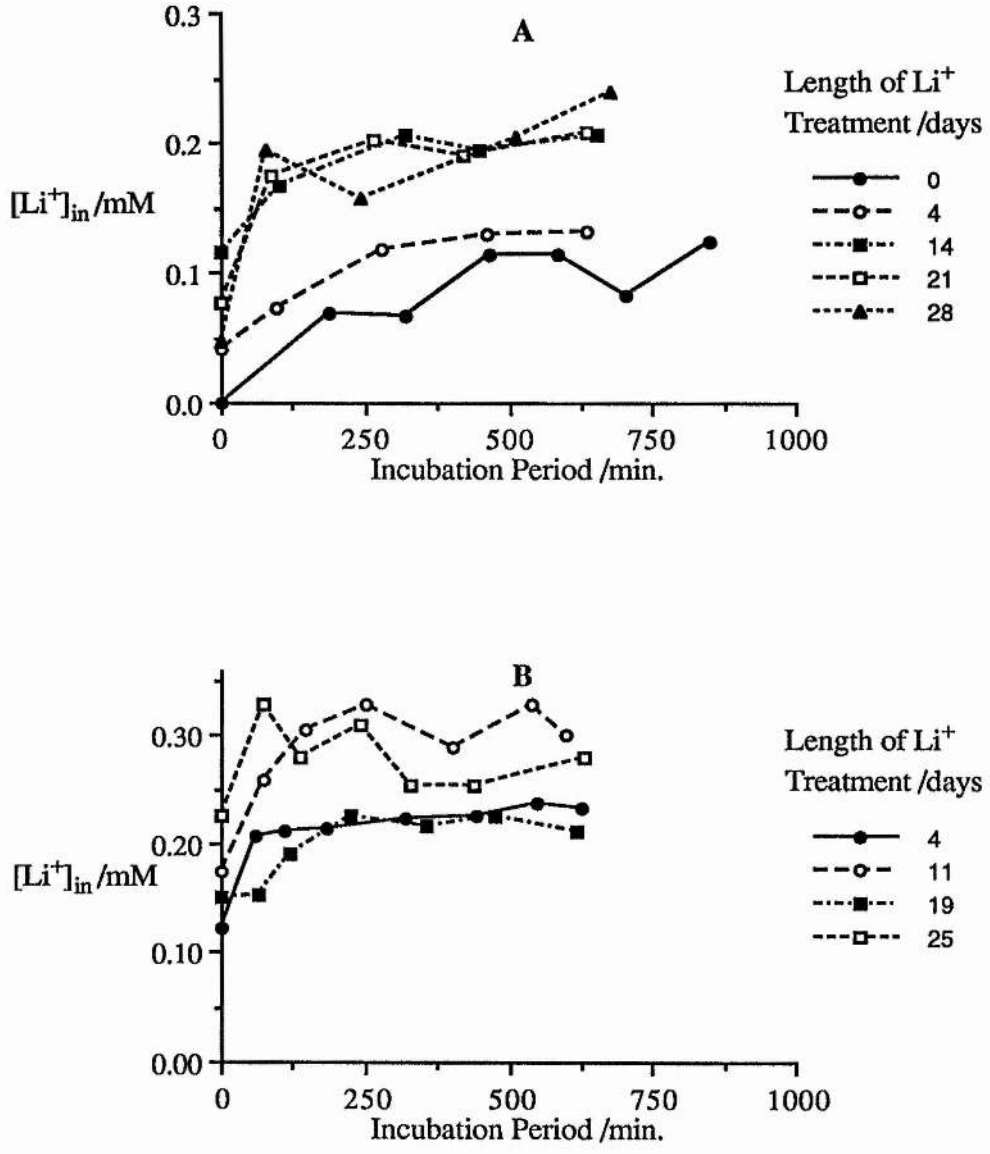

Figure 3.6 The effect of commencing lithium treatment on the Li^+ uptake behaviour of erythrocytes from 2 patients suffering from bipolar affective disorder, who had: **(A)** never been treated with Li^+ previously, **(B)** been treated with Li^+ previously but had not taken it for many years

Patient MP, a female in-patient, had taken Li^+ before but the treatment had been stopped 6 months previously, as she was not compliant. with the medication. Li^+ was used as a prophylactic treatment; she was also taking ECT and chloropromazine. Figure 3.7A illustrates that there was a very slight change in the uptake profiles after only 3 days therapy, and thereafter the uptake curves were very similar.

Patient BK, a female in-patient, had taken Li^+ before but had stopped 5 months previously. This patient was depressed and showed no obvious response after 7 days therapy. She was also taking carbamazepine. Figure 3.7B illustrates that there was no change in the Li^+ uptake behaviour of the erythrocytes of this patient; the uptake followed the pretreatment curve, even after 42 weeks therapy.

Patient CT, a 58 year old female, had previously been treated with Li^+ but had not taken it for 8 months. She had previously had a long period of depression followed by acute mania and this period of Li^+ therapy was started while she was suffering from depression in order to try to avoid the manic episode. This person was an out-patient and was not compliant with her medication, reducing her dosage by two-thirds soon after commencing the treatment. At 4, 21 and 28 days, the erythrocytes of this patient accumulated a significant amount of Li^+ (ratio of 0.13). However, after only 14 days, the uptake curve was similar to the pretreatment profile, possibly as a consequence of the patient's non-compliance (Figure 3.7C).

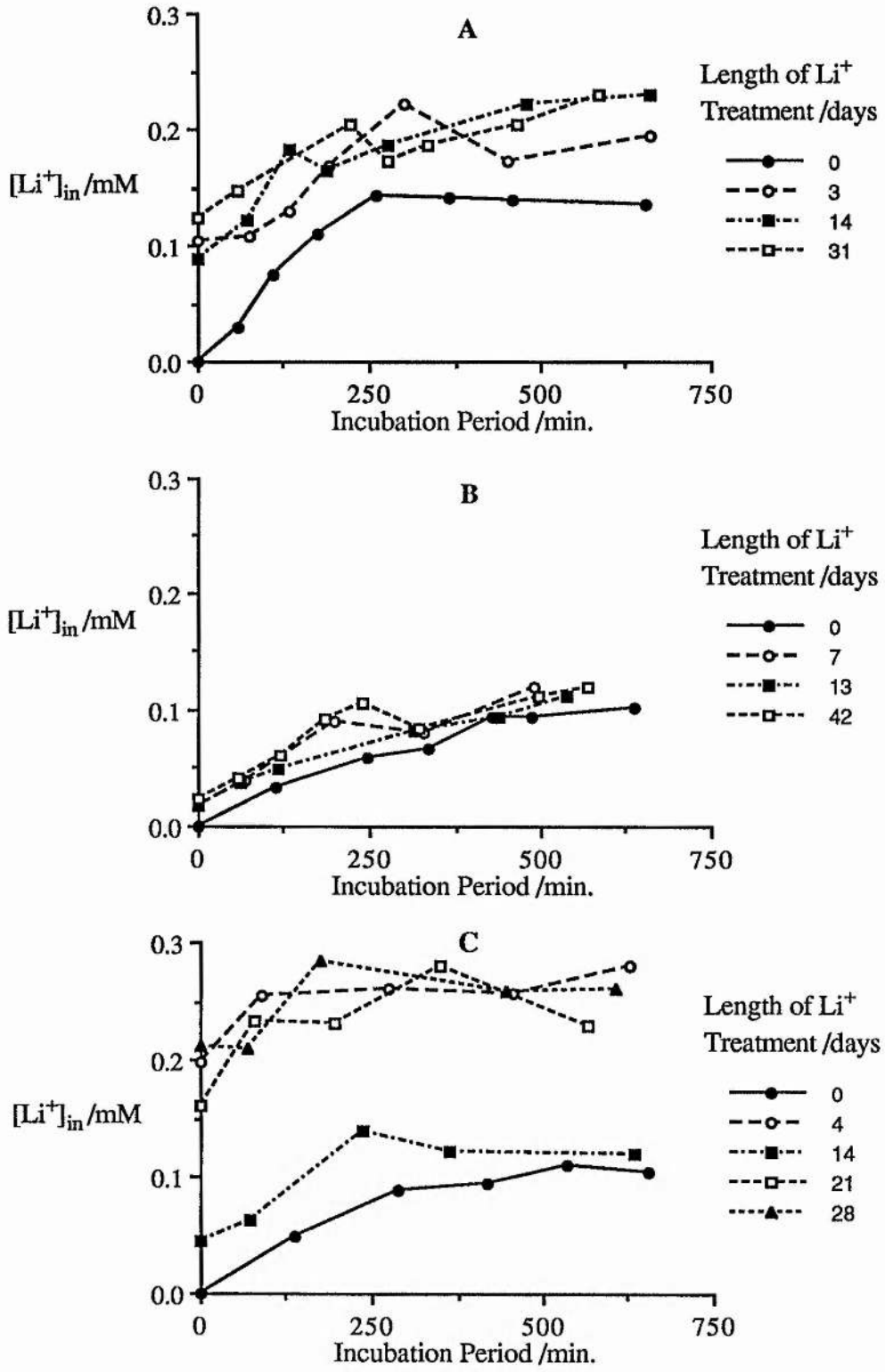

Figure 3.7 The effect of commencing lithium treatment on the Li^+ uptake behaviour of erythrocytes from 3 patients suffering from bipolar affective disorder, who had been treated with Li^+ previously but had not taken it for: **(A)** 6 months; **(B)** 5 months; and **(C)** 8 months

3.2.6 Effect of Extracellular [K+] on Li+ Uptake into Erythrocytes

In the above studies the extracellular [K+] was 16.8mM. To investigate the Li+ uptake into erythrocytes at physiological [K+] similar experiments were performed at 5mM K+ by replacing of some K+ in the incubating medium with Na+. In Figure 3.8 the results are compared with those at 16.8mM K+ and those at a higher [K+] of 32mM. The latter concentration was used for comparison purposes only. The uptake behaviour is very similar for all 3 concentrations; there is no significant difference between the Li+ uptake at 16.8 and 32mM K+. At 5mM K+, the $[Li^+]_{in}$ appears to be very slightly higher than for the higher K+ concentrations but this only becomes significant after approximately 10h.

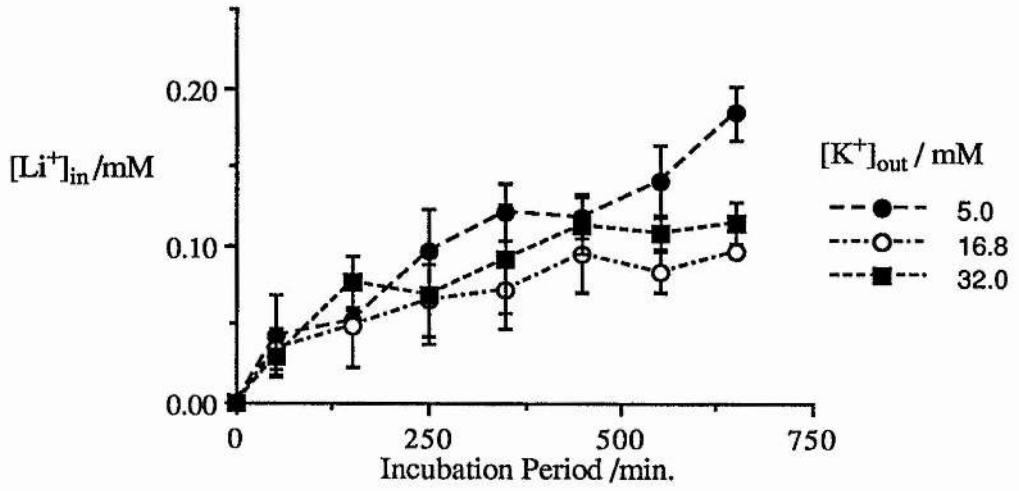

Figure 3.8 The effect of extracellular [K+] on the uptake of Li+ into erythrocytes from healthy individuals

3.3 Uptake of Li^+ into Rat and Rabbit Erythrocytes

Using identical experimental protocols to that in the previous studies, the uptake of Li^+ into both rat and rabbit erythrocytes was studied. The results are shown in Figure 3.9. In rat erythrocytes the uptake of Li^+ was linear with time, with a rate of 0.05mM Li^+h^{-1}, no saturation was observed in the time period studied and, after 10h the $[Li^+]_{in}$ was approximately 0.5mM (Figure 3.9A). This is much higher than was observed in any of the human studies. However, in rabbit erythrocytes, the initial uptake was very rapid and saturation at approximately 0.14mM Li^+_{in} was attained within approximately 2h (Figure 3.9B).

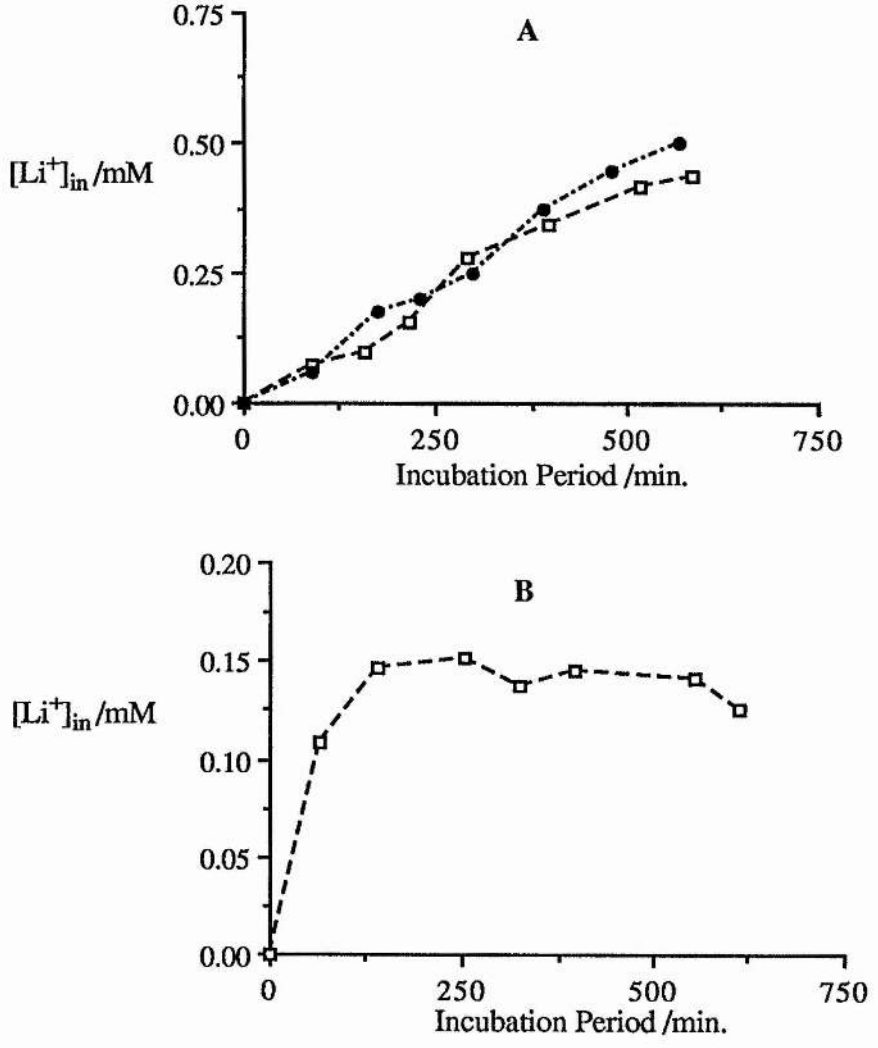

Figure 3.9 The uptake of Li^+ into erythrocytes of **(A)** 2 rats and **(B)** 1 rabbit

3.4 Discussion

The results obtained illustrate the potential for the non-invasive study of Li^+ transport in the erythrocytes of psychiatric patients. The accumulation of Li^+ in erythrocytes is low compared to the extracellular concentration, as observed previously *(7,8)*. The higher accumulation of Li^+ in the patients group in Figure 3.4 is consistent with the higher Li^+ ratio observed for psychiatric patients on Li^+ therapy, and may be due to the inhibition of the Na^+-Li^+ countertransport, the predominant mechanism of Li^+ efflux in erythrocytes *(15,23)*. Assuming there is no change in the two Li^+ influx pathways in erythrocytes, the 'leak' and the anion-exchange routes, inhibition of the Li^+ efflux pathway will result in a higher intracellular [Li^+] at steady-state. Interestingly, in the erythrocytes of all the psychiatric patients who were studied prior to commencing lithium therapy, the uptake of Li^+ was similar to that of the control group. This is contrary to the studies which report an altered Na^+-Li^+ countertransport mechanism in affective patients *(24)*.

The data from the control group, for the uptake of Li^+ into erythrocytes over the first 10h, gives a 1st order rate constant of 4.93×10^{-3} min^{-1} (correlation coefficient of 0.977), and a corresponding half-life of 2.3h. This is faster than that of a similar experiment in which a rate constant of 3.33×10^{-4} min^{-1} for the uptake of Li^+ was reported *(8)*. The difference may be because the reported value was calculated from data over a much longer time period than this work (33h compared to 10h), or may be due to differences in the experimental conditions. Perhaps more importantly the reported value was the result of only a single experiment, compared to the averaged data for twelve such experiments in this work.

The results for the male control on commencing lithium treatment clearly show a Li^+-induced change in the uptake of Li^+ which occurred after 3 weeks treatment (Figure 3.5A). Thus it may be that treatment with Li^+ is also responsible for the altered Li^+ uptake behaviour observed in the patients stabilised on lithium compared to the controls

(Figure 3.4). This is consistent with the Li^+-induced inhibition of the Na^+-Li^+ countertransport previously reported *(23)*. A similar Li^+-induced effect on the uptake of Li^+ into erythrocytes was observed after 2 weeks Li^+ treatment for patient AR (Figure 3.6A), and after only a few days treatment for patients MP, CT and JD (Figures 3.7A, C and 3.6B, respectively). However, in the latter case, this cannot be confirmed since no pre-treatment experiment was performed. The different time delays before an effect was obtained may be related to the observed variability in the time periods before a clinical effect of Li^+ occurs in patients, or alternatively may be related to the psychotic state of the patients on commencing therapy.

The absence of an effect in the female control after 4 weeks Li^+ treatment (Figure 3.5B) and in one of the patients after 6 weeks therapy (Figure 3.7B) may be due to other medical factors, such as the illness suffered by the control, or to the additional medications, or alternatively it may possibly indicate that these people are non-responders to Li^+ treatment. It is also possible that these people need to take Li^+ for longer periods before the Li^+ uptake behaviour is altered.

In the patients commencing Li^+ therapy, there was no control over many factors which may have contributed to the inconsistent Li^+ uptake results. For instance, the time the blood sample was taken relative to the previous administration of Li^+ or of other medications, or to the time of the previous meal, was not controlled. Also, the psychiatric state of the patient at the time of acquiring the sample was not known. An extended study, with more control over such factors, and with a larger number of patients would be required to determine the origin of these inconsistencies. Additionally, similar studies with patients suffering from different psychiatric disorders (bipolar, unipolar) or with patients in different psychotic phases (mania, depression, normal) could be undertaken. It has been reported that the Li^+_{in} / Li^+_{out} ratio and/or the activity of the Na^+-Li^+ countertransport process may be related to the nature of the disorder *(11,13,14,24)*, or to the psychotic state of the patient *(25)*.

At first glance, the absence of any effect of changing the extracellular [K^+] upon the transport of Li^+ might have been predicted. The two passive Li^+ influx pathways and the Na^+-Li^+ countertransport mechanism are not directly affected by the $[K^+]_{out}$. However, changes in the $[K^+]_{out}$ were achieved by corresponding changes in the $[Na^+]_{out}$ to maintain the osmolarity of the medium. Therefore, the transmembrane Na^+ and K^+ concentration gradients were altered and this might be expected to interfere with the Na^+-dependent Li^+ efflux mechanism. Unfortunately, under the conditions used there was no apparent effect on the Li^+ transport behaviour.

The linear uptake of Li^+ into rat erythrocytes and the higher accumulation of Li^+ (Figure 3.9A), relative to human erythrocytes, is consistent with the absence of a Na^+-Li^+ countertransport system in the erythrocytes of this mammal *(26)*. However, this transport mechanism is present in the erythrocytes of many other mammals, including rabbits, and generally the activity of this process is increased relative to that in human erythrocytes *(26)*.

3.5 References

1 Laszlo, P. (1982), in *The Multinuclear Approach to NMR Spectroscopy*, Lambert, J.B. and Riddell, F.G. (eds), D. Reidel Publishing Co., Holland, chapter 12.

2 Espanol, M.C. and Mota de Freitas, D. (1986), *Biophys. J.*, **49**, 326a.

3 Espanol, M.C. and Mota de Freitas, D. (1987), *Inorg. Chem.*, **26**, 4356-4359.

4 Pettegrew, J.W., Post, J.F.M., Panchalingham, K., Withers, G. and Woessner, D.E (1987), *J. Mag. Res.*, **71**, 504-519.

5 Gullapalli, R.R., Hawk, R.M. and Komoroski, R.A. (1991), *Mag. Res. Med.*, **20**, 240-252.

6 Partridge, S., Hughes, M.S., Thomas, G.M.H. and Birch, N.J. (1988), *Biochem. Soc. Trans.*, **16**, 205-206.

7 Hughes, M.S., Flavell, K.J. and Birch, N.J. (1988), *Biochem. Soc. Trans.*, **16**, 827-828.

8 Riddell, F.G., Patel, A. and Hughes, M.S. (1990), *J. Inorg. Biochem.*, **39**, 187-192.

9 Abraha, A., Dorus, E. and Mota de Freitas, D. (1991), *Lithium*, **20**, 118-121.

10 Seo, Y., Murakami, M. Suzuki, E. and Watari, H. (1987), *J. Mag. Res.*, **75**, 529-533.

11 Espanol, M.C., Ramasamy, R. and Mota de Freitas, D. (1989), in *Biological and Synthetic Membranes*, Butterfield, D.A. (ed.), Alan R. Liss Inc., N.Y., 33-43.

12 Mota de Freitas, D., Espanol, M.C., Ramasamy, R. and Labotka, R.J. (1990), *Inorg. Chem.*, **29**, 3972-3979.

13 Bansal, V.K., Mota de Freitas, D. and Ramasamy, R. (1989), *Kidney Internat.*, **35**, 322.

14 Ramasamy, R., Mota de Freitas, D., Bansal, V.K., Dorus, E. and Labotka, R.J. (1990), *Clin. Chim. Acta*, **188**, 169-176.

15 Mota de Freitas, D., Silberberg, J., Espanol, M.C., Dorus, E., Abraha, A., Dorus, W., Elenz, E. and Whang, W. (1990), *Biol. Psychiat.*, **28**, 415-424.

16 Shinar, H., Navon, G. and Klaui, W. (1986), *J. Am. Chem. Soc.*, **108**, 5005-5006.

17 Riddell, F.G., Arumugam, S. and Cox, B.G.(1987), *J. Chem. Soc. Chem. Commun.*, 1890-1891.

18 Riddell, F.G., Arumugam, S. (1988), *Biochim. Biophys. Acta*, **945**, 65-72.

19 Riddell, F.G., Arumugam, S. (1989), *Biochim. Biophys. Acta*, **984**, 6-10.

20 Mota de Freitas, D., Espanol, M.C. and Ramasamy, R. (1987), *Receuil des Travaux Chim. des Pays-Bas*, **106**, 389.

21 Gupta, R.K. (ed.) in *NMR Spectroscopy of Cells and Organisms*, **2**.

22 Ramasamy, R., Espanol, M.C., Long, K.M., Mota de Freitas, D. and Geraldes, C.F.G.C. (1989), *Inorg. Chim. Acta*, **163**, 41-52.

23 Rybakowski, J.K., Frazer, A., Mendels, J. and Ramsey, T.A. (1978), *Commun. Psychopharmacol.*, **2**, 99-104.

24 Pandey, G.N., Dorus, E., Casper, R.C., Janicek, P. and Davis, J.M. (1984), *Prog. Neuropsychopharmacol. Biol. Psychiat.*, **8**, 547-555.

25 Rybakowski, J.K., Potok, E. and Strzyzewski, W. (1981), *J. Affect. Dis.*, **3**, 59-64.

26 Duhm, J. and Becker, B.F. (1979), *J. Memb. Biol.*, **51**, 263-286.

Chapter 4

Lithium NMR Spectroscopy of Cells and Organs

4.1 Nmr Spectroscopy of Cells and Organs

In addition to the study of the metabolism of erythrocytes, nmr spectroscopy can be applied to similar studies of other intact cells and of perfused organs, and to *in vivo* studies.

4.1.1 Techniques for Studying Cell Suspensions

The main difficulty associated with the study of cell suspensions is the high cell density required to be maintained in the relatively small volume within the detection coil of the spectrometer, for adequate signal-to-noise ratio to be obtained without depleting the cells of the nutrients and oxygen required to sustain life. Thus the majority of research has centred on yeast, bacteria and protozoa which can be successfully grown to high density in suspension. However, a number of ingenious techniques has been developed to allow continual perfusion of the cells whilst avoiding the problem of the cells flowing with the perfusate.

Some tumour-derived cell types and continuous cell lines can be grown as free cells in suspension however most cells can only be cultured on solid supports. Free cells in suspension tend to flow with the perfusate and block the filters employed to restrain them. Two methods have been developed to avoid this problem. First, the cells can be embedded within a perfusible gel matrix, for example agarose, which can then be drawn out into fine threads and restrained within the nmr tube by a filter, thus maintaining the cells in a fixed position and optimizing the flow of nutrients to the cells *(1)*. Secondly, the cell suspension can be perfused by the use of a continuous loop of fine, hollow-fibre dialysis tubing through which the oxygenated medium can be pumped *(2)*. These fibres only occupy a small fraction (approximately 1/6) of the sample volume, however this method does require modification of the nmr tube so that it is hermetically sealed.

Alternatively for anchorage-dependent cells, high densities can be achieved by growing the cells on solid supports, such as microcarrier beads or fibres, which can be easily transferred to a nmr tube and perfused with medium. To minimize detachment of the cells from the solid support, the flow rate of the perfusate is kept low. Cells have been grown on the outer surfaces of hollow fibres, through which the medium is perfused in a similar manner to that used for the free cells in suspension *(3,4)*, on the surfaces of microcarrier beads *(5,6)* and on polyester fibres *(6)*. In the latter two methods, nylon mesh screens were employed as filters to restrain the supports in the nmr tube. The ^{31}P nmr spectra of human breast cancer cells grown either on polyacrolein microcarriers or on polyester fibres were more reproducible than the spectra of cells embedded in gel threads, and investigation by scanning electron micrographs revealed differences in the assembly and shape of the cells cultured by the three methods *(6)*. Not surprisingly, the cells grown on the beads and the fibres retained the shape and appearance of cells grown regularly in a monolayer, whilst those embedded in the gel were dispersed and spherical, lacking the surface filaments that provide contact between cells. The main disadvantage of these solid supports is the significant proportion of the sample volume they occupy; a value of 65% is reported in an experiment using microcarrier beads of 160-300μm diameter *(7)*.

4.1.2 ^{23}Na-, and ^{7}Li-Nmr Spectroscopy of Cells and Organisms

Nmr spectroscopy has been applied by a number of groups to the study of intracellular Na^+, but to date is very limited with respect to intracellular Li^+. Using methods similar to those used for suspensions of erythrocytes, ^{23}Na-nmr spectroscopy has been applied to the study of human lymphocytes *(8)*, rat cardiac myocytes *(9)*, amphibian oocytes *(10)*, rat kidney tubules *(11)*, frog sartorius muscle *(12)* and rat abdominal muscle *(13)*. In all these systems, the cells and tissues were suspended in

an isotonic medium containing a shift reagent, usually $Dy(P_3O_{10})_2^{7-}$, and were not perfused.

In one ^{23}Na study of a suspension of Na^+-rich yeast cells, using $Dy(NTA)_2^{3-}$, to separate the intra-, and the extracellular ^{23}Na resonances, the efflux of Na^+ from the cells was monitored with respect to time *(14)*. The cells were free in suspension and were not perfused, however occasional gentle pipetting prevented the cells settling. This study also demonstrated the potential of ^7Li-nmr for the study of intracellular Li^+ using the same shift reagent. Similarly, ^7Li-nmr has been used to study the Li^+ content of, and the transport of Li^+ into a suspension of rat hepatocytes using the shift reagent $Dy(P_3O_{10})_2^{7-}$ *(15)*. The initial uptake of Li^+ into the hepatocytes was rapid and saturation of the intracellular Li^+ occurred within 1h. As observed with erythrocytes, the $[Li^+]_{in}$ at saturation was low compared to the $[Li+]_{out}$ - the ratio $[Li^+]_{in}$ / $[Li^+]_{out}$ was approximately 0.04, 0.06 and 0.07 at $[Li+]_{out}$ of 8.3, 10.2 and 12.5mM, indicating the presence of a transport mechanism to maintain this low $[Li^+]_{in}$. It should be noted that this study used a very short interpulse delay (3s) which is probably insufficient for complete magnetic relaxation all the Li^+ species present, even though the applied pulse was only 45°, and therefore the absolute values for the $[Li^+]$ should be treated with caution.

The applicability of the methods described above for nmr studies of intact, anchorage-dependent cells was demonstrated in a ^{31}P- and ^{23}Na-nmr study of resting and stimulated mast cells *(7)*. The cells were grown as a monolayer on microcarrier beads and perfused with an oxygenated medium. The intra-, and extracellular Na^+ resonances were distinguished using a Hepes buffer containing $Dy(P_3O_{10})_2^{7-}$, and the viability of the cells was determined by monitoring the phosphorous metabolites using ^{31}P nmr spectroscopy.

4.2 Nmr Spectroscopy and Imaging of Organs

Cells, small tissue samples and small organs can be studied in suspension in standard, or sometimes modified, nmr tubes placed within the existing RF coils of the spectrometer. However, for the study of larger organs and whole bodies, magnetic resonance spectroscopy (MRS) employing specially adapted surface coils or magnetic resonance imaging (MRI) in which the whole body or organ is surrounded by the detection coil can be employed. Both methods have been extensively developed and produce excellent resolution for *in vivo* studies, with minimal risk to the subject (animal or human).

For MRS, the surface coil is placed on the surface of the individual adjacent to the organ or tissue of interest or, for longer term studies, the coil can be surgically implanted in the animal. The intensity of the RF field decreases with distance from the plane of a surface coil and the sampling volume is roughly hemispheric. A considerable amount of work has gone into coil design to achieve optimum coverage of the surface of interest. Thus a surface coil placed over the head, for example, will detect signals from nuclei in overlying muscle and bone as well as from the brain.

Localisation techniques, which are really extensions of MRI techniques, can be employed with MRS to investigate defined volumes, for example the various anatomic regions within the brain. By applying magnetic field gradients across the volume of interest, the frequency of the signal becomes a function of the distance from the coil, thus providing spatial resolution of the signal. In MRI, magnetic field gradients are superimposed in 3 orthogonal directions on the organ or body of interest. The field gradients are varied in 2 of these directions such that the frequency becomes a function of the position, producing spatial resolution. MRI can image in all planes and can therefore produce a 3 dimensional reconstruction of a particular nucleus within an organ.

4.2.1 ^{23}Na-, and ^{7}Li-Nmr Spectroscopy of Perfused Organs

The continuous measurement of tissue contents of electrolytes (Na^+, Li^+ and Cl^-) in intact *ex vivo* organs by nmr spectroscopy was demonstrated by a study on the perfused salivary gland from a rat, suspended inside a 10mm nmr tube *(16)*. No shift reagent was employed in this study and therefore a single resonance was observed for each of the ions. The kinetics for both the decrease in the intensity of the Na^+ signal and the increase in that of the Li^+ signal, were followed with time when Li^+ was substituted for Na^+ in the perfusate.

The study of intracellular Na^+, K^+ and Li^+ in a perfused organ, by nmr spectroscopy, was demonstrated by cannulating the venous input and allowing the perfusate to mimic the normal blood flow through the excised heart of a frog *(17)*. The heart and cannular apparatus were placed in a 20mm nmr tube with the heart being completely submerged in the perfusate. Using $Dy(P_3O_{10})_2^{7-}$ (3.0mM) to separate the intra-, and the extracellular resonances, chemical shifts of approximately 6.5ppm for Na^+, 3.5ppm for K^+, and 3.2ppm for Li^+ (perfusate containing 80mMLi^+) were obtained. The T_1 and T_2 relaxation times for the intracellular Li^+ were 700 and 31ms, respectively.

4.2.2 *In vivo* ^{23}Na-Nmr Spectroscopy

The use of *in vivo* ^{1}H and ^{31}P nmr-spectroscopy and nmr-imaging is now widespread and certain other nuclei, such as ^{23}Na, ^{19}F, ^{13}C and ^{2}H are being investigated. The potential use of shift reagents *in vivo* has been demonstrated by ^{23}Na-nmr spectroscopy. $Dy(TTHA)^{3-}$ was continuously infused into the bloodstream of a gerbil by introduction into the femoral vein to distinguish between the intra-, and the extracellular ^{23}Na resonances *in vivo* in both the brain and the leg muscle *(18)*. In the spectra of the leg muscle, the two expected signals were observed however, in the

spectra of the brain, 3 signals were observed and were assigned to the intracellular Na^+, the extracellular-extravascular Na^+, and the intravascular Na^+. The appearance of the signal from the extravascular-extracellular Na^+ indicates the permeability of the blood-brain barrier to the shift reagent and demonstrates a further potential application of this technique. Once again, ^{31}P nmr spectroscopy was employed to monitor changes in either the phosphorous metabolites or in the intracellular pH.

4.2.3 *In Vivo* ^{7}Li-Nmr Spectroscopy and Imaging

To date, very few studies of *in vivo* ^{7}Li-nmr spectroscopy and imaging have been reported. ^{7}Li-nmr imaging is an ideal method to monitor the Li^+ distribution non-invasively in the human brain. It has the potential to lead to insights in the locus of action of Li^+ in psychiatric therapy and, for instance, differences in the distribution of Li^+ in the brain may be related to differences in the clinical response or the efficacy of the drug.

Using surface coils, *in vivo* ^{7}Li-nmr spectroscopy has been applied to humans, following the oral administration of Li_2CO_3. By the careful use of Li^+ standards made from agarose phantoms, quantification of the $[Li^+]$ in the brain and in the calf muscle has been performed and compared with that in the serum. Following ingestion of a single dose of the drug by a healthy individual, the Li^+ level in the serum increased rapidly and peaked after approximately 4h, whereas the levels in the muscle and the brain rose more slowly and were still increasing after 8h *(19)*. The T_1 of Li^+ in the muscle was 7s. Monitoring of the $[Li^+]$ during several days of treatment, showed that the accumulation of Li^+ in the serum was more rapid and to a higher level than that in the muscle, which was in turn more rapid and to a higher level than that in the brain. When the treatment was stopped, Li^+ was eliminated rapidly from both the serum and the muscle, whereas the level in the brain decreased very slowly *(19,20)*. Similar data was reported for a patient suffering from bipolar affective disorder commencing Li^+

therapy, however in this case the level in the brain rose more rapidly than that in the muscle *(20)*. A patient suffering from schizoaffective disorder, who had been taking Li^+ for 6 months, was monitored by ^{7}Li-nmr for several months over which time the [Li^+] in the brain fluctuated over the range 0.45 - 0.84mM *(20)*. The reason behind the fluctuating levels is not understood, however the brain [Li^+] did correlate with that in the serum. Similarly, in two studies of a number of patients suffering from bipolar affective disorder and stabilised on Li^+ therapy, the levels in the brain and the muscle were consistently lower than that in the serum, and there was a positive correlation between the serum [Li^+] and the brain [Li^+] *(21,22)*. In one particular individual it was noted that, although the brain [Li^+] was lower than the serum [Li^+] during both the depression and the mania, during the switch from the depressive to the manic episode, the level in the brain exceed that in the serum *(22)*. A T_1 of 3.4 ± 0.5s for Li^+ in the brain of patients suffering bipolar disorder was reported *(23)*.

In vivo ^{7}Li-nmr spectroscopy has also been applied to the study of anaesthetized rats following injection with LiCl, when a dose dependent increase in the intensity of the ^{7}Li signals in the brain was reported *(24,25)*. Following a single dose of LiCl, in the range 2-10mmol.kg^{-1}, the [Li^+] in the brain reached a maximum after approximately 8h and then decreased to only half its value in approximately 20h *(25)*. Localised spectroscopy, of 0.5ml sample volumes from the front, centre and rear of the brain, suggested that the Li^+ was uniformly distributed. This technique also showed that there was no reduction in the signal intensity even 20h after administration of the LiCl, suggesting that the decrease observed by non-localised spectroscopy may be due to elimination of Li^+ from the extracranial tissue *(25)*. The T_1 for Li^+ in the rat brain was 4.1s.

The first ^{7}Li-nmr image of a body section was of the upper abdomen of a rat, which had been administered 2 doses of LiCl i.p. (10mmol.kg^{-1}), with a 24h interval between doses, prior to sacrificing *(26)*. The image, recorded over 4h with a resolution of 5mm, showed a higher [Li^+] in both the perivertebral muscle and the liver, relative to

that in the stomach. Two T_2 values, of 10ms and 100ms, were determined; the biphasic behaviour being ascribed to weak macromolecular binding of Li^+. The same group then applied ^{7}Li-nmr imaging to the head of an anaesthetized puppy, following administration of i.p. injections of LiCl *(27)*. The low resolution of the resulting image, recorded over 4h, did not allow any anatomical features to be distinguished. Both T_1 and T_2 showed biexponential behaviour, which was again ascribed to a rapid exchange between free and bound Li^+. However, the 2 different relaxation times may simply be due to Li^+ species in different pools, for example in the intracellular fluid, in the CSF, in the blood or in extracranial tissue.

A recently reported Li-nmr image of a rat head shows a significant improvement in definition, where the brain stem and the spinal cord region can be distinguished *(25)*. The most intense signal is from the muscle in the neck behind and below the brain, which is approximately twice that in the brain. The tongue also shows substantial signal intensity. Within the brain region itself, the [Li^+] is relatively uniform, with the level in the cerebellum approximately 30% lower than that in the front of the brain.

The reports described above illustrate the wide potential for both ^{7}Li-nmr spectroscopy and ^{7}Li-nmr imaging *in vivo* in psychiatric research. Applying a method modified from that used for ^{23}Na-nmr spectroscopy of mast cells *(7)*, the following section reports an original investigation into the potential of employing ^{7}Li-nmr spectroscopy to study intracellular Li^+ in human brain cells, using a cell line derived from a brain tumour. The use of shift reagents *in vivo* has also been investigated in order to study Li^+ in the various environments within rat brain.

4.3 ^{7}Li-, and ^{23}Na-Nmr Spectroscopy of Human 1321 N1 Astrocytomas

Human 1321 N1 astrocytomas, a cell line derived from a brain tumour, were cultured on the surface of microcarrier beads (250μm diameter) to facilitate the nmr experiment. This produced a density of approximately 4 x 10^7 cells (80mg protein) per ml of beads packed under gravity *(28)*. ^{7}Li-, and ^{23}Na-nmr spectra were recorded after resuspending the beads/cells in a buffer containing $Dy(P_3O_{10})_2^{7-}$ to distinguish the intra-, and extracellular resonances for both cations. Typical spectra, illustrating the excellent resolution achieved for both ^{7}Li and ^{23}Na, are shown in Figures 4.1 and 4.2, respectively. In both figures, the lower trace is simply an expansion of the upper trace. In the ^{7}Li spectrum, the shift difference is 4.3ppm and the $\omega_{1/2}$ are 80 and 33Hz for the signals from the Li^+_{in} and Li^+_{out}, respectively. In the ^{23}Na spectrum, the chemical shift difference is 6.74ppm and the $\omega_{1/2}$ are 98 and 78Hz for the signals from the Na^+_{in} and Na^+_{out}, respectively. ^{31}P nmr spectroscopy was employed to monitor the viability of the cells throughout the experiment (see Section 2.2.1).

4.3.1 Astrocytomas Preloaded with Li^+

A sample of astrocytomas was preloaded with Li^+ by including LiCl (16.6mM) in the culture medium for 24h prior to the nmr experiment. This ensured that sufficient Li^+ was present inside the cells to be easily observed by ^{7}Li-nmr spectroscopy. The nmr spectra were recorded after resuspending the beads/cells in a buffer containing $Dy(P_3O_{10})_2^{7-}$ (3mM) and LiCl (10mM). In the ^{7}Li spectrum, the integral of the intracellular signal (I_{in}) was approximately 6.1% that of the extracellular signal (I_{out}) and in the ^{23}Na spectrum, the I_{in} was approximately 2.4% of the I_{out}. This latter value compares with I_{in} of 2.5% of I_{out} reported for the ^{23}Na-nmr spectrum of mast cells, cultured on the same beads, in a similar buffer not containing Li^+ *(7)*. Analysis of both the ^{23}Na-, and the ^{7}Li-nmr spectra of both the suspension of beads/cells and the

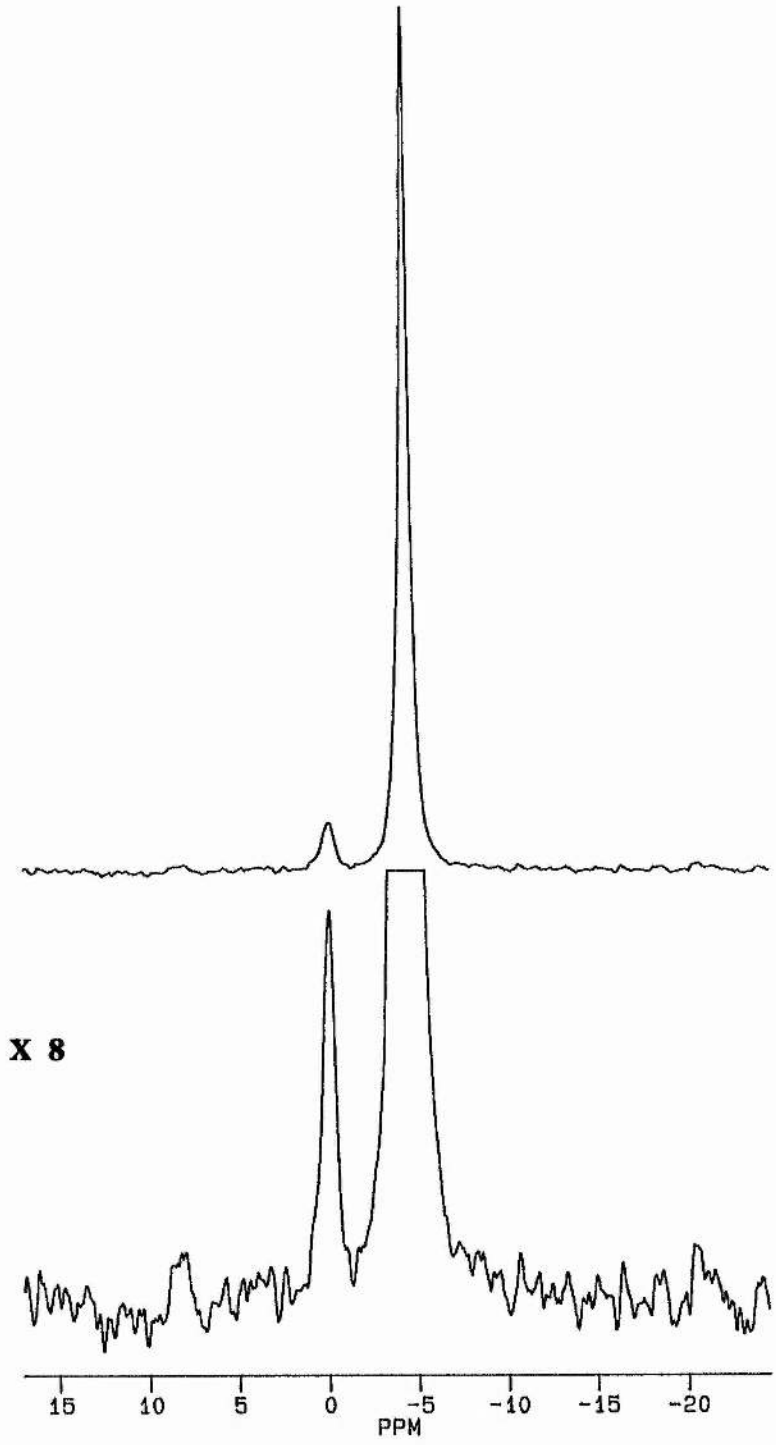

Figure 4.1 ^{7}Li-nmr spectra of astrocytomas on microcarrier beads, in a buffer containing $Dy(P_3O_{10})_2^{7-}$

(Each spectrum is the sum of 48 acquisitions recorded at 194MHz, $[Li^+]_{out}$ = 10mM)

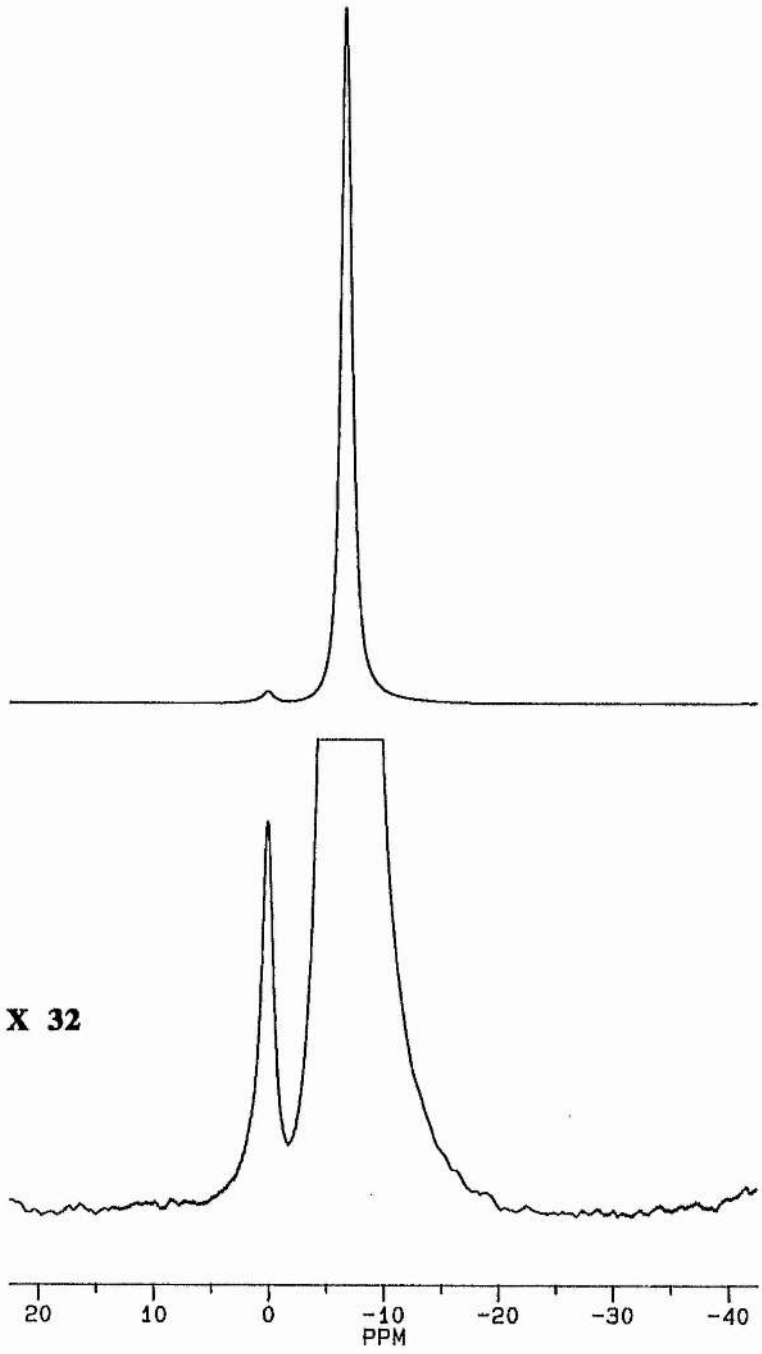

Figure 4.2 ^{23}Na-nmr spectra of astrocytomas on microcarrier beads, in a buffer containing $Dy(P_3O_{10})_2^{7-}$

(Each spectrum is the sum of 1200 acquisitions recorded at 132MHz, $[Na^+]_{out}$ = 90mM)

corresponding buffer, established that the microcarrier beads occupied approximately 50%, and the intracellular volume was approximately 8.5%, of the total sample volume (see Section 2.2.3). This compares with the reported values of 65% occupied by beads and 4% by the mast cells *(7)*. Assuming the $[Na^+]_{in}$ was 20mM, the $[Li^+]_{in}$ was calculated to be approximately 3.1mM, giving the ratio $[Li^+]_{in}$ / $[Li^+]_{out}$ of approximately 0.3.

4.3.2 Uptake of Li^+ into Astrocytomas

The uptake of Li^+ into the astrocytomas was monitored with respect to time by ^{7}Li-nmr. The cells were incubated at 37°C in a buffer containing either 10mM Li^+, when data was acquired for 25min. per spectrum, or 50mM Li^+, when data was acquired for 4min. per spectrum. The higher concentration improved the time resolution for the initial uptake of Li^+ by achieving adequate signal-to-noise with fewer scans. From both the ^{23}Na and the ^{7}Li nmr data, the volume occupied by the beads was approximately 30%, the lower value probably being due to the modified procedure of filling the the nmr tube with buffer to prolong the life of the cells (see Section 2.2.2), and the intracellular volume was approximately 6.7%.

Figure 4.3 shows the time dependence of the integral of the Li^+_{in} resonance as a percentage of that of the Li^+_{out} resonance, at both concentrations of Li^+_{out}. At 10mM Li^+_{out}, it can be seen that the initial uptake of Li^+ is rapid and that saturation occurs within 60min., when the I_{in} is approximately 9% of the I_{out}. This corresponds to a $[Li+]_{in}$ of approximately 4.5mM, and thus the ratio $[Li^+]_{in}$ / $[Li^+]_{out}$ is approximately 0.45. At 50mM Li^+_{out}, the I_{in} is approximately 3% of I_{out} after 30min. which corresponds to $[Li^+]_{in}$ of approximately 16mM and thus a ratio of $[Li^+]_{in}$ / $[Li^+]_{out}$ of approximately 0.32. The graphs show that the uptake appears to follow 1st order kinetics and a rate constant of $5.5 \times 10^{-2} \pm 0.75 \times 10^{-2}$ min.$^{-1}$ has been determined for a

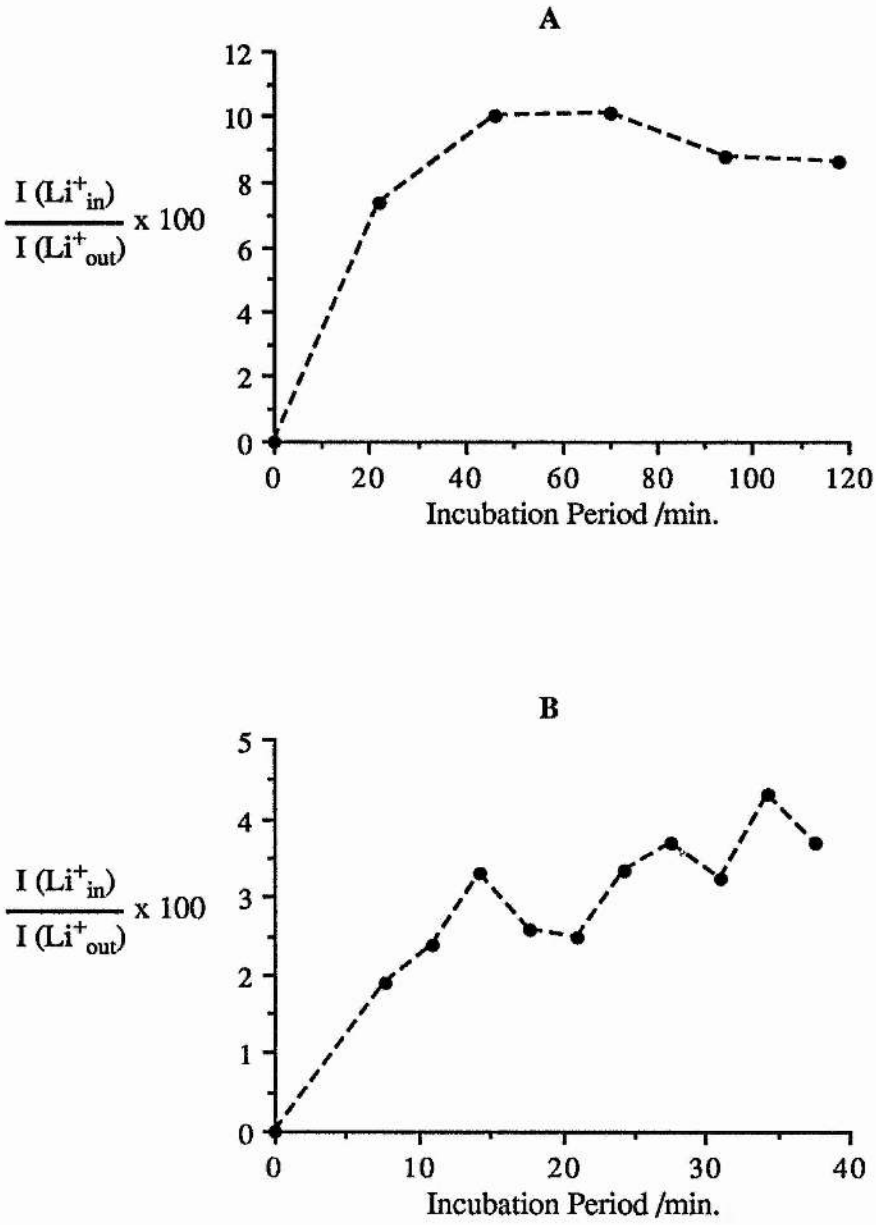

Figure 4.3 The time dependence of the integral of the intracellular Li^+ resonance, $I(Li^+_{in})$, as a percentage of that of the extracellular resonance, $I(Li^+_{out})$, in astrocytomas at **(A)** 10mM and **(B)** 50mM Li^+_{out}

$[Li^+]_{out}$ of 50mM. This corresponds to a half-life of approximately 12.6min..

4.4 *In Vivo* Li-Nmr Spectroscopy of Rat Brain

In vivo ^{7}Li-nmr spectra of the head of anaesthetised rats, pretreated with LiCl, were obtained by using a surface coil placed on the scalp. Contrast reagents were injected into the bloodstream of the rats via the tail vein, in order to distinguish the various Li^+ pools within the brain. High quality ^{7}Li spectra were obtained within 15min. of administering the LiCl to the rats, i.e. as soon as the animal could be positioned in the magnet after dosing. Li^+ doses of 1-10mmol.kg^{-1}, and contrast reagent doses of 0.5-2.0mmol.kg^{-1}, were administered.

All the spectra obtained showed only a single ^{7}Li resonance, with $\omega_{1/2}$'s in the range 30-80Hz, depending on the homogeneity of the field. No separation of the resonances from Li^+ in different environments was achieved with any of the shift reagents, even in the spectra from the rats treated with several doses of Li^+ for up to 2 days prior to the experiment. No significant changes in either the $\omega_{1/2}$ or the integral of the resonance was observed, and in general, the chemical shift of the resonance did not change significantly with any of the reagents employed. In only one experiment was a significant shift difference of 2.76ppm obtained, and as can be seen in Figure 4.4, even this did not show any separation of resonances from the different Li^+ pools. Although quantification was not possible under the conditions used, increasing the dose administered from 1 or 2mmol.kg^{-1}, to 10mmol.kg^{-1}, did not appear to increase the intensity of the signal, indicating that the signal was probably saturated.

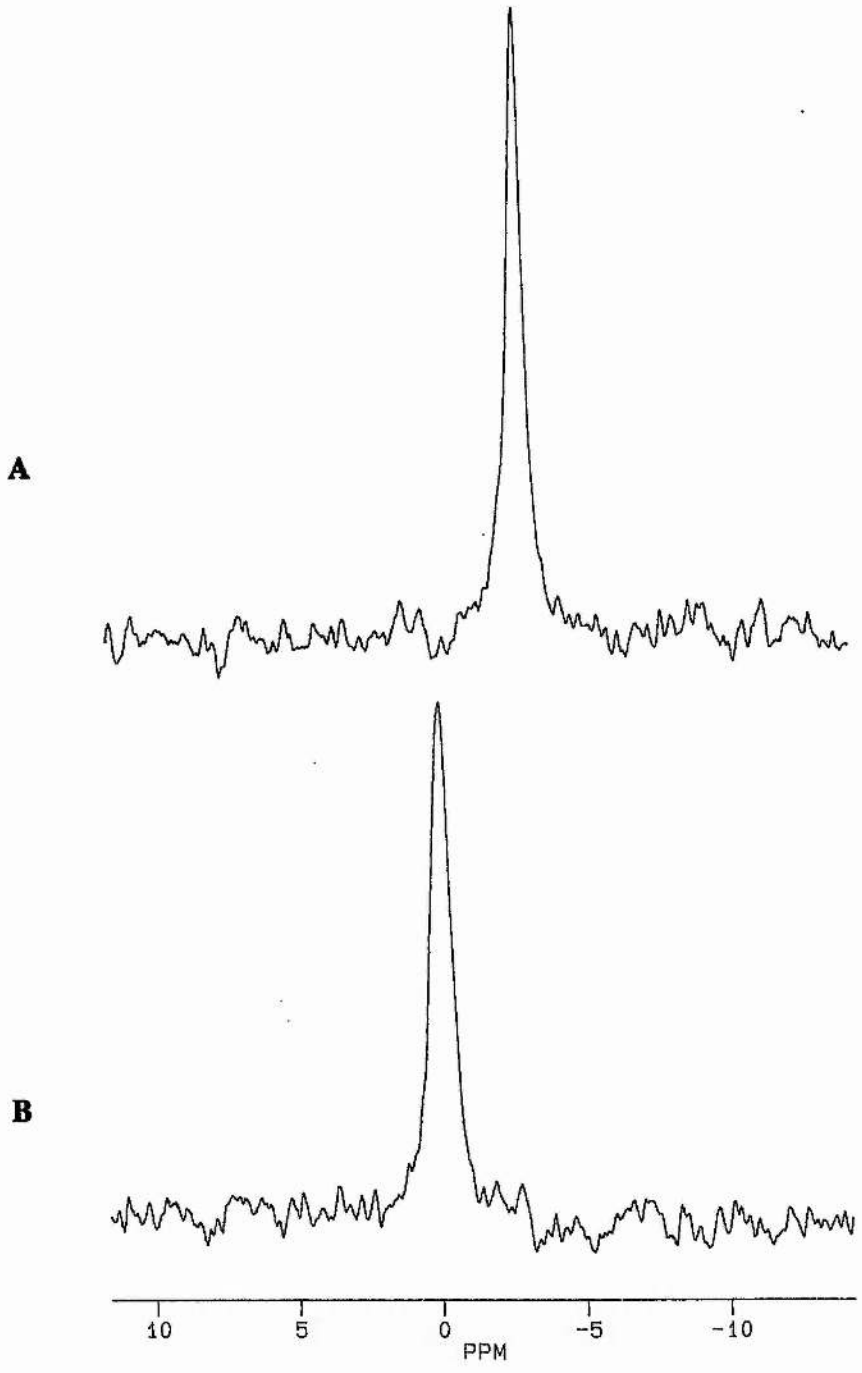

Figure 4.4 *In vivo* ^{7}Li-nmr spectra of the head of an anaesthetised rat after administration of: **(A)** LiCl (10.8mmol.kg^{-1}), $Dy(TTHA)^{3-}$ (1.8mmol.kg^{-1}) and $GdNO_3$ (2mmol.kg^{-1}); and **(B)** LiCl (7.2mmol.kg^{-1}) and $Dy(TTHA)^{3-}$ (1.2mmol.kg^{-1})

4.5 Discussion

The results obtained with the astrocytomas demonstrates the potential for the non-invasive nmr study of intracellular Li^+ in excitable cells. Although absolute values for the intracellular concentrations were not obtained in this study, the data suggests that the intracellular [Li^+] is low with respect to the extracellular concentration, as in erythrocytes. This is in agreement with data obtained by AAS on primary nerve cells from chick embryos *(29,30)* and on cultured mouse neuroblastoma x glial hybrids *(31)*, but it is in contrast to the data from cultured rat glioma cells *(32)* and mouse neuroblastoma cells *(33)*, which reported that, even in the resting state, these cells accumulate Li^+ against the chemical gradient. Obviously, these differences may be due to the two experimental techniques employed, but are more likely to be due to the different cell lines or the different species studied, and illustrates the danger of extrapolating such data to human brain cells. The relatively low intracellular [Li^+] in the astrocytomas indicates the presence of a mechanism for transporting Li^+ out of the cells against its concentration gradient, possibly a Na^+-Li^+ countertransport system similar to that found in human erythrocytes. A Na^+-Li^+ exchange process has been reported in primary nerve cells *(29)* and in mouse neuroblastoma x glial hybrids *(34)*. If this Li^+ efflux mechanism is absent in rat glioma cells, as is the case in rat erythrocytes *(35)*, this may explain the high levels of intracellular Li^+ accumulated by these cells.

The uptake of Li^+ into the astrocytomas is rapid, being approximately 10 times faster than that into erythrocytes (Section 3.4). Equilibration is achieved within 60min. and this appears to represent the true steady-state for Li^+ movement, since the ratio $[Li^+]_{in}$ / $[Li^+]_{out}$ after 60min. was similar to that obtained after 24h. This rapid initial uptake followed by saturation is typical of the behaviour of Li^+ uptake in the other brain cells studied by AAS *(29,31,32,33,36)* and illustrates how the Li^+ transport behaviour in brain cells differs from that in erythrocytes. Indeed, the movement of Li^+ though the

voltage-dependent Na^+ channel has previously been demonstrated in nerve cells *(31,34)*. This transporter is absent in electrically passive tissue, such as erythrocytes.

Li^+ transport processes and intracellular concentrations in the brain can be approached by using nerve cell culture as a intact model system. Obviously, the study of human nerve cells is likely to be more relevant to the study of the mechanism of action of Li^+ in psychiatric therapy, than either the study of human erythrocytes or the study of nerve cells from other mammalian species. However, it should be remembered that different behaviour between cells from immortalized cell lines and those present in normal mammalian brain may also be significant.

This preliminary study illustrates the potential for ^{7}Li-nmr spectroscopy in this field of research. Once the relaxation times and nmr-visibility of the cations have been established, detailed quantitative analysis of intracellular [Li^+] and transport behaviour can be studied at physiological [Li^+] in any *in vitro* cell system.

Although the object of the *in vivo* work, to observe intracellular Li^+ in rat brain, was not achieved, the potential for this method remains. It appears likely that, under the conditions of the experiment, the shift reagents were not entering the bloodstream and were, therefore, not reaching the brain, or that the shift reagent was not able to cross the blood brain barrier. It may be that continuous infusion of the shift reagent into the animal is required to attain and maintain the necessary concentration in the brain. It is also likely that the repetition rate employed (2s) was too short to give acceptable signal to noise for the intracellular Li^+ resonance, even if the extracellular signal had been shifted - a T_1 of 4.1s for total Li^+ in rat brain in the absence of a shift reagent, has been reported *(25)*. Given that the ^{23}Na signals have been reported to be distinguished *in vivo* in the various compartments within the gerbil brain using continuous infusion of $Dy(TTHA)^{3-}$ *(18)*, and that Li^+ signals have been distinguished *ex vivo*, in perfused organs using chemical shift reagents *(16,17)*, there is no apparent reason why intracellular Li^+ may not be observed *in vivo*, under the right conditions. It

may be that the blood brain barrier in rats is impermeable to the shift reagents employed, a problem apparently not experienced in the study with the gerbil. The toxicity of these reagents means their use in human studies *in vivo* is unlikely, although their applicability to animal studies remains a valuable asset.

4.6 References

1 Foxall, D.L. and Cohen, J.S. (1983), *J. Mag. Res.*, **52**, 346-349.

2 Karczmar, G.S., Koretsky, A.P., Bissell, M.J., Klein, M.P. and Weiner M.W. (1983), *J. Mag. Res.*, **53**, 123-128.

3 Gonzalez-Mendez, R., Wemmer, D., Wade-Jardetzky, N. and Jardetzky, O. (1982), *Biochim. Biophys. Acta*, **720**, 274-280.

4 Hrovat, M.I., Wade, C.G. and Hawkes, S.P. (1985), *J. Mag. Res.*, **61**, 409-417.

5 Ugurbil, K., Guernsey, D.L., Brown T.R., Glynn, P., Tobkes, N. and Edelman, I.S. (1980), *Proc. Natl. Acad. Sci. USA*, **78**, 4843-?

6 Neeman, M., Rushkin, E., Kadoun, A. and Degani, H. (1988), *Mag. Res. Med.*, **7**, 236-242.

7 Pilatus, U., Degani, H. and Pecht, I. (1990), *Febs Letts*, **269**, 292-296.

8 Gupta, R.K., Gupta, P. and Negendank, W. (1982), in *Ions, Cell Proliferation and Cancer,* Academic Press, New York.

9 Wittenberg, B.A. and Gupta, R.K. (1985), *J. Biol. Chem.*, **260**, 2031-2034.

10 Morrill, G.A., Weinstein, S.P., Kostellow, A.B. and Gupta, R.K. (1985), *Biochim. Biopyhys. Acta*, **844**, 377-392.

11 Rayson, B.M. and Gupta, R.K. (1985), *J. Biol. Chem.*, **260**, 7276-7280.

12 Gupta, R.K. and Gupta, P. (1982), *J. Mag. Res.*, **47**, 344-350.

13 Matwiyoff, N.A., Gasporovic, C., Wenk, R., Wicks, J.D. and Rath, A. (1986), *Mag. Res. Med.*, **3**, 164-168.

14 Balschi, J.A., Cirillo, V.P. and Springer, C.S. (1982), *Biophys. J.*, **38**, 323-326.

15 Thomas, G.M.H., Hughes, M.S., Partridge, S., Olufunwa, R.I., Marr, G. and Birch, N.J. (1988), *Biochem. Soc. Trans.*, **16**, 208.

16 Murakami,M. Seo, Y., Matsumoto, T. Ichikawa, O., Ikeda, A. and Watari, H. (1986), *Jpn. J. Physiol.*, **36**, 1267-1274.

17 Burstein, D. and Fossel, E.T. (1987), *Mag. Res. Med.*, **4**, 261-273.

18 Naritomi, H., Kanashiro, M., Sasaki, M., Kuribayashi, Y. and Sawada, T. (1987), *Biophys. J.*, **52**, 611-616.

19 Renshaw, P.F. and Wicklund, S. (1988), *Biol. Psychiat.*, **23**, 465-475.

20 Komoroski, R.A., Newton, J.E.O., Walker, E., Cardwell, D., Jagannathan, N.R., Ramaprasad, S. and Sprigg, J. (1990), *Mag. Res. Med.*, **15**, 347-356.

21 Gyulai, L., Wicklund, S.W., Greenstein, R., Bauer, M.S., Ciccione, P., Whybrow, P.C., Zimmerman, J., Kovachich, G. and Alves, W. (1991), *Biol. Psychiat.*, **29**, 1161-1170.

22 Kato, T., Takahashi, S. and Inubushi, T. (1992), *Psychiat. Res. Neuroimag.*, **45**, 53-63.

23 Kushnir, T., Itzchak, Y., Valevski, A., Lask, M. Modai,I., Stoker, S. and Navon, G. (1991), *Proc. 10th Ann. Scientific Meeting, S.M.R.M.*, 1063.

24 Preece, N.E., Gadian, D.G., Houseman, J. and Williams, S.R. (1992), *Lithium*, **3**, in press.

25 Ramaprasad, S., Newton, J.E.O., Cardwell, D., Fowler, A.H. and Komoroski, R.A. (1992), *Mag. Res. Med.*, **25**, 308-318.

26 Renshaw, P.F., Haselgrove, J.C., Leigh, J.S. and Chance, B. (1985), *Mag. Res. Med.*, **2**, 512-516.

27 Renshaw, P.F., Haselgrove, J.C., Bollinger, L., Chance, B. and Leigh, J.S. (1986), *Mag. Res. Imag.*, **4**, 193-198.

28 Batty, I., *personal communication.*

29 Janka, Z., Szentistvanyi, I., Rimanoczy, A. and Juhasz, A. (1980), *Psychopharmacol.*, **71**, 159-163.

30 Szentistvanyi, I., Janka, Z., Rimanoczy, A., Latzkovits, L. and Juhasz, A. (1980), *Cell. Mol. Biol.*, **25**, 315-321.

31 Reiser, G., Scholz, F. and Hamprecht, B. (1982), *J. Neurochem.*, **39**, 228-234.

32 Gorkin, R.A. and Richelson, E. (1979), *Brain Res.*, **171**, 365-368.

33 Gorkin, R.A. and Richelson, E. (1981), *Neuropharmacol.*, **20**, 791-801.

34 Reiser, G. and Duhm, J. (1982), *Brain Res.*, **252**, 247-258.

35 Duhm, J. and Becker, B.F. (1979), *J. Memb. Biol.*, **51**, 263-286.

36 Saneto, R.P. and Perez-Polo, J.R. (1982), *J. Neurosci. Res.*, **7**, 413-418.

Chapter 5

Effect of Lithium upon the Composition of the Erythrocyte Membrane

5.1 Effect of Li^+ upon Erythrocyte Membrane Processes

Several specific transport processes in erythrocytes are altered after the initiation of Li^+ treatment, including the Na^+/K^+ pump, the Ca^{2+} pump, choline transport and the Na^+-Li^+ countertransport. The inhibition of this latter process is most likely responsible for the altered Li^+ transport behaviour observed in this work, in Chapter 3. Any of these changes could be important in the therapeutic action of Li^+ and/or may be the underlying molecular basis of bipolar affective disorder. Alternatively, these abnormalities may be the consequence of a more general defect in membrane composition and structure, and it has been suggested that a membrane defect could be indicative of a predisposition to the affective disorders.

Membrane lipids serve as the molecular cement for membranes and regulate the lateral movement of membrane-proteins. Changes in lipid composition would be expected to result in changes in forces between membrane components, such as receptors and transport systems. For instance, changing the relative amounts of acidic and neutral lipids would alter the charge density and could result in a dramatic change in membrane binding. It has been shown that the activity of the enzyme Na^+/K^+ ATPase is significantly dependent on the membrane lipid content *(1)*. Since the transport of neurotransmitters and their precursors occurs at the membrane, and the receptor complexes are located on the membrane surface, it is not unreasonable to suggest that membrane defects are likely to have significant effects on neurotransmitter availability and the transduction of receptor-mediated signals.

Li^+ inhibits *myo*-inositol monophosphatase, the enzyme responsible for the formation of *myo*-inositol from inositol-1-phosphate, $I(1)P_1$, thus leading to a decline in the levels of *myo*-inositol. Both choline and *myo*-inositol are precursors for the synthesis of membrane phospholipids: choline for phosphatidylcholine (PC) and sphingomyelin (Sph), and *myo*-inositol for phosphatidylinositol (PI) and the polyphosphoinositides. Therefore, since Li^+ alters the metabolism of both these

precursors, it is possible that Li^+ is involved in altering the composition of the tissue phospholipids.

5.1.1 Effect of Li^+ upon the ATPases

Erythrocyte membrane abnormalities in bipolar disorder were first observed in studies of the enzyme Na^+/K^+-ATPase. A Li^+-induced increase in the activity of the Na^+/K^+-ATPase was observed in the erythrocytes of Li^+-treated bipolar and unipolar patients *(2,3)*, and the concentration of the enzyme Ca^{2+}-ATPase was found to be increased in the erythrocyte membranes of Li^+-treated bipolar patients compared to those of controls *(4)*.

5.1.2 Effect of Li^+ upon Choline Transport

Choline transport across the erythrocyte membrane is irreversibly reduced by 90% as a consequence of chronic Li^+ treatment *(5)*. In the erythrocytes of Li^+-treated patients, significant accumulation of intracellular choline occurs despite unchanged levels of endogenous choline in plasma *(6,7)*. The affinity of the transport system for choline was found to be unchanged by Li^+ treatment whereas the V_{max} was reduced 3-fold, implying that either the number of transporting molecules had been reduced or that the ability of the choline-carrier complex to cross membrane was impaired *(8)*. This implied that an irreversible change in the composition of the membrane had occurred, either as a result of a change in the amount of specific constituents or a conformational change in the complex. Following chronic treatment with Li^+, increased uptake of choline into the brain and stimulation of the conversion of choline into the neurotransmitter acetylcholine in rats has been reported *(9)*. Hence, the beneficial effect of Li^+ may be due to an increase in the availability of acetylcholine in response to lithium therapy.

5.1.3 Na^+-Li^+ Countertransport and Membrane Composition

The molecular structure of the carrier in the erythrocyte membrane which is responsible for the Na^+-Li^+ countertransport has not yet been elucidated, however it is known that the carrier is significantly influenced by the lipid components of the membrane. Therefore, a deficiency in the Na^+-Li^+ countertransport system may be associated with abnormalities in membrane lipid composition. There is evidence that the Na^+-Li^+ countertransport activity is altered by changes in the concentrations of plasma lipids and, since the erythrocyte membrane lipids are in a dynamic equilibrium with the plasma lipids, any change in the levels of the plasma lipids may alter the composition of the erythrocyte membrane *(10)*. In hypertensive patients, the activity of the Na^+-Li^+ countertransport in erythrocytes was found to correlate positively with total cholesterol and triglycerides, and negatively with high density lipoprotein (HDL) cholesterol *(11)*. The activity was also found to correlate positively with the saturated, and to correlate negatively with the unsaturated fatty acids of erythrocyte lipids of normotensive subjects *(12,13)*. In patients suffering bipolar affective disorder, a negative association between the activity of Na^+-Li^+ countertransport in erythrocytes and HDL cholesterol has been reported *(14)*.

In erythrocytes, the Na^+-Li^+ countertransport activity is reduced *in vitro* by increases in the level of cholesterol *(15)*, and is considerably altered by subtle changes in the fatty acid composition of PC, induced by the *in vitro* replacement of some of the native PC *(15,16)*.

5.1.4 Erythrocyte Lipids in Li^+-Treated Psychiatric Patients

There is some evidence that abnormalities exist in the erythrocyte membranes of patients suffering psychiatric illnesses. Studies of the lipid content of the membranes of erythrocyte ghosts from Li^+-treated patients suffering various forms of

schizophrenia reported that, compared to healthy Li^+-treated controls, the membranes of the patients had a significantly lower levels of PC, and this was accompanied by increased levels of phosphatidylethanolamine (PE) and Sph *(17)*, by increased levels of phosphatidylserine (PS) *(18)*, or by increased levels of PS and decreased levels of PE *(19,20)*. Schizophrenic patients also appeared to have different levels of sphingomyelin fatty acids than the controls *(17)*. However, no differences were observed in the cholesterol/phospholipid ratio, a primary factor in determining membrane fluidity *(17)*. The membrane composition of manic patients was found to be similar to the controls *(19)*.

These changes in the relative concentrations of the various phospholipids can be rationalised by considering the normal enzymatic biosynthesis of PC in membranes which involves the decarboxylation of PS followed by successive N-methylations of PE *(21)*:

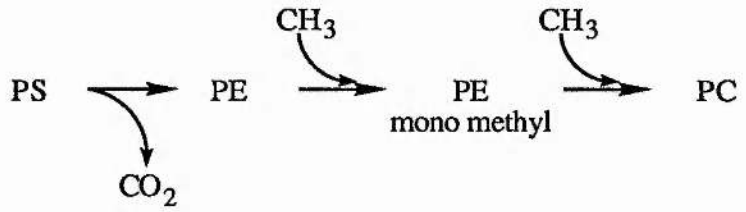

Therefore, inhibition of the decarboxylation step would lead to a build up of PS at the expense of PE and PC. Similarly, inhibition of the methylation steps would lead to a build up of PE at the expense of PC. Interestingly, neuroleptic drugs are known to block the methylation reactions and hence, it has been suggested that a decrease in PE may play a role in psychotic symptoms *(20)*.

5.1.5 Effect of Li^+ upon Cortical Phospholipids in Rat

Acute treatment of Li^+, using relatively high doses (9 or 12mmol.kg^{-1}), produced a significant decrease in the level of PE and an increase in the relative level of

Sph in rat cerebral cortex *(22)*. Chronic dietary administration of Li^+ produced a significant decrease in PI and PE with an increase in PC. Interestingly, a decrease in PI is postulated from the inhibition of inositol monophosphatase. The decrease in PE accompanied by an increase in PC, and in Sph following acute treatment, may again reflect changes in the choline metabolism since choline is a precursor for both of these. PE is converted to PC by N-methylation, and subsequently to choline *(21)*.

5.1.6 Effect of Li^+ upon Membrane Proteins

A difference in the concentration of a minor membrane-associated protein has been observed in the erythrocytes of Li^+-treated patients. The spectrin-actin cytoskeleton of erythrocytes is linked to some of the integral membrane proteins by ankyrins. The major ankyrin in human erythrocytes is ankyrin 2.1, however higher than normal levels of ankyrin 2.3 have been reported in patients suffering from bipolar affective disorder, both before and during Li^+ therapy *(23,24)*.

5.2 Li^+ Treatment and Erythrocyte Membrane Composition

The abnormal transport behaviour observed on the initiation of Li^+ therapy observed in this work, in Chapter 3, may be the consequence of a Li^+-induced change in the composition of the erythrocyte membrane. The human erythrocyte membrane is primarily composed of protein (approximately 50%) and lipid (approximately 44%). Therefore, to investigate the effect of Li^+ treatment on the composition of this membrane, the erythrocytes of Li^+-free healthy controls and of Li^+-treated patients were analysed for membrane lipid content by high performance thin-layer chromatography (HP-TLC), and for membrane protein content by gel electrophoresis. Comparisons were made to investigate any differences between the 2 groups of individuals to account for this observed Li^+ transport behaviour.

5.2.1 Effect of Li^+ Therapy upon the Lipid Content of Human Erythrocyte Membranes

The lipids were extracted from the erythrocyte membranes of both Li^+-free healthy controls and from Li^+-treated patients. The lipids were then separated by HP-TLC, using the a 2-solvent system which produced a complete separation of the phospholipids and cholesterol. The lipids were revealed after charring with a copper acetate spray reagent, identified using authentic samples and were quantified by densitometric analysis *(25)*.

A typical chromatogram of the erythrocyte lipids from 3 patients and 3 controls is shown in Figure 5.1, and the corresponding R_f values are shown in Table 5.1. As can be seen the neutral lipids from human erythrocytes consist almost exclusively of cholesterol, in comparison to the standard lipid mixture derived from cod roe, which contains substantial amounts of cholesterol esters (CE), triacylglycerol (TAG) and free fatty acids (FFA). The phospholipids detected are Sph, PC, PS, PI and PE and, in contrast to the erythrocyte membranes, the standard sample contains no PS and a significant amount of PI.

Table 5.2 compares the cholesterol and phospholipid content of the erythrocyte membranes from Li^+-free healthy controls and Li^+-treated patients. The data indicates that the proportion of cholesterol present appears to be slightly increased in the patient group, however this difference is not statistically significant (i.e. below the 95% confidence limits).

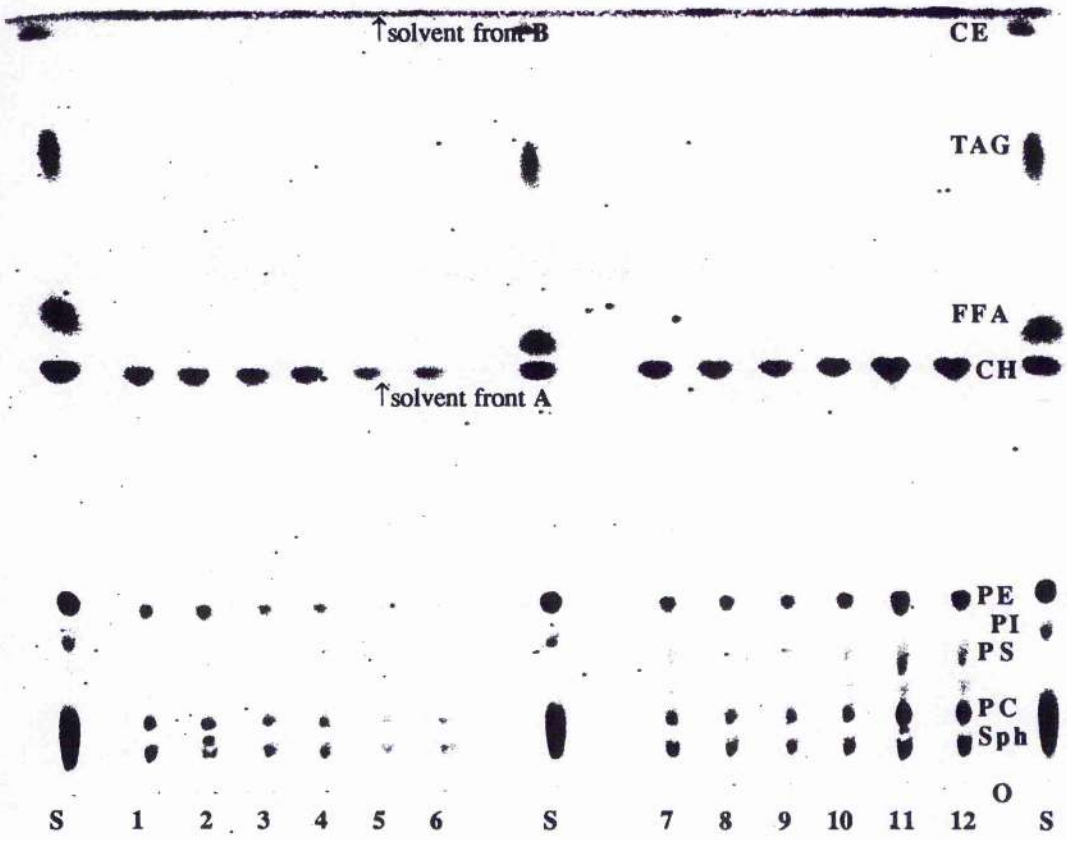

Figure 5.1 TLC of human erythrocyte membrane lipids from 3 controls (**1-6**) and 3 Li^+-treated patients (**7-12**) in duplicate, developed in solvent systems: (**A**) chloroform-*i*-propanol-methyl acetate-methanol-0.25% w/v KCl (25:25:25:10:9); (**B**) hexane-diethyl ether-acetic acid (80:10:2).

Abbreviations: **O**-origin; **S**-standard (cod roe); **CE**-cholesterol esters; **TAG**-triacylglycerol; **FFA**-free fatty acids; **CH**-cholesterol; **PE**-phosphatidylethanolamine; **PI**-phosphatidylinositol; **PS**-phosphatidylserine; **PC**- phosphatidylcholine; **Sph**-sphingomyelin

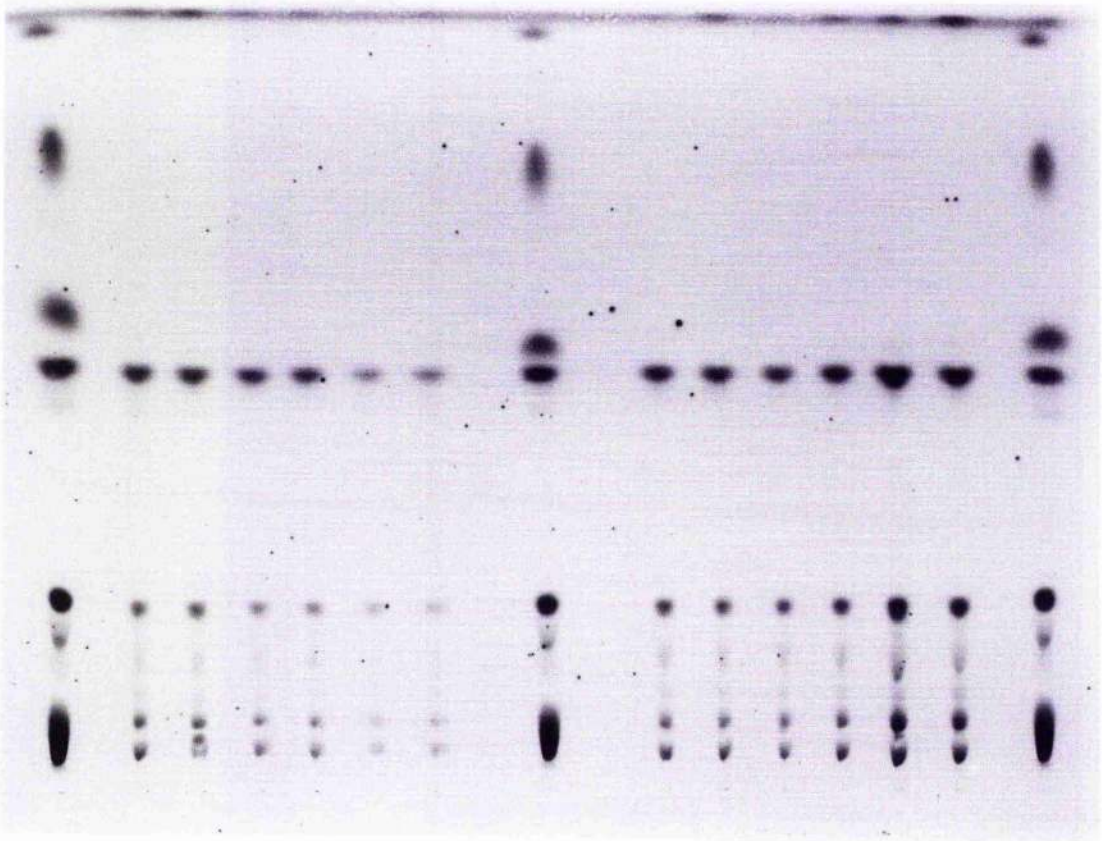

Table 5.1 R_f values of human erythrocyte lipids on TLC in the solvent systems: (A) chloroform - *i*-propanol - methyl acetate - methanol - 0.25% w/v KCl (25 : 25 : 25 : 10 : 9) and (B) hexane - diethyl ether - acetic acid (80 : 10 : 2).

LIPID COMPONENT	R_f
Sphingomyelin	0.05
Phosphatidylcholine	0.09
Phosphatidylinositol	0.16
Phosphatidylethanolamine	0.24
Cholesterol	0.54

Table 5.2 Comparison of the cholesterol (unesterified) and phospholipid content of human erythrocyte membranes as a percentage of the total, from Li^+-free controls and Li^+-treated patients

	Phospholipid (PL)	Cholesterol (Ch)	PL / Ch
Controls (n=6)	55.50 ± 4.0	44.50 ± 4.0	1.2
Patients (n=6)	63.29 ± 4.1	36.71 ± 4.1	1.7

Both Table 5.2 and 5.3 show that there is a significant amount of variation in the results obtained and this was found even in the duplicates of the same sample, indicating that this behaviour is primarily due to the experimental procedure.

There is also considerable variation reported in the literature for the concentrations of the individual phospholipids in erythrocyte membranes, depending upon the methods employed. However, Table 5.3 indicates that the results obtained in this work using HP-TLC are comparable to levels quoted by Nelson, which are the mean values from a number of different studies chosen from the literature *(26)*. In general, there is very little difference in the phospholipid content between the Li^+-free

and Li^+-treated groups. The level of Sph appears to be very slightly decreased (11%) and that of PS is increased (21%) in the Li^+-treated group, however these differences are not statistically significant. The levels in the control group are consistently closer to those of the literature data for 'normal' human erythrocytes, implying that the deviations observed in the patient group are probably reliable. Figure 5.2 illustrates the phospholipid composition of the erythrocyte membranes for the two groups.

Table 5.3 Comparison of phospholipid content of human erythrocyte membranes, as a percentage of total phospholipid, from Li^+-free controls and Li^+-treated patients

Phospholipid	Controls (n=6)	Patients (n=6)	Reference *(26)*
Sph	24.5 ± 1.8	21.9± 1.7	25.8 ± 2.2
PC	29.6 ± 3.2	28.8 ± 2.5	32.2 ± 2.8
PS	14.4 ± 1.8	17.4 ± 1.8	13.0 ± 3.1
PI	3.3 ± 2.2	3.2 ± 1.6	1.8 ± 0.8
PE	28.0 ± 2.1	28.4 ± 1.5	27.2 ± 3.0

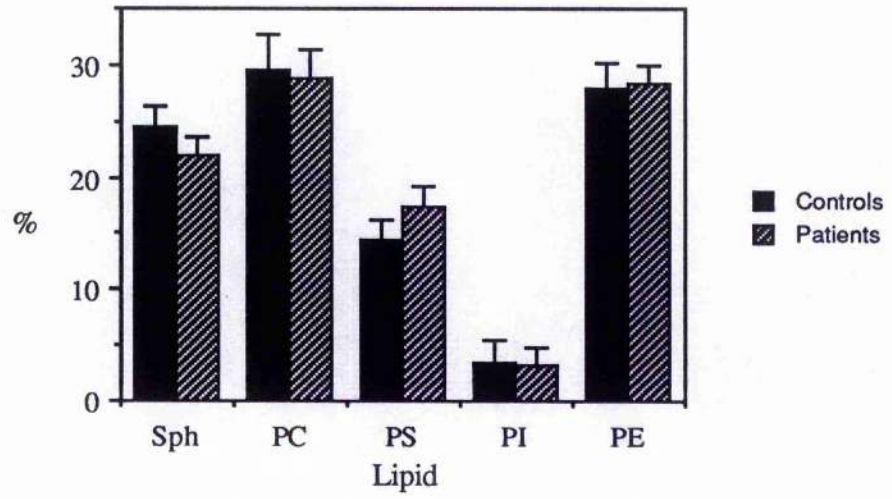

Figure 5.2 Comparison of the phospholipid content of erythrocyte membranes, as a percentage of the total phospholipids, from Li^+-treated psychiatric patients and Li^+-free controls

5.2.2 Lipid Content of Rabbit Erythrocyte Membranes

For comparative purposes, the lipid content of rabbit erythrocytes was also determined by HP-TLC. The proportion of cholesterol (56.6 ± 3.9 %) was higher than that in humans, giving a lower PL/C ratio of 0.8. Table 5.4 shows that there are a couple of significant differences in the proportions of the individual phospholipids compared to the human erythrocyte membrane (Table 5.3). There is a decrease in the proportion of Sph and a corresponding increase in the proportion of PE, as predicted from the literature *(26)*.

Table 5.4 Phospholipid content of rabbit erythrocyte membranes, as a percentage of total phospholipid

Phospholipid	Rabbits	Reference *(26)*
Sph	13.7 ± 2.6	19.0
PC	29.5 ± 0.1	34.2
PS	16.7 ± 0.7	12.2
PI	2.1 ± 0.8	1.6
PE	38.0 ± 2.7	31.9

5.2.3 Effect of Li^+ Therapy upon the Protein Content of Human Erythrocyte Membranes

Erythrocyte ghosts were prepared from the erythrocytes of Li^+-free controls and of Li^+-treated patients, the membrane proteins were solubilised using sodium dodecyl sulphate (SDS) and the mixture was fractionated by polyacrylamide gel electrophoresis (SDS-PAGE). This produced a size-dependent separation of the membrane proteins which were revealed by staining the gel with Coomassie Brilliant Blue.

Figure 5.3 SDS-PAGE profile of human erythrocyte membrane proteins from 3 controls **(2, 6, 8)**, 3 Li^+-treated patients **(1, 3, 4)** and 2 controls after a 24h *in vitro* incubation in Li^+-containing medium **(5, 7)**

(**o** = standard mixture of protein molecular weight markers (Biorad Lab. Ltd); the gel was stained with Coomassie Brilliant Blue)

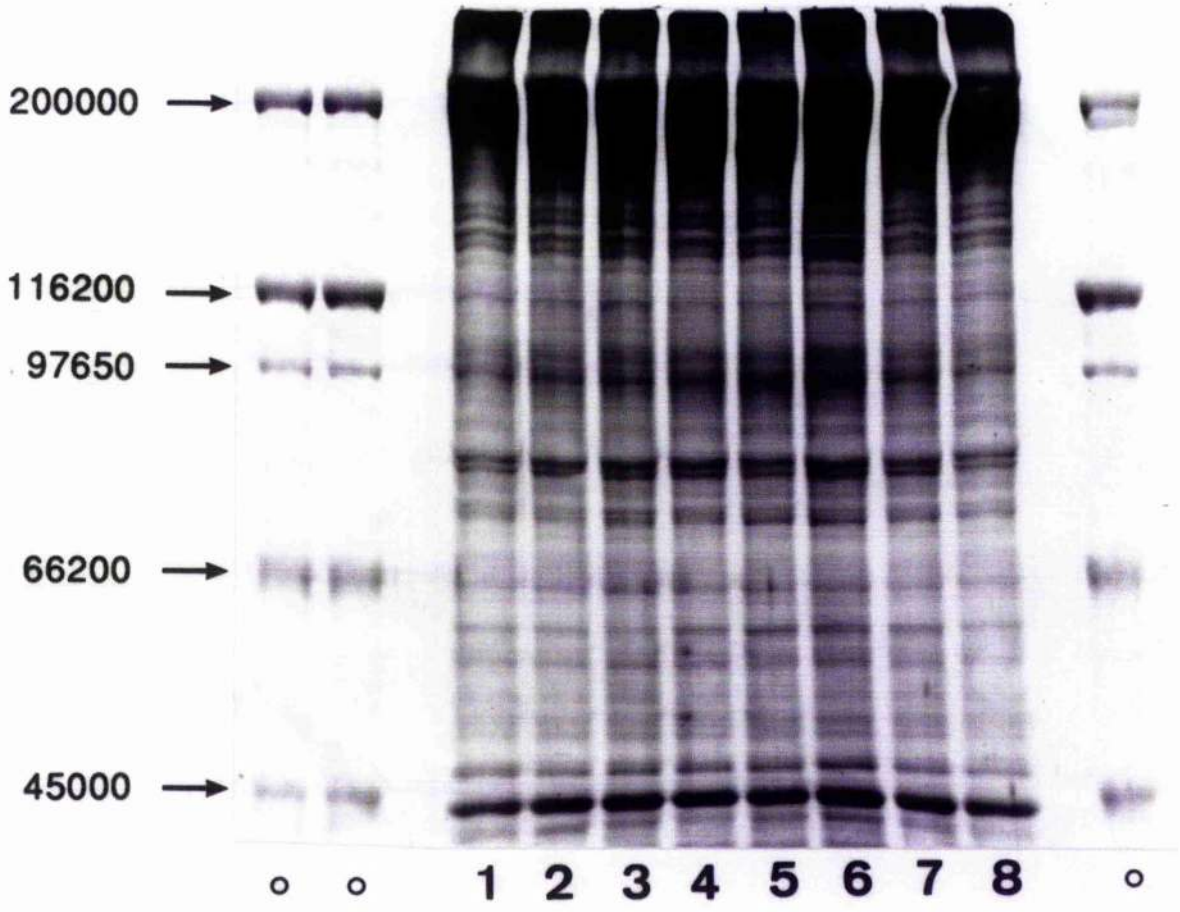
200000
116200
97650
66200
45000
o o 1 2 3 4 5 6 7 8 o

A photograph of a typical gel of the erythrocyte membrane proteins from 3 patients and from 3 controls is shown in Figure 5.3. Also included on this gel are the proteins from 2 of the controls after a 24h *in vitro* incubation of the erythrocytes in Li^+-containing medium. A visual comparison of the chromatograms showed that there are no significant differences in the major protein components of the erythrocyte membranes of any of these samples. The following general assignments are as according to Steck *(27)* : the very intense band around the 200,000 protein molecular weight (m.w.) marker comprises a doublet arising from α–, and β-spectrin; the doublet at approximately 78,000 m.w. arises from the Band 4.1 and 4.2 proteins; and the intense band at 43,000 m.w. is actin (Band 5). The Band 3 protein, which contains the anion channel, occurs as a diffuse zone around the 97650 m.w. marker.

5.3 Discussion

The main conclusion to draw from this data, using these analytical techniques, is that there is very little difference between the concentrations of the major components of the erythrocyte membranes of Li^+-treated psychiatric patients and of Li^+-free healthy controls. No significant differences were observed for either the major lipid or the major protein content of the erythrocyte membranes. The slightly lower level of Sph and corresponding higher level of PS in the Li^+-treated patients is not in accordance with any of the reported membrane effects of Li^+. Interestingly, the levels of PC and PE for the 2 groups were virtually identical, in contrast to the data reported for the Li^+-treated schizophrenic patients *(17,18,19,20).*

The use of other techniques may be required to identify an abnormality in a specific membrane component that was not analysed for in this work. For instance, differences in the levels of the fatty acid components of the individual phospholipids can be determined by GLC, as observed for Sph from the erythrocytes of the

schizophrenic patients *(17)*, or alternatively subtle differences in the changes of minor protein components can be determined by their isolation and analysis, as in the abnormality observed in the ankyrins in bipolar patients *(23,24)*.

Success in identifying a specific membrane fault in bipolar affective disorder could lead to a new category of therapeutic drugs to correct for the primary biochemical errors in bipolar illnesses, in contrast to present psychopharmacological drugs which balance a neurochemical abnormality. Such drugs would regulate either the insertion of specific proteins into the membrane, or the mode of linkage of integral membrane proteins to the underlying cytoskeleton.

5.3 References

1 Grisham, C.M. and Barnett, R.E. (1973), *Biochem.*, **12**, 2635-2637.

2 Hokin-Nearvson, M., Burchardt, W.A. and Jefferson, J.W. (1976), *Res. Commun. Chem. Pathol. Pharmacol.*, **14**, 117-126.

3 Mallinger, A.G., Hanin, I., Himmelhoch, J.M., Thase, M.E. and Knopf, S. (1987), *Psychiat. Res.*, **22**, 49-59.

4 Meltzer, H.L., Kassir, S., Goodnick, P.J., et al (1988), *Neuropsychobiol.*, **20**, 169-173.

5 Lee, G., Lingsch, C., Lyle, P.T. and Martin, K. (1974), *Brit. J. Clin. Pharmacol.*, **1**, 365.

6 Jope, R.S., Jenden, D.J., Ehrlich, B.E. and Diamond, J.M. (1978), *N. Eng. J. Med.*, **299**, 833-834.

7 Jones, A.J. and Kuchel, P.W. (1980), *Clin. Chim. Acta*, **104**, 77-85.

8 Lingsch, C. and Martin, K. (1976), *Br. J. Pharmacol.*, **57**, 323.

9 Jope, R.S. (1979), *J. Neurochem.*, **33**, 487.

10 Rutherford, P.A., Thomas, T.H. and Wilkinson, R. (1992), *Clin. Sci.*, **82**, 341-352.

11 Hunt, S.C., Williams, R.R., Smith, J.B. and Ash, K.O. (1986), *Hypertension*, **8**, 30-36.

12 Corrocher, R., Ferrari, S., Bassi, A. et al (1987), *Life Sci.*, **41**, 1171-1178.

13 Duhm, J. and Behr, J. (1986), *Scand. J. Clin. Lab. Invest. (Supplement)*, **46**, 82-95.

14 Rybakowski, J.K., Amsterdam, J.D., Dyson, W.L. Frazer, A., Winokur, A. and Kurtz, J. (1989), *Pharmacopsychiat.*, **22**, 16-20.

15 Engleman, B. and Duhm, J. (1991), *J. Memb. Biol.*, **122**, 231-238.

16 Engleman, B., Op den Kamo, J.A.S. and Roelofsen, B. (1990), *Am. J. Physiol.*, **258**, C682-C691.

17 Hitzman, R.J. and Garver, D.L. (1982), in *Biological Markers In Psychiatry and Neurology*, Pergamon Press, ed. Usdin, E. and Hanin, I., 177-182.

18 Hitzman, R.J. and Garver, D.L. (1982), *Pharmacol. Bull.*, **18**, 190-193.

19 Stevens, J.D. (1972), *Schizo. Bull.*, **6**, 60-61.

20 Henn, F.A. and Henn, S.W. (1982), in *Biological Markers In Psychiatry and Neurology*, Pergamon Press, ed. Usdin, E. and Hanin, I., 183-186.

21 Pelech, S.L. and Vance, D.E. (1984), *Biochim. Biophys. Acta*, **779**, 217-251.

22 Joseph, N.E., Renshaw, P.F. and Leigh, J.S. (1987), *Biol. Psychiat.*, **22**, 540-544.

23 Zhang, Y. and Meltzer, H.L. (1989), *Psychiat. Res.*, **27**, 267-275.

24 Zhang, Y., Placidi, G.F. and Meltzer H.L. (1990), *Clin. Pharmacol. Ther.*, **47**, 136.

25 Hedegard, E. and Jensen, B. (1981), *J. Chromatog.*, **225**, 450-454.

26 Nelson, G.J., ed. (1979), in *Blood Lipids and Lipoproteins: Quantitation, Composition and Metabolism.*, Robert E. Kreiger Publishing Co., p334.

27 Steck, T.L. (1974), *J. Cell. Biol.*, **62**, 1-19.

Chapter 6

Interaction of Lithium with Inositol Monophosphatase

6.1 Li^+ and Inositol Monophosphatase

One popular hypothesis for the therapeutic effect of Li^+ is its interference with inositol lipid metabolism by virtue of its ability to inhibit the enzyme inositol 1-monophosphatase. Many neurotransmitters act by stimulating the inositol lipid metabolism which results in the activation of 2 second messengers: inositol 1,4,5-trisphosphate, Ins(1,4,5)P_3, which releases Ca^{2+} from intracellular stores *(1)*, and 1,2-diacylglycerol, 1,2-DG, which activates protein kinase C *(2)*. Thus, it is proposed that Li^+ alleviates bipolar affective disorder by interfering with the inositol phospholipid-dependent intracellular signalling behaviour of actively stimulated, but not resting neurones.

Li^+ was first found to interfere with inositol lipid metabolism when decreased levels of *myo*-inositol were observed in the brains of Li^+-treated rats *(3)*. Subsequent work revealed a corresponding increase in the levels of inositol 1-phosphate, I(1)P_1, *(4)*, and this behaviour was found to be the result of the inhibition of inositol 1-monophosphatase by Li^+ ($K_i \approx$ 1mM), the enzyme which converts I(1)P_1 to free inositol *(5)*.

6.1.1 The Phosphoinositide Cycle and its Interference by Li^+

In the phosphoinositide cycle illustrated in Figure 6.1, the activation of the membrane receptor by specific agonists stimulates the hydrolysis of phosphatidylinositol 4,5-bisphosphate, PI(4,5)P_2, catalysed by the enzyme phosphoinositidase C, PIC; a GTP-dependent protein is responsible for coupling the activated receptor to PIC (reviewed in reference *6*). This then generates the 2 second messengers, inositol 1,4,5-trisphosphate, I(1,4,5)P_3, and sn(1,2)-diacylglycerol, (DAG). PIC also interacts with other inositol phospholipids to give inositol 1,4-bisphosphate, I(1,4)P_2, and inositol 1-phosphate, I(1)P_1. I(1,4,5)P_3 is then recycled

through two pathways: by dephosphorylation by a 5-phosphatase to produce $I(1,4)P_2$, or by phosphorylation catalysed by a 3-kinase to produce inositol 1,3,4,5-tetrakisphosphate, $I(1,3,4,5)P_4$, which is thought to be another second messenger. Subsequently, $I(1,4)P_2$ and inositol 1,3,4-trisphosphate, $I(1,3,4)P_3$, the product of dephosphorylation of $I(1,3,4,5)P_4$, are both dephosphorylated by inositol polyphosphate 1-phosphatase, and all the inositol monophosphate isomers, $I(1)P_1$, $I(4)P_1$ and $I(3)P_1$, are dephosphorylated by inositol monophosphatase to generate free inositol. Both of these latter enzymes, inositol polyphosphate 1-phosphatase and inositol monophosphatase, are uncompetitively inhibited by Li^+ *(5,7)*.

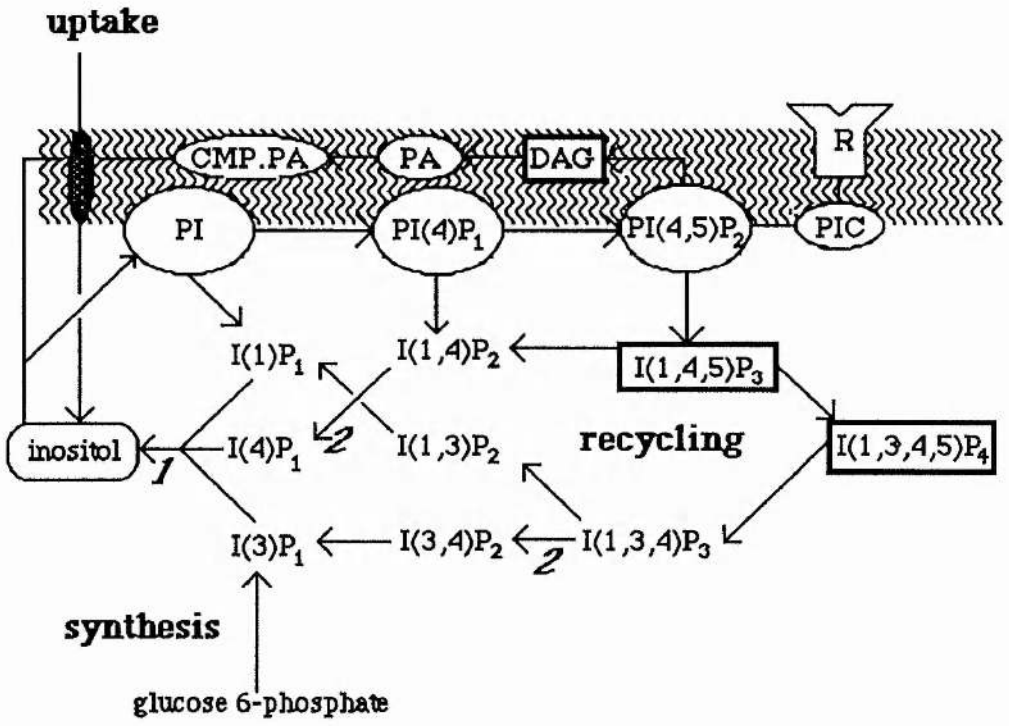

Figure 6.1 Scheme of the phosphoinositide recycling pathway, showing the 2 enzymes which are uncompetitively inhibited by Li^+ and the sources of cellular inositol

(*1* = inositol monophosphatase; *2* = inositol polyphosphate 1-phosphatase)

$PI(4,5)P_2$, the precursor used by the membrane receptor to generate the second messengers, is formed by the phosphorylation of phosphatidylinositol, PI, which, in turn, is synthesized from free inositol and cytidine monophosphoryl-phosphatidate, CMP.PA, by the action of a synthase, *myo*-inositol 3-phosphatidyl transferase. Therefore, the supply of $PI(4,5)P_2$ available to the receptor, depends upon maintenance of the levels of cellular inositol - a reduction in the level of cellular inositol will reduce the supply of $PI(4,5)P_2$ and consequently will impair the activation of the receptor in response to an agonist and the subsequent formation of the second messengers.

There are 3 sources which contribute to free inositol in cells (illustrated in Figure 6.1): *de novo* synthesis from glucose, in which the penultimate step is the cyclisation of glucose-6-phosphate to $I(3)P_1$, which is then dephosphorylated; from the phosphoinositide cycle, whereby the final step is dephosphorylation of the inositol monophosphates; and uptake from the extracellular environment. Since Li^+ inhibits inositol 1-monophosphatase, the enzyme responsible for the dephosphorylation of the inositol monophosphates including $I(3)P_1$, the first 2 sources of inositol are both sensitive to Li^+ and, therefore, in the presence of Li^+ the extracellular supply of inositol becomes the only source of cellular inositol. It has been reported that the blood brain barrier is relatively impermeable to inositol *(8)*, and proposed that, in consequence, nerve cells are primarily dependent upon the Li^+ sensitive pathways for free inositol. Therefore, nerve cells may be particularly vulnerable to the inhibitory action of Li^+ particularly during periods of intense stimulation, in comparison to peripheral cells which are exposed to supplies of inositol in plasma. This behaviour has two interesting aspects in relation to the therapeutic action of Li^+. First, the time delay before a response to Li^+ treatment is observed could be accounted for by the reservoir of PI available in cells, which has to be depleted before the inhibitory effect of Li^+ becomes significant. Secondly, the inhibitory effect of Li^+ will be significant only in cells when the receptors are being hyperstimulated, as might be expected in nerve cells during periods of severe mania or depression.

However, it should be noted that the concentrations of inositol in plasma are approximately 50-100μM whereas in cerebrospinal fluid the concentrations are several fold higher, and also, in a number of cell types, a transport mechanism has been identified which allows inositol to accumulate in cells against the electrochemical gradient *(9)*. Thus, if the rate of inositol uptake is comparable with the stimulated rate of PIC activity, the proposed influence of Li^+ on the second messenger system may be minimal and might not be responsible for the therapeutic action of Li^+ in bipolar affective disorder.

6.1.2 Mechanism of Hydrolysis of I(1)P_1 and Inhibition by Li^+

The mechanism of the inhibition of inositol monophosphatase by Li^+ was confirmed to be uncompetitive *(10)*. This type of inhibition of an enzyme is extremely rare in nature, and can arise when the inhibitor, I, binds to the enzyme-substrate complex, ES, rather than to the free enzyme, E. In comparison, in competitive inhibition, E can combine with either the substrate, S, to give the complex ES, or with I to give EI. This type of inhibition usually occurs when I is a substrate analogue and sits in the active site normally occupied by I. In competitive inhibition, S and I have a linear relationship over a wide concentration range - thus the inhibition of E, caused by an increase in the concentration of I can be overcome by a proportionate increase in the concentration of S. In uncompetitive inhibition however, an increase in the concentration of I requires a disproportionately large increase in the concentration of S to maintain the same metabolic turnover of E, and at higher inhibitor concentrations the inhibition may not be overcome at all.

Inositol monophosphatase is completely dependent upon Mg^{2+} for activity, and is competitively inhibited by Ca^{2+}, Mn^{2+} and *myo*-inositol 2-phosphate *(11)*; Ca^{2+} is a competitive inhibitor for Mg^{2+} binding. The inhibition by Li^+ is uncompetitive, with no evidence that Li^+ is competitive with either Mg^{2+} or I(1)P_1. Through detailed

kinetic studies on this enzyme, the mechanism of the phosphate ester hydrolysis and the inhibitory effect of Li^+ is being investigated (for a recent review see reference *9*). The hydrolysis of *myo*-inositol 1-phosphate, as it is currently understood, involves a ternary complex mechanism which is summarised in Figure 6.2. The enzyme binds the substrate, $I(1)P_1$, with H_2O being the second substrate (step *1* in Figure 6.2) and the ester is then hydrolysed to give inositol and P_i (step *2*). Inositol is the first product off (step *3*) with P_i debinding last (step *4*). The co-factor, Mg^{2+}, appears to bind to the enzyme after $I(1)P_1$ does, implying that the substrate either modifies, or creates the binding site for Mg^{2+}. Mg^{2+} is only required for the catalytic steps and Li^+ binds to the active site which vacated by Mg^{2+} before P_i is released. Li^+ can bind to either the E:S complex, where it apparently does not prevent inositol from debinding, or to the E:P_i complex. In complexation with Li^+, the activity of the enzyme is severely reduced.

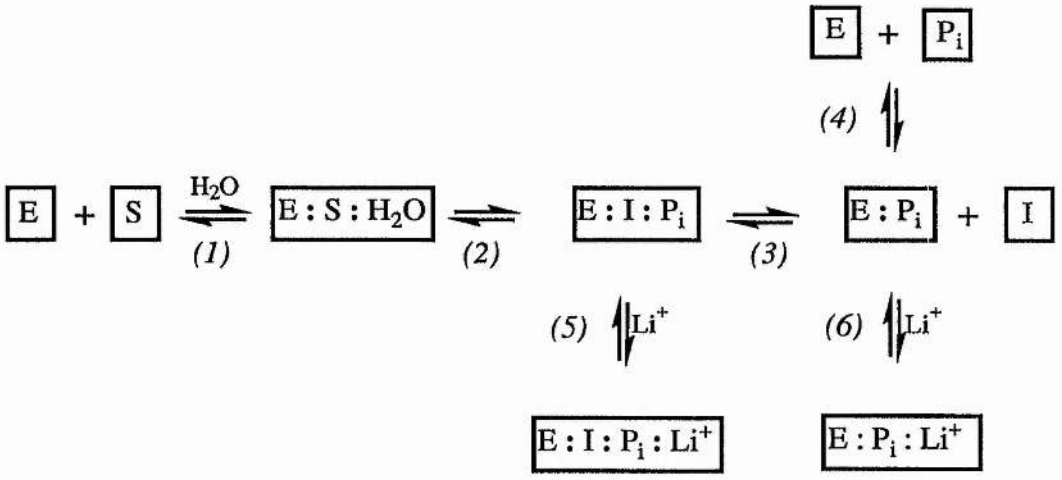

Figure 6.2 Postulated mechanism of the hydrolysis of inositol 1-monophosphate, (S), by inositol 1-monophosphatase, (E), and the interaction by Li^+

(I = inositol, $P_i = HPO_4^{2-}$)

6.1.3 Structure of Inositol Monophosphatase

Both of the inositol monophosphatases purified from rat brain and from bovine brain are homodimers with molecular weights of 55,000 *(12)* and 58,000 *(11)*, respectively. By expression in *Escherichia coli*, the bovine enzyme has been successfully sequenced and cloned *(13)*, and subsequently both the human and rat brain inositol monophosphatases have been cloned and purified *(14)*.

The structure of the human inositol monophosphatase, purified from *Escherichia coli* , has recently been determined using X-ray crystallography *(15)*. Figure 6.3 is a ribbon representation of the inositol 1-monophosphatase dimer, showing the secondary structure of the enzyme. The dimer consists of identical subunits, with Gd^{3+} (orange sphere) and SO_4^{2-} (ball and stick) bound at identical sites on each subunit. Gd^{3+}, was employed as a heavy metal substitute for Ca^{2+}, which competes with the normal co-factor, Mg^{2+}, and occupies the same position on the enzyme as Ca^{2+} does. Therefore, the position occupied by Gd^{3+} on the enzyme in this crystal structure is probably the active site normally occupied by Mg^{2+} *in vivo*. Similarly, SO_4^{2-} is expected to interact with the enzyme in the same manner as the phosphate group of the substrate or phosphate product of the hydrolysis reaction, and therefore the position of SO_4 in the crystal structure is likely to be significant also. These active sites appear to sit in a relatively large, and predominantly hydrophilic 'cavern' within the enzyme, which is much larger than is required to accommodate the substrate, $I(1)P_1$. Knowledge of the structure of the enzyme should now lead to a better understanding of the mechanism of the hydrolysis and also to the design of inhibitors of the enzyme to confirm (or disprove) that the inhibitory effect of Li^+ is responsible for its therapeutic action.

Figure 6.3 Ribbon Representation of the Secondary Structure of the Inositol Monophosphatase Dimer *(15).*

(Gd^{3+} is shown as an orange sphere and SO_4 is represented by a ball and stick model)

Photograph donated by, and reproduced with the kind permission of Dr C.I. Ragan, Director of Biochemistry at Merck, Sharpe & Dohme Research Laboratories, Harlow, Essex.

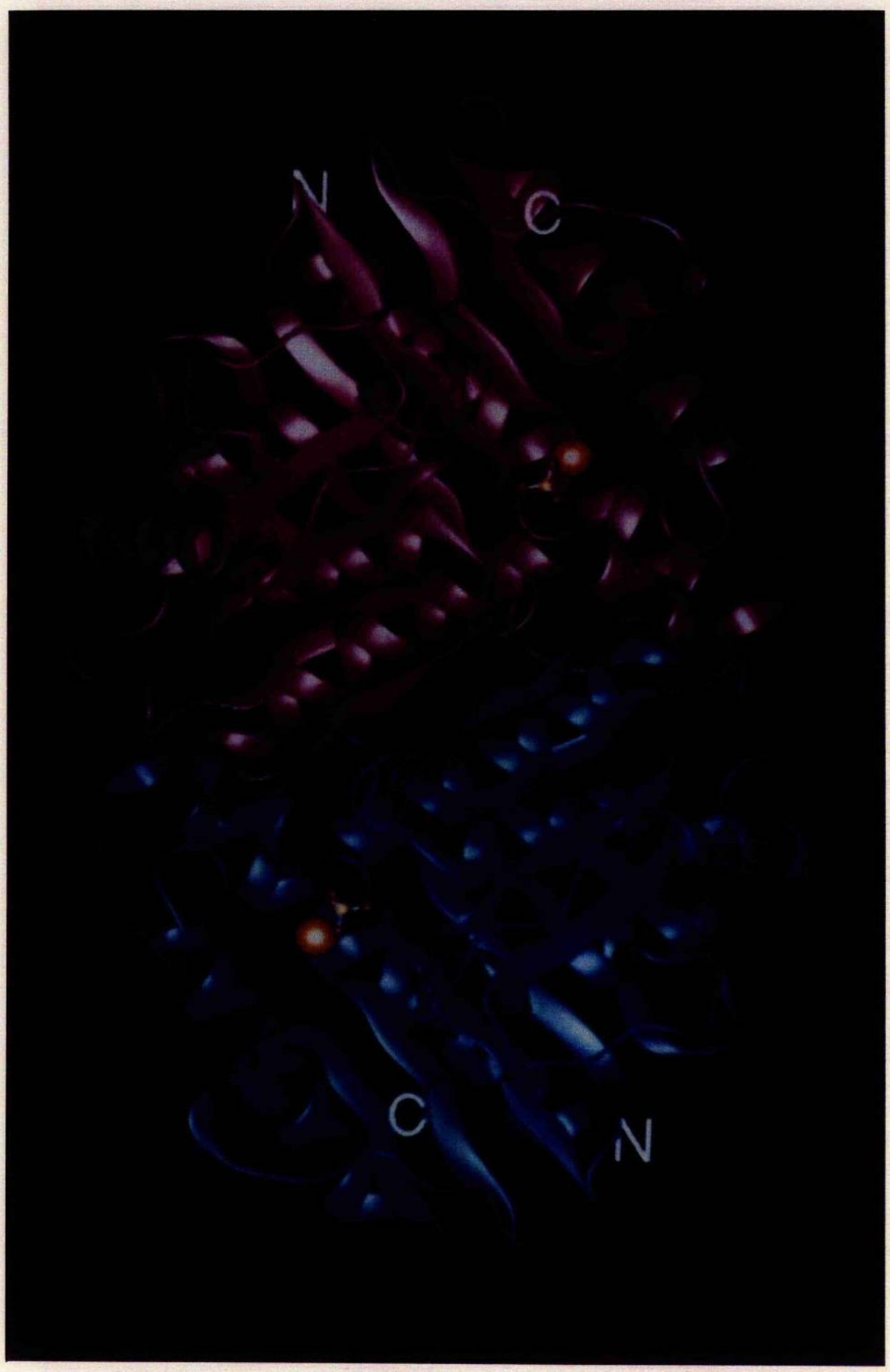
N
C
C
N

6.1.5 Changes in Inositol Levels in Human Brain

The study of the phosphoinositide cycle in humans is obviously very limited, however *in vivo* ^{31}P-nmr spectroscopy has the potential to explore the concentrations of phosphorous metabolites in all human tissue, including the brain. The *in vivo* ^{31}P-nmr spectroscopy of the brains of bipolar patients treated with Li^+ showed elevated levels of phosphomonoesters (PME) in patients in the manic state, compared to those in the euthymic state and to Li^+-free controls *(16)*. This was believed to be due to elevation of the level of I(1)P_1, which is known to appear in this region of the ^{31}P-nmr spectrum, however, that it could arise from elevation of other substance, such as phosphorylethanolamine or phosphorylcholine, could not be ruled out. High-resolution ^{31}P-nmr spectroscopy of the brain extracts of Li^+-treated cats had previously confirmed that the elevated level of PME observed in the cat brains by *in vivo* ^{31}P-nmr spectroscopy using surface coils, was predominantly due to I(1)P_1 *(17)*. Similar results have also been reported recently by the *in vivo* ^{31}P-nmr spectroscopy of rat brain *(18)*.

6.2 ^{7}Li-Nmr Studies of Interaction of Li^+ with Enzymes

The potential of ^{7}Li-nmr spectroscopy as a probe in enzyme studies was demonstrated by a study on the cation binding sites of Na^+/K^+-ATPase *(19)*. By substituting Li^+ for K^+ in the K^+ binding site on the enzyme, the ^{7}Li-nuclear relaxation rate increased with increasing [Mn^{2+}]. Mn^{2+}, a paramagnetic cation, was used in this study as a substitute for Mg^{2+}, which is diamagnetic. The paramagnetic effect upon the ^{7}Li relaxation rate was used to estimate the distance between the Mn^{2+} and the Li^+ on the enzyme, and hence to give information on the distances of the K^+ and Mg^{2+} binding sites on the enzyme. No change in T_1 was observed on addition of increasing amounts of Mg^{2+} to similar solutions of the enzyme and Li^+.

In the research for this thesis, ^{7}Li-nmr spectroscopy has been employed to investigate the interaction of Li^+ with the enzyme, inositol 1-monophosphatase. Any binding of Li^+ to the enzyme was expected to be observable in the ^{7}Li-nmr spectrum. The inclusion of a chemical shift reagent in the solution should produce a shift difference in the Li-nmr spectrum between the resonances of the two Li^+ species (the bound and the free aqueous Li^+). If the exchange rate between these two species is relatively slow (on the NMR timescale), both signals will be observed in the spectrum. However, if the exchange rate is rapid, only one signal will be observed at a chemical shift intermediate between that of the two separate resonances. The T_1 relaxation time of the bound Li^+ is expected to be considerably shorter than that of the free ion, and the overall measurable T_1 relaxation time of the Li^+ resonance in a solution containing the enzyme will represent a weighted average of those of the free and bound Li^+ species, and should, therefore, be significantly lower than that of the Li^+ resonance in the absence of the enzyme.

6.2.1 ^{7}Li-Nmr Studies of the Interaction of Li^+ with Inositol 1-Monophosphatase

Aqueous solutions of homogeneous bovine brain inositol 1-monophosphatase, containing K^+ (250mM), Mg^{2+} (3mM) and Tris (50mM) at pH 7.5, with varying concentrations of LiCl, inositol 1-monophosphate, HPO_4^{2-}, inositol and $Dy(P_3O_{10})_2^{7-}$ were examined by ^{7}Li-nmr spectroscopy to investigate the interaction between the enzyme and Li^+.

$Dy(P_3O_{10})_2^{7-}$ was initially employed to distinguish between the ^{7}Li resonances arising from the free Li^+ and any Li^+ bound to the enzyme. Although the FID's were accumulated for long periods of time and with relatively large sweep widths of up to 50,000Hz, only a single resonance was observed under any condition, in all the solutions used.

T_1 measurements were then performed, using the inversion-recovery technique, for the Li^+ species present in the various solutions. $Dy(P_3O_{10})_2^{7-}$ was included in the buffer to allow relatively rapid data acquisition and the results recorded in Table 6.1 show a range of T_1's from 185-350ms. A slight decrease in the T_1 of approximately 10% occurred on addition of the enzyme to the Li^+-containing buffer, however this was probably due to a concentration, or a viscosity, effect rather than to a specific Li^+-enzyme interaction. This was confirmed by a decrease in the T_1, of approximately 20%, following the addition of bovine serum albumin (BSA) to the Li^+-containing buffer. BSA is a protein of similar molecular weight (66,700) to the inositol monophosphatase dimer, with no known interaction with Li^+ and, therefore binding to Li^+ is unlikely to produce an effect upon the relaxation behaviour

No correlation was found between the T_1 and the concentration of $I(1)P_1$ in solutions containing Li^+ and the enzyme. Similarly, no significant change in T_1 was observed on the addition of inorganic phosphate, P_i, to the Li^+/enzyme mixture however in this case, the subsequent addition of inositol produced a reduction in the T_1. Since a similar reduction was observed on the addition of inositol to solutions of Li^+ and BSA, this behaviour was probably due to the significant increase in the viscosity of the solution observed upon the addition of inositol.

Table 6.1 The effect of inositol monophosphatase (E) on the T_1 of ^7Li in a variety of aqueous solutions

Solutes in Buffer* (mM)	T_1 / ms
Li^+ (1)	349
Li^+ (1) + E (0.2)	296
Li^+ (1) + E (0.2) + I(1)P_1 (0.8)	312
Li^+ (1) + E (0.2) + I(1)P_1 (1.6)	296
Li^+ (1) + E (0.2) + I(1)P_1 (3.1)	286
Li^+ (1) + E (0.2) + I(1)P_1 (10.6)	337
Li^+ (1) + E (0.3) + P_i§ (10)	339
Li^+ (1) + E (0.3) + P_i (10) + inositol (100)	244
Li^+ (1) + E (0.3) + P_i (10) + inositol (200)	247
Li^+ (1) + E (0.3) + P_i (10) + inositol (400)	238
Li^+ (10)	295
Li^+ (10) + E (0.4)	268.
Li^+ (10) + E (0.4) + P_i (3)	284
Li^+ (10) + E (0.4) + P_i (3) + inositol (200)	244
Li^+ (10) + BSA† (0.37)	235
Li^+ (10) + BSA (0.37) + inositol (200)	186
Li^+ (10)) + inositol (200)	258

*buffer = KCl (175mM), $MgCl_2$ (3mM), $K_5P_3O_{10}$ (15mM), Tris (50mM) and $DyCl_3$ (1mM) at pH 7.5;

§P_i = inorganic phosphate, K_2HPO_4; †BSA = bovine serum albumin

6.3 Discussion

The conditions employed in these studies were selected to optimise the possibility of observing a Li^+:enzyme interaction. At a Li^+ concentration of 1mM and an enzyme concentration of 0.2mM, it was estimated that approximately 50% of the Li^+ is likely to be bound to the enzyme. First, the substrate, $I(1)P_1$, was added to solutions of Li^+ and the enzyme to force the equilibriums in the forward directions (in Figure 6.2) and then, in similar experiments, the products of the hydrolysis reaction, inositol and P_i, were added to force the equilibria in the reverse directions, in order to obtain significant levels of the $E:I:P_i:Li^+$ complex and/or the $E:P_i:Li^+$ complex.

The presence of only a single resonance in the Li^+/enzyme mixtures on the addition of the shift reagent is probably indicative of a relatively fast exchange rate for the bound and free Li^+ species. However, the reason for the absence of any observable effect upon the relaxation behaviour of the Li^+ ion is unknown. It may be that the effect of the shift reagent, of reducing the T_1 of all the Li^+ species in these solutions, is masking any effect due to a Li^+:enzyme interaction. Therefore, these experiments should ideally be performed in the absence of $Dy(P_3O_{10})_2^{7-}$, however this would impractical due to the extremely long acquisition times that would be required in order to obtain adequate signal-to noise in each spectrum. Apart from the disadvantage of limited spectrometer availability, the instability of the enzyme preparation, which is contaminated with a small amount of a protease, makes this approach unrealistic.

Under all the conditions employed in this study it was not possible to observe any interaction between Li^+ and inositol 1-monophosphatase.

6.4 References

1 Berridge, M.J and Irvine, R.F. (1984), *Nature*, **312**, 315-321.

2 Nishizuka, Y. (1984), *Nature*, **308**, 693-697.

3 Allison, J.H. and Stewart, M.A. (1971), *Nature (New Biol.)*, **233**, 267-268.

4 Allison, J.H. and Blisner, M.E. (1976), *Biochem. Biophys. Res. Commun.*, **68**, 1332-1338.

5 Hallcher, L.M. and Sherman, W. R. (1980), *J. Biol. Chem.* **255**, 10896-10901.

6 Nahorski, S.R., Ragan, C.I. and Challiss, R.A.J. (1991), *Tips*, **12**, 297-303.

7 Gee, N.S., Reid, G.G., Jackson, R.G., Barnaby, R.J. and Ragan, C.I., (1988), *Biochem. J.*, **253**, 777-782.

8 Lewin, L.M., Yanna, Y., Sulimovici, S. and Kraicer, P.F. (1976), *Biochem. J.*, **156**, 375-380.

9 Gani, D., Downes, C.P., Batty, I. and Bramham, J. (1993), *Biochem. Biophys. Acta*, in press.

10 Shute,J.K., Baker, R., Billington, D.C. and Gani, D. (1988), *J. Chem. Soc. Chem. Commun.*, 626-628.

11 Gee, N.S., Ragan, C.I., Watling, K.J., Aspley, S., Jackson, R.G., Reid, G.G., Gani, D. and Shute, J.K. (1988), *Biochem. J.*, **249**, 883-889.

12 Takimoto, K., Okada, M., Matsuda, Y. and Nakaga, H. (1985), *J. Biochem.*, **98**, 363-370.

13 Diehl, R.E., Whiting, P., Potter, J., Gee, N., Ragan, C.I., Lienmeyer, D., Schoepfer, R., Bennet, C. and Dixon, R.A.F. (1990), *J. Biol. Chem.*, **265**, 5946-5949.

14 McAllister, G., Whiting, P., Hammond, E.A., Knowles, M.R., Atack, J.R., Bailey, F.J., Maigetter, R. and Ragan, C.I. (1992), *Biochem. J.*, **284**, 749-754.

15 Bone, R., Springer, J.P. and Atack, J.R. (1992), *Proc. Natl. Acad. Sci., USA*, **89**, 10031-10035.

16 Kato, T., Shiori, T., Takahashi, S. and Inubushi, T. (1991), *J. Affective Disorders*, **22**, 185-190.

17 Renshaw, P.F., Summers, J.J., Renshaw, C.E., Hines, K.G. and Leigh, J.S. (1986), *Biol. Psychiat.*, **21**, 691-694.

18 Preece, N.E., Gadian, D.G., Houseman, J. and Williams, S.R. (1992), *Lithium*, **3**, in press.

19 Grisham, C.M. and Hutton, W.C. (1978), *Biochem. and Biophys. Res. Commun.*, **81**, 1406-1411.

Chapter 7

Caesium NMR Spectroscopy of Erythrocytes

7.1.1 Biological Effects of Cs^+

Cs^+ is an ultra-trace element in humans, however the biochemistry of this cation has not been investigated in any depth. A role for Cs^+ in the treatment of depression has been reported *(1)*. Additionally, a membrane abnormality, or an abnormality in the distribution of Cs^+ across the erythrocyte membrane, has been postulated to be a consequence of alcoholism. The concentration of Cs^+ in the serum of patients suffering from alcohol dependence syndrome correlated positively with the degree of saturation in the fatty acids of the erythrocyte phospholipids *(2)*. This correlation was not observed in either healthy controls or in patients suffering from schizophrenia *(3)*. Also, the concentration of Cs^+ in the erythrocytes of abstinent alcoholic subjects (approximately 2.3 $ngml^{-1}$) was significantly higher than that the erythrocytes of age-matched, healthy controls (approximately 1.3 $ngml^{-1}$) *(4)*. This latter abnormality was independent of the length of abstinence, which ranged from 1 day to 5 years, and did not appear to be related to liver damage. If these high Cs^+ levels are attributable to alcohol ingestion, the relatively short lifetime of erythrocytes indicates a long term, or permanent alcohol-induced abnormality. It may be that this observation could be employed as a biological marker for, and may indicate a predisposition to alcohol dependence.

7.1.2 Transport of Cs^+ in Biological Systems

Very few studies have been reported on the transport of Cs^+ through biological membranes. In the systems which have been investigated, the transport of Cs^+ into cells is sensitive to ouabain inhibition *(5,6)* and in the absence of extracellular K^+, Cs^+ can activate the Na^+/K^+-ATPase, being translocated in the process *(7)*. It is probable that Cs^+ is transported at least in part by the Na^+/K^+ pump, substituting for, or competing with K^+, however in general Cs^+ is less effective than Rb^+ in substituting

for K^+. Cs^+ also appears to be able to block the Na^+, and the K^+ voltage-dependent channels in excitable membranes *(8)*.

7.1.3 ^{133}Cs-Nmr Spectroscopy of Biological Systems

In studies of both human erythrocytes in aqueous suspension and excised rat hearts perfused with Cs^+-containing medium, it was found that the intra-, and the extracellular Cs^+ resonances could be distinguished without the use of the paramagnetic shift reagents required for the study of other alkali metal ions *(6)*. The study reported that the Cs^+ species in the suspensions of erythrocytes exhibited 100% nmr-visibility and the spin-lattice relaxation times, T_1, for Cs^+ were 4.5s in the erythrocytes compared to 13.6s in the extracellular buffer, and 2.5 in the rat heart compared to 12s in the perfusate. The uptake of Cs^+ both into the erythrocytes and into the perfused heart was monitored with respect to time. The observed inhibition of uptake in erythrocytes due to the presence of ouabain was comparable to the ouabain-inhibited uptake of K^+ or Rb^+, implying that Cs^+ is transported into erythrocytes *via* an active transport pathway that is very similar to, or is the same as a specific K^+ transporter.

A detailed investigation of the intracellular Cs^+, and the effects of various shift reagents upon the chemical shifts of the extracellular Cs^+ resonances in the ^{133}Cs-nmr spectra of erythrocyte suspensions have been reported *(9)*. The resolution of the intra-, and the extracellular Cs^+ signals in the absence of a shift reagent was ascribed to the interactions of Cs^+ with the intracellular phosphates, in particular 2,3-diphosphoglycerate (DPG), in which a 1:1 complex is formed with DPG acting as a tridentate ligand.

^{133}Cs-nmr spectroscopy has also been employed to study subcellular compartmentation and ion uptake in perfused maize seedling roots *(10)*. Without incorporating a shift reagent, 3 resonances were observed in the spectra obtained and

these were assigned to Cs^+ in the perfusate, and to Cs^+ in the cytoplasm and the vacuole of the maize root cells. The uptake of Cs^+ into the 2 pools was monitored with respect to time.

The ionophore-induced transport of Cs^+ across membranes has been investigated in phospholipid vesicles, using the $P_3O_{10}^{5-}$ anion to generate a chemical shift difference between the intra-, and the extracellular Cs^+ resonances *(11)*. In contrast to studies on other alkali metal ions, no paramagnetic lanthanide was required and the observed shift difference was attributed to the different anionic compositions of the intra-, and the extracellular fluids. The ionophore employed was nigericin, an efficient ionophore for the transport of K^+.

7.2 Nmr Study of Cs^+ Transport in Human Erythrocytes

Following the observation of elevated Cs^+ levels in the erythrocytes of patients suffering from alcohol-dependence syndrome, and the postulate of an abnormality in the transport of Cs^+ transport and/or in the trans-membrane distribution of Cs^+ *(4)*, the transport of Cs^+ in erythrocytes of healthy controls and of alcoholic individuals was investigated by ^{133}Cs-nmr spectroscopy.

7.2.1 ^{133}Cs-Nmr Spectroscopy of Erythrocytes

The uptake of Cs^+ into human erythrocytes was monitored *in vitro* by isolating erythrocytes from whole blood and resuspending them at 37°C in an isotonic medium containing 10mM Cs^+. After the determination of the 90° pulse width and the T_1 values for the different Cs^+ species, the intracellular concentrations were determined by quantitative ^{133}Cs-nmr spectroscopy, using the same method employed for Li^+ in Chapter 3.

The suspension medium employed, containing no shift reagent, (see Section 2.7.2) produced a shift difference of typically 1.1ppm between the intra-, and the extracellular Cs^+ resonances. The T_1's were 3.38 ± 0.03s and 11.24 ± 0.15s for the intra-, and the extracellular Cs^+ resonances, respectively. These compare with reported T_1's of 4.5s and 13.6s for erythrocytes incubated in a different suspension medium *(6)*. Therefore an interpulse delay of 60s (i.e. > 5 x T_1) was employed to ensure complete relaxation of both Cs^+ species, and thus valid quantification of the $[Cs^+]_{in}$.

7.2.2 ^{133}Cs-Nmr Spectroscopy of Erythrocytes from Healthy Controls and Patients Suffering from Alcohol-Dependence Syndrome

The uptake of Cs^+ into the erythrocytes of 2 abstinent, healthy volunteers was monitored with respect to time. These people had never previously imbibed alcohol, as far as they were aware. Figure 7.1 shows a series of ^{133}Cs-nmr spectra from a typical experiment. The spectra show two signals, one at -1.09ppm assigned to the extracellular Cs^+ ($\omega_{1/2}$ = 13Hz) and one at 0ppm assigned to the intracellular Cs^+ ($\omega_{1/2}$ = 19Hz).

This experiment was then repeated several times with erythrocytes from a number of healthy individuals, who were neither abstinent nor alcohol-dependent, and with erythrocytes from a number of patients suffering from alcohol-dependence syndrome. In all cases the results were very similar. The time dependence of the $[Cs^+]_{in}$ from 2 typical experiments, 1 on an abstinent control and 1 on an alcoholic patient, is illustrated in Figure 7.2. In both cases, the uptake is approximately linear over the time period studied (8h) and the rate is approximately 0.33mM h^{-1}, with no evidence for saturation.

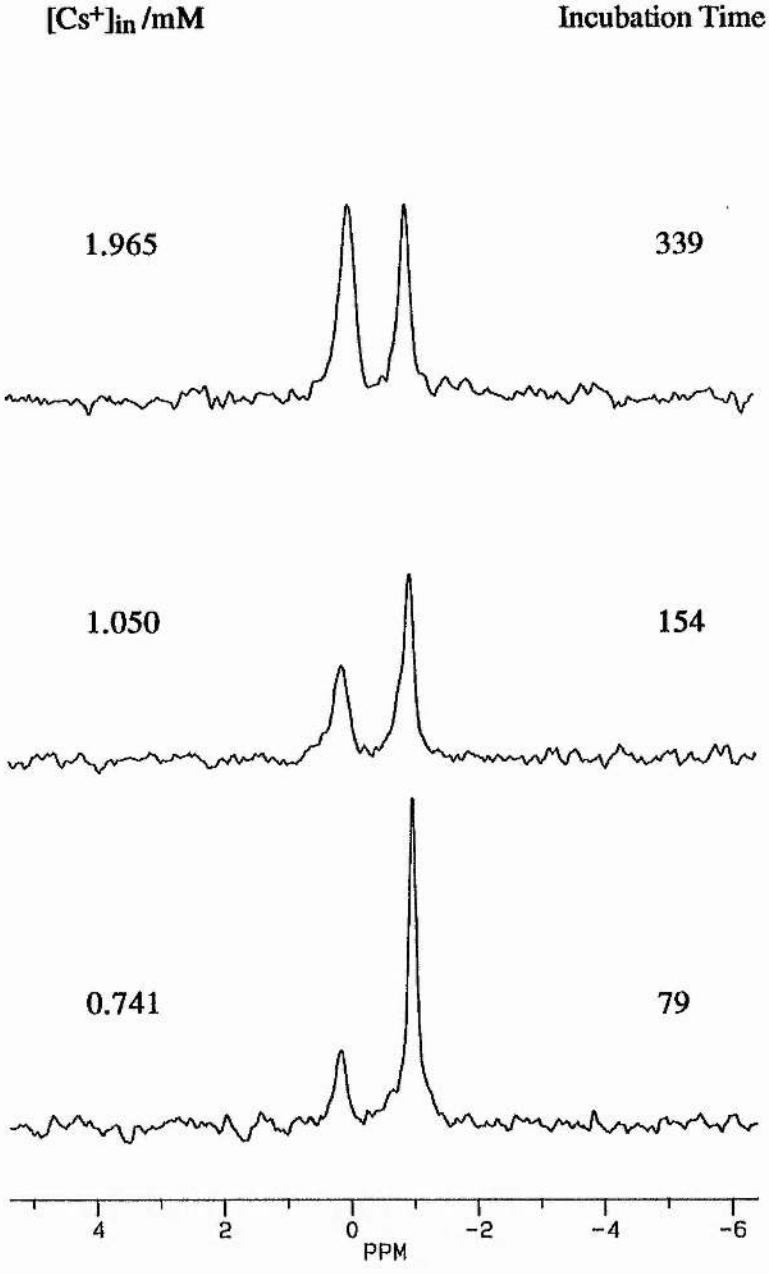

Figure 7.1 ^{133}Cs-nmr spectra of human erythrocytes incubated in phosphate buffer containing 10mM Cs^+, showing time dependence of the intracellular [Cs^+] (Each spectrum is the sum of 8 acquisitions recorded at 66MHz on the MSL500 nmr spectrometer)

Incubation of erythrocytes in the suspension medium (10mM Cs^+, 24h, 37°C, 4% haematocrit) resulted in an intracellular [Cs^+] of approximately 5mM. The efflux of Cs^+ from the Cs^+-loaded erythrocytes was monitored by resuspending the erythrocytes in Cs^+-free isotonic medium at 37°C for up to 8h, however under these conditions, no reduction in the intracellular [Cs^+] was observed.

The effect of extracellular Cs^+ on the intracellular concentrations of Na^+ and K^+ was investigated by ^{23}Na- and ^{39}K-nmr spectroscopy, by substituting Na^+ for Cs^+ in the extracellular medium. Although the absolute values should be treated with caution since the effects of nmr invisibility have not been taken into account, the changes in the intracellular levels of these cations are illustrated in Figure 7.3. As expected, the $[Cs^+]_{in}$ increases with increasing $[Cs^+]_{out}$. A slight decrease in the $[Na^+]_{in}$ is observed with increasing $[Cs^+]_{out}$, although this is probably due to the efflux of Na^+ from the erythrocytes as a result of the significant reduction in $[Na^+]_{out}$. More interesting is the considerable reduction in $[K^+]_{in}$ with increasing $[Cs^+]_{out}$, despite the fact that the $[K^+]_{out}$ remains constant.

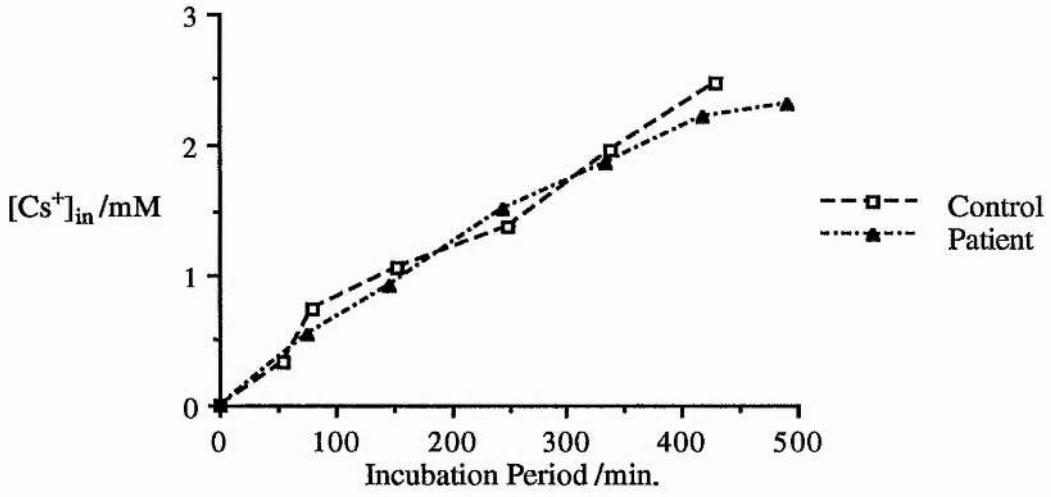

Figure 7.2 The uptake of Cs^+ into the erythrocytes of an abstinent healthy control and a patient suffering from alcohol-dependence syndrome, at $[Cs^+]_{out}$ of 10mM

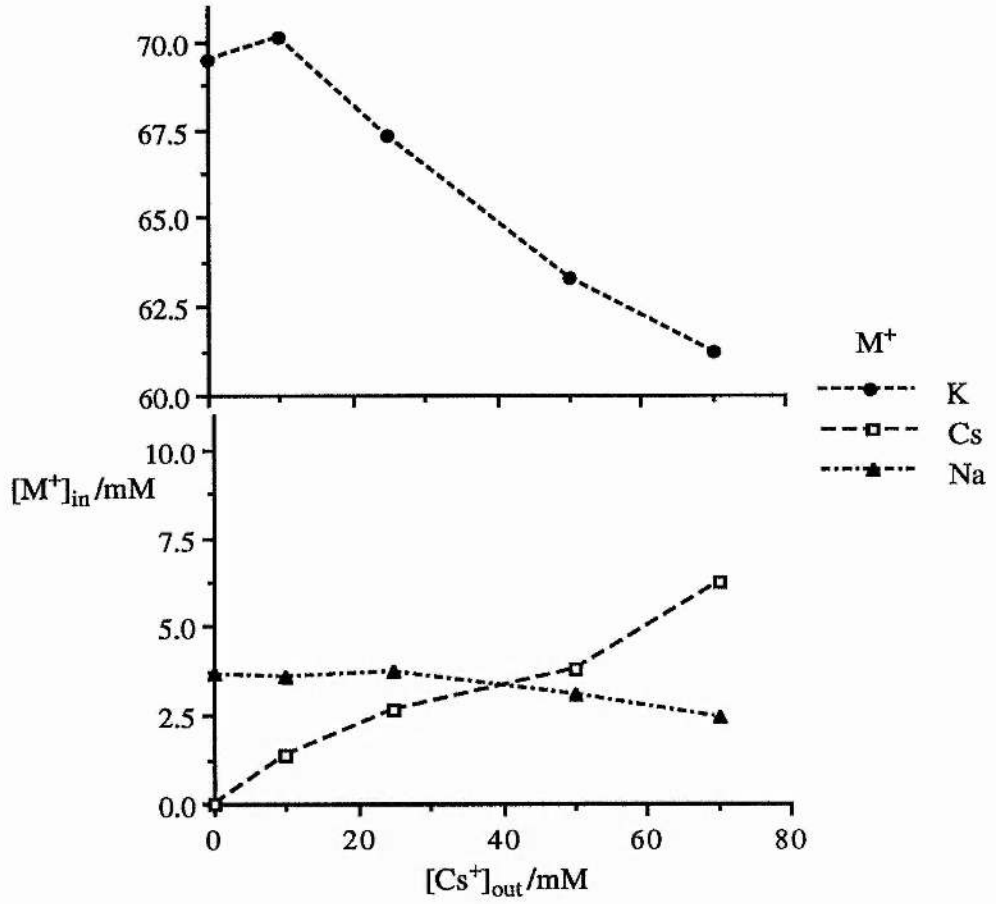

Figure 7.3 The effect increasing the extracellular [Cs^+] on the intracellular [Cs^+], [Na^+] and [K^+] in suspensions of human erythrocytes

7.3 Discussion

^{133}Cs-nmr spectroscopy is aided by the fact that the natural abundance of ^{133}Cs is 100% and that the chemical shifts of Cs^+ are more anion dependent than those of the other alkali metal ions, because of the larger ionic radius of this cation.

The resolution of the intra-, and the extracellular Cs^+ resonances was achieved without the incorporation of a chemical shift reagent as expected from a previous study *(6)*. The linear uptake of Cs^+ occurred at a rate of $0.33mMh^{-1}$, which is approximately half that previously observed in a study which employed the same $[Cs^+]_{out}$ but which used a different suspension medium, not containing K^+ *(6)*. Since it is likely that the uptake of Cs^+ is, at least in part, mediated by a K^+ transport mechanism *(6,7)*, the presence of K^+ in the suspension medium employed in this study, is probably responsible for the lower uptake rate, with Cs^+ in competition with K^+ for the transporter. The decrease in the intracellular concentration of K^+ as the concentration of the extra-, and consequently the intracellular Cs^+ increases, confirms that Cs^+ can behave as a substitute for K^+ in erythrocytes. It appears that there is no effective efflux mechanism available for the transport of Cs^+ out of erythrocytes as indicated by the absence of efflux from the Cs^+-loaded cells.

Interestingly, the uptake of Cs^+ into erythrocytes from completely abstinent healthy controls was virtually identical to that from the alcoholic patients, indicating a lack of transport abnormality under these concentrations and conditions. However, it should be noted that Cs^+ is only an ultra-trace element in humans, a level of $1.3ngml^{-1}$ has been quoted for the concentration of Cs^+ in the erythrocytes of healthy individuals *(4)*, and the transport of Cs^+ at endogenous concentrations may well be completely different from the relatively high concentration employed in this study (10mM). Unfortunately, the relative insensitivity of nmr spectroscopy means that transport studies at physiological concentrations are impossible by this technique.

7.4 References

1 Messiha, F.S. (1978), *Br. J. Pharm.*, **64**, 9-12.

2 Corrigan, F.M., Glen, A.I.M., Glen, E.M.T., Skinner, E.R., Horrobin, D.F. and Ward, N.I. (1989), *Trace Elements in Medicine*, **6**, 108-113.

3 Corrigan, F.M., Van Rhijn, A.G., Skinner, E.R., Horrobin, D.F. and Ward, N.I. (1991), *Trace Elements in Medicine*, **8**, 101-105.

4 Corrigan, F.M., Besson, J.A.O. and Ward, N.I. (1991), *Alcohol and Alcoholism*, **26**, 309-314.

5 Beauge, L.A. and Sjodin, R.A. (1968), *J. Physiol.*, **194**, 105-123.

6 Davis, D.G., Murphy, E. and London, R.E. (1988), *Biochem.*, **27**, 3547-3551.

7 Whittam, R. and Ager, M.E. (1964), *Biochem. J.*, **93**, 337-348.

8 Mullins, L.J. (1975), *Biophys, J.*, **15**, 921-931.

9 Wittenkeller, L., Mota de Freitas, D., Geraldes, C.F.G.C. and Tome, A.J.R. (1991), *Inorg. Chem.*, **31**, 1135-1144.

10 Pfeffer, P.E., Rolin, D.B., Brauer, D., Tu, S, and Kumosinski, T.F. (1990), *Biochim. Biophys. Acta*, **1054**, 169-175.

11 Riddell, F.G., Arumugam, S. and Patel, A. (1990), *Inorg. Chem.*, **29**, 2397-2398.